学位論文

Design, Synthesis and Biological Evaluation of 2-Pyrrolone Derivatives as Radioprotectors Regulating p53-Dependent Apoptosis and Their Mechanistic Study

(p53 依存性アポトーシス制御型放射線防護剤としての 2-ピロロン類の設計、合成、活性評価及びその作用機序解析)

Doctoral Thesis

Tokyo University of Science

２０２３年（令和５年）３月

Hidetoshi Satoh

(Supervisor: Prof. Shin Aoki)

Contents

Abbreviation ---- 1

Chapter 1. General Introduction ---- 6

[1-1] Radiation therapy and radioprotectors ---- 7

[1-2] p53 and the regulation of its behavior for radioprotection ---- 10

[1-3] Aim and contents of this thesis ---- 13

Chapter 2. Design, Synthesis and Biological Evaluation of 2-Pyrrolone Derivatives as Radioprotectors ---- 16

[2-1] Introduction ---- 17

[2-2] Results and discussion ---- 22

[2-2-1] Synthesis ---- 22

[2-2-2] Evaluation of radioprotective activity and cytotoxicity ---- 35

[2-2-3] Evaluation of p53-suppressing activity ---- 44

[2-3] Conclusion ---- 46

Chapter 3. A Novel RNA Synthesis Inhibitor, STK160830, Has Negligible DNA-Intercalating Activity for Triggering A p53 Response, and Can Inhibit p53-Dependent Apoptosis ---- 47

[3-1] Introduction ---- 48

[3-2] Results ---- 52

[3-2-1] STK160830 suppresses DNA damage-induced apoptosis in a p53-dependent manner ---- 52

[3-2-2] Correlation between changes in intracellular protein expression and viability by STK160830 ---- 56

[3-2-3] STK160830 is a novel mRNA synthesis inhibitor with a different spectrum of action from Act.D ---- 59

[3-2-4] STK160830 has negligible DNA-intercalating activity for triggering a p53 response---------- 63
[3-3] Discussion ---------- 66

Chapter 4. Concluding Remarks ---------- 70

Chapter 5. Experimental Section ---------- 73
[5-1] Materials and Methods for Chapter 2 ---------- 74
[5-2] Materials and Methods for Chapter 3 ---------- 125

Chapter 6. References ---------- 130

Acknowledgement ---------- 143

List of Publications ---------- 145

Abbreviation

5CHQ	5-chloro-8-quinolinol
AS-2	5,7-bis(*N*-methylaminosulfonyl)-2-methyl-8-quinolinol
AcOEt	ethyl acetate
AcOH	acetic acid
ACTB	mRNA encoding beta-actin
Act.D	actinomycin D
ADDP	1,1′-(azodicarbonyl)dipiperidine
aq.	aqueous
ATR	attenuated total reflection
Ball-1	human leukemia B cells
BBC3	bcl2-binding components 3, mRNA encoding PUMA
BCA assay	bicinchoninic acid assay
Bispicen	*N*,*N*'-bis(2-pyridylmethyl)-1,2-ethylenediamine
brs	broad signal
ca.	circa, about
CAN	ammonium cerium(IV) nitrate
CCD	charge-coupled device
CCDC	Cambridge crystallographic data center
CCRF-CEM	human leukemia, lymphoblastic T cells
CDKN1A	cyclin-dependent kinase inhibitor 1, mRNA encoding p21
CIF	crystallographic information file
cm^{-1}	wavenumber(s)
ctDNA	calf thymus DNA
DDR	DNA damage response
DMF	*N*,*N*-dimethylformamide

DMSO	dimethyl sulfoxide
DNA	deoxyribonucleic acid
DRB	5,6-dichloro-1-β-D-ribofuranosylbenzimidazole
ECL	enhanced chemiluminescence
equiv	equivalent
ESI	electrospray ionization
Et_2O	diethyl ether
EtBr	ethidium bromide
EtOH	ethanol
EU	5-ethynyl uridine
FAB	fast atom bombardment
FBS	fetal bovine serum
FDA	food and drug administration
GAPDH	glyceraldehyde-3-phosphate dehydrogenase
HEPES	4-(2-hydroxyethyl)-1-piperazineethanesulfonic acid
HRMS	high-resolution mass spectrometry
HRP	horseradish peroxidase
Hz	hertz
IR	ionizing radiation; infrared
KU812	human leukemia, chronic myeloid
KY821	human leukemia, acute myeloid
LED	light-emitting diode
LET	linear energy transfer
M	molar, mega
m-	meta
m/z	mass-to-charge ratio
M^+	parent molecular ion

Me	methyl
MeCN	acetonitrile
MeOH	methanol
min	minute(s)
mL	milliliter
mol	mole(s)
MOLT-4	human leukemia, T lymphoblastic cells
mp	melting point
mRNA	messenger ribonucleic acid
MS	mass spectrometry
MW	microwave
NMR	nuclear magnetic resonance
NOE	nuclear overhauser effect
NOESY	nuclear overhauser effect spectroscopy
ORTEP	Oak Ridge Thermal-Ellipsoid Plot Program
***o*-**	ortho
***p*-**	para
p53DINP1	p53-dependent damage-inducible nuclear protein 1
PAGE	poly acrylamide gel electrophoresis
PBS	phosphate buffered saline
PFTα	pifithrin α
PPh_3	triphenylphosphine
P-TEFb	positive transcription elongation factor b
***p*-TsOH**	*p*-toluenesulfonic acid
PUMA	p53 upregulated modulator of apoptosis
PVDF	polyvinylidene fluoride
pPCR	quantitative polymerase chain reaction

quant.	quantitative yield
RIPA	radioimmunoprecipitation assay
RNA	ribonucleic acid
RT	radiation therapy
rt	room temperature
ROS	reactive oxygen species
rpm	revolutions per minute
SAR	structure-activity relationships
SD	standard deviation
SDS	sodium dodecyl sulfate
SNU283	human adenocarcinoma, rectal
SW837	human adenocarcinoma, rectal
***t*-BuOH**	tertiary-butyl alcohol
***t*-BuOK**	potassium tertiary-butoxide
TBST	tris buffered saline with tween 20
TFA	trifluoroacetic acid
THF	tetrahydrofuran
TLC	thin-layer chromatography
T_m	melting temperature
TMS	tetramethylsilane
TP53	tumor protein p53, mRNA encoding p53
TP53INP1	tumor protein p53-inducible nuclear protein, mRNA encoding P53DINP1
U937	human lymphoma
UV	ultraviolet
vis	visible
WST-8	water soluble tetrazolium salt; 2-(2-Methoxy-4-nitrophenyl)-3-(4-

	nitrophenyl)-5-(2,4-disulfophenyl)-2H-tetrazolium Sodium Salt; 5-(2,4-disulfophenyl)-3-(2-methoxy-4-nitrophenyl)-2-(4-nitrophenyl)-2H-tetrazolium, inner salt, monosodium salt
Zn	zinc
Å	angstrom(s)
°C	degrees Celsius
$\Delta\Psi_m$	mitochondrial membrane potential
µ	micro
γ	gamma

Chapter 1.

General Introduction

[1-1] Radiation therapy and radioprotectors

Radiation therapy (RT) is a common cancer treatment that is broadly applied to cancer patients for its advantages such as non-invasive anti-cancer activity and the coverage of radiation to tumor tissues with spatial control. In RT, reactive oxygen species (ROS) generated by ionizing radiation (IR) causes cellular DNA damages, resulting in cancer cell death. The efficacy and safety of RT have been considerably improved by the understanding of the biological events responding to the damage caused by IR as well as the development and improvement of irradiation instruments and techniques. These developments contribute to the increase in the number of people receiving RT and it is estimated that half of the current cancer patients receive RT during the cancer treatment.[1] On the other hand, it is known that IR-induced DNA damages take place not only in cancer cells but also in normal cells, resulting in serious acute side effects and restriction of clinical dose of radiation.

To date, some types of drugs such as radiosensitizers, radiomitigators and radioprotectors have been proposed to tackle the limitation of RT described above. The use of these drugs suppresses the undesired side effects by expanding the radiosensitivity between normal tissues and cancer tissues[2] (Figure 1-1), allowing the use of higher radiation dose.

We have been interested in chemical radioprotectors that protect normal tissues from IR-induced injury. Several mechanisms of action for radioprotection include ROS scavenging, the suppression of inflammatory cytokines, promoting cellular recovery processes and molecular-targeting inhibition of the apoptotic signaling pathways.[3] To date, amifostine (**1** in Scheme 1-1), a ROS scavenger, is the only chemical drug that has been approved as a radioprotector by the Food and Drug Administration (FDA) in the US. It is very likely that the thiophosphate group of amifostine is hydrolyzed by alkaline phosphatase to afford the corresponding thiol product, which quenches the ROS species generated by IR. However, the clinical use of amifostine is limited due to its side effects such as severe nausea and vomiting possibly derived from its thiol structure that is required for ROS quenching.[4] Therefore, the development of new radioprotectors that possess different mechanism with a high radioprotective activity and low side effects is a subject of considerable interest.

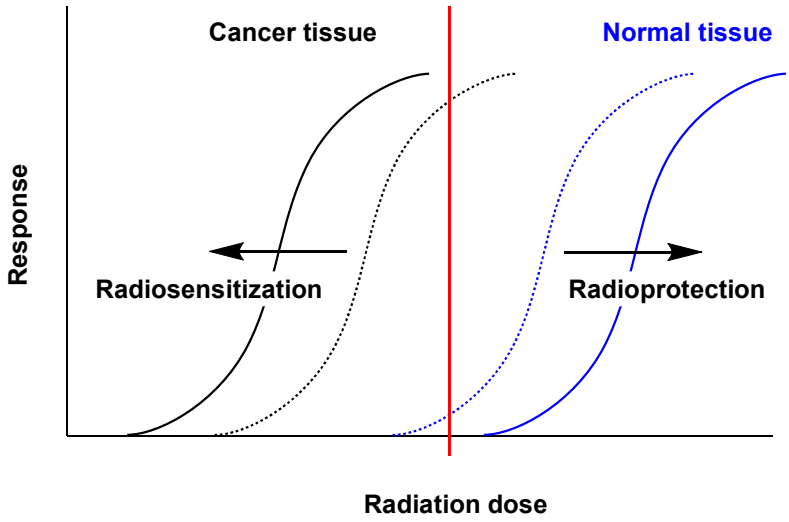

Figure 1-1. The image of dose-response curve of normal (blue) and cancer tissues (black) against radiation. Plain curves show original response of each tissue and dashed curves show the controlled responses by drugs. Red line shows the dose of cancer treatment. Generally, the greater difference between response curve of cancer tissue and that of normal tissue, the more effective treatment.

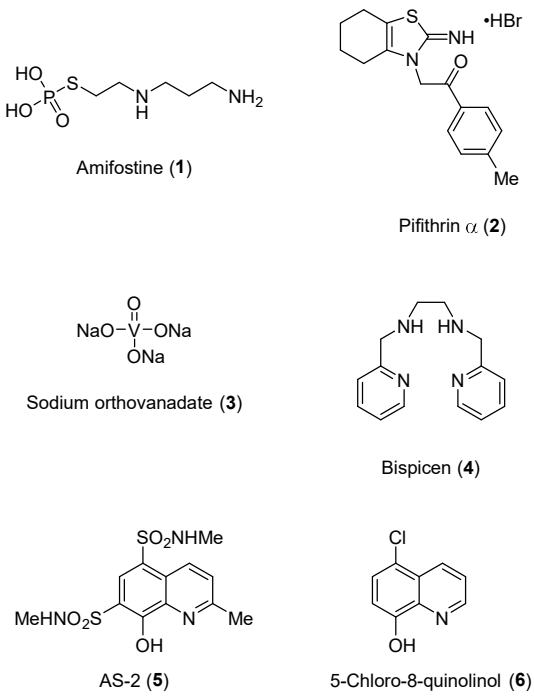

Scheme 1-1. Representative radioprotective compounds targeting p53 reported by our and other research groups.

[1-2] p53 and the regulation of its behavior for radioprotection

p53 was initially identified as a tumor suppressor in 1989; subsequently, it was found to be the most frequently mutated gene in cancer.[5] It is known that p53 is activated by genomic stress and plays a central role in DNA damage response (DDR), including cell cycle arrest, DNA repair and apoptosis. These functions of p53 are considered to contribute to the suppression of tumorigenesis, for which p53 is often referred to as 'guardian of the genome'. Although *TP53* is the most studied human gene, there are still many questions concerning the regulation of p53 activity by cellular stresses.[6] The effect of p53 on radiosensitivity has been well studied and it was found that the loss of p53 provides different consequences dependent on target tissues (Figure 1-2).[7] For example, because of the protective effect of p53, its inhibition results in radiosensitization in endothelial cells. In contrast, p53-mediated apoptosis is a major cause of IR-induced cell death in bone marrow, thymus and spleen, and hence the temporal inhibition of p53 would protect normal tissues from radiation. These results indicate that the regulation of p53 function is a potential strategy for both radiosensitization and radioprotection.

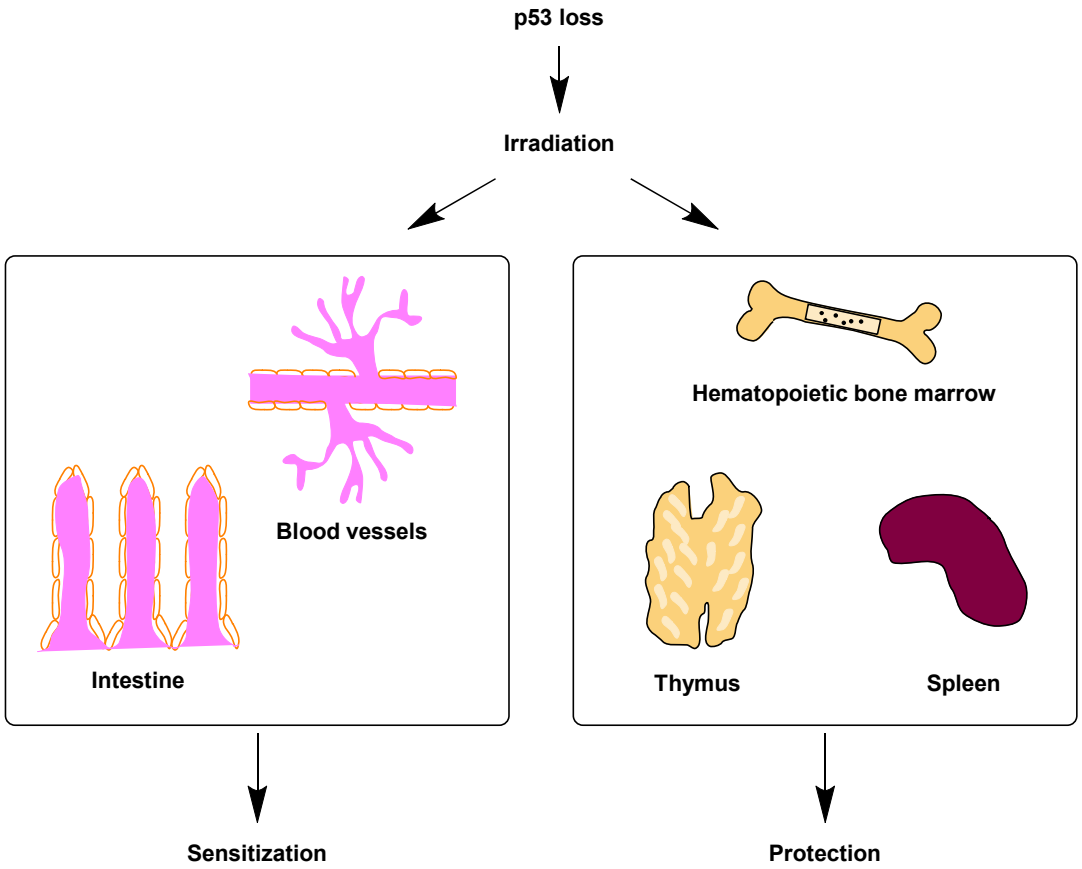

Figure 1-2. The tissue-dependent role of p53 and the effect of p53 loss on the tissues. The p53 loss sensitizes the gut and cardiac endothelial cells to radiation. On the other hand, the p53 loss protects the hematopoietic and lymphoid cells from radiation.

In this context, Komarov and co-workers reported that a p53 inhibitor, pifithrin α (PFT α, **2** in Scheme 1-1), protects mice from IR-induced injury by blocking p53-induced transactivation.[8] They also found that the drug-mediated temporal inhibition of p53 would not increase the risks of IR-induced tumorigenesis. Several recent reports have suggested that modifying p53 behavior with small molecules is one of the effective

approaches for cancer therapy and minimizing toxicity in healthy cells by suppressing p53 signaling pathway.[9]

It is known that p53 binds to DNA for the transactivation of target genes in DDR. The crystal structure of a DNA-p53 complex (PDB: 1TUP) revealed that a zinc (Zn^{2+}) ion is included in its DNA binding site.[10] We previously reported that sodium orthovanadate (**3** in Scheme 1-1) and Zn^{2+} chelators such as *N*,*N*'-bis(2-pyridylmethyl)-1,2-ethylenediamine (bispicen, **4**) induce a conformational change in p53, which resulted in the inhibition of p53-mediated apoptosis.[11] Further investigation revealed that 5,7-bis(*N*-methylaminosulfonyl)-2-methyl-8-quinolinol (AS-2, **5**), a Zn^{2+} chelator, exhibited good radioprotective activity with less cytotoxicity.[12] In addition, it has been reported that 5-chloro-8-quinolinol (5CHQ, **6**) shows a unique p53-modulating activity that shifts its transactivation from proapoptotic to protective responses, including the activation of cyclin-dependent kinase p21 and the suppression of the pro-apoptotic protein PUMA.[13] In these studies, MOLT-4 cells were used as a model of normal cells because MOLT-4 cells express wild-type p53 and undergo p53-mediated apoptosis in response to IR stress.[11-13] These compounds are of great interest since they confer strong radioprotective activity by modulating the activity of p53 and provide clues regarding the function of p53 in the cellular response to radiation.

[1-3] Aim and contents of this thesis

In this thesis, we report on the design, synthesis and biological evaluation of 2-pyrrolone derivatives as radioprotectors and their mechanistic study. STK160830 (**7a** and also referred as HSt-2), a 2-pyrrolone derivative, was found as one of new candidates of radioprotector in a phenotypic screening of 9600 compounds included in a chemical library of the Drug Discovery Initiative at The University of Tokyo (Scheme 1-2).

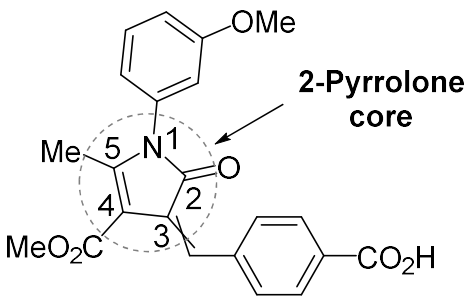

STK160830 (7a, HSt-2)

Scheme 1-2. A chemical structure of STK160830 (**7a**, HSt-2) discovered in a chemical library of The Drug Discovery Initiative at The University of Tokyo (HSt-2 is the alternative compound number of **7a** named after the author of this Ph. D thesis).

In Chapter 2, we report on the design, synthesis and biological evaluation of STK160830 and its derivatives. The 2-pyrrolone derivatives that were synthesized in this study have two stereoisomers for the *exo*-olefin part of the 2-pyrrolone core and we found that the *Z*-form compound was more biologically active than the corresponding *E*-form compound. Radioprotective activity was evaluated by dye exclusion assays using MOLT-4 cells, as a model of normal cells. The result of a structure-activity relationships (SAR) study revealed several structural requirements for radioprotective activity. Mechanistic study suggests the down-regulation of p53 evaluated by STK160830 and the results indicated that the radioprotective activity is dependent on the suppression of p53.

In Chapter 3, we report on the mechanistic study of radioprotection by STK160830. We have found that STK160830 acts on the upstream of the mitochondria or on the mitochondria themselves by checking the percentage of cells losing the mitochondrial membrane potential ($\Delta\Psi_m$). Then, we verified the p53-specificity of radioprotection of STK160830 by checking anti-apoptotic activity using several cell lines having p53-mutation. The anti-apoptotic activity of STK160830 was shown in the cell lines bearing wild-type p53, as we expected. To examine the effect on p53, the expression level was confirmed by western blot analysis and the result suggested that STK160830 suppressed p53 accumulation upon the IR-irradiation. Further mechanistic study revealed that

STK160830 inhibited nascent mRNA synthesis of *TP53*, an encoding gene of p53, without the intercalation with DNA.

Finally, the conclusion of this thesis is described in Chapter 4.

Chapter 2.

Design, Synthesis and Biological Evaluation of 2-Pyrrolone Derivatives as Radioprotectors

(放射線防護剤としての 2-ピロロン類の設計と合成及び生物学的評価)

[2-1] Introduction

Radiation therapy (RT) is a common cancer treatment that is broadly applied to cancer patients for its advantages such as non-invasive anti-cancer activity and the coverage of radiation to tumor tissues with spatial control. In RT, reactive oxygen species (ROS) generated by ionizing radiation (IR) causes cellular DNA damages, resulting in cancer cell death. However, IR-induced DNA damages also take place in normal cells, resulting in toxicity and acute side effects.[7]

It is important to develop chemical agents that protect normal tissues from IR-induced injury (radioprotectors) for achieving a more efficient and safer RT by ROS scavenging, the suppression of inflammatory cytokines, promoting cellular recovery processes and molecular-targeting inhibition of the apoptotic signaling pathways as described in Chapter 1.

In this context, we focused on the development of radioprotectors targeting p53. As described in Chapter 1, we conducted a phenotypic screening of 9600 compounds included in a chemical library of the Drug Discovery Initiative at The University of Tokyo (Scheme 1-2). We selected 178 compounds that suppress IR-induced p53-dependent apoptosis in MOLT-4 cells by WST-8 assay at the first step (Scheme 2-1). In a secondary screening, dose-dependent WST-8 assay was carried out, which allowed us to select 7

compounds of interest. Finally, STK160830 (**7a** or HSt-2), a 2-pyrrolone derivative, was selected as a potent radioprotector by dye exclusion assay. We also reported that **7a** suppresses the level of p53 expression that is induced by IR-irradiation and that it exhibits an anti-apoptotic activity in MOLT-4 cells. Moreover, the anti-apoptotic activity was not observed in most of the cell lines having a p53 mutation. It was also found that nascent mRNA synthesis of p53 was inhibited by **7a** without DNA intercalation. Therefore, it is very likely that **7a** exerts its radioprotective activity in different mechanisms from those of other radioprotective compounds **1-6** described in Figure 3 of Chapter 1.

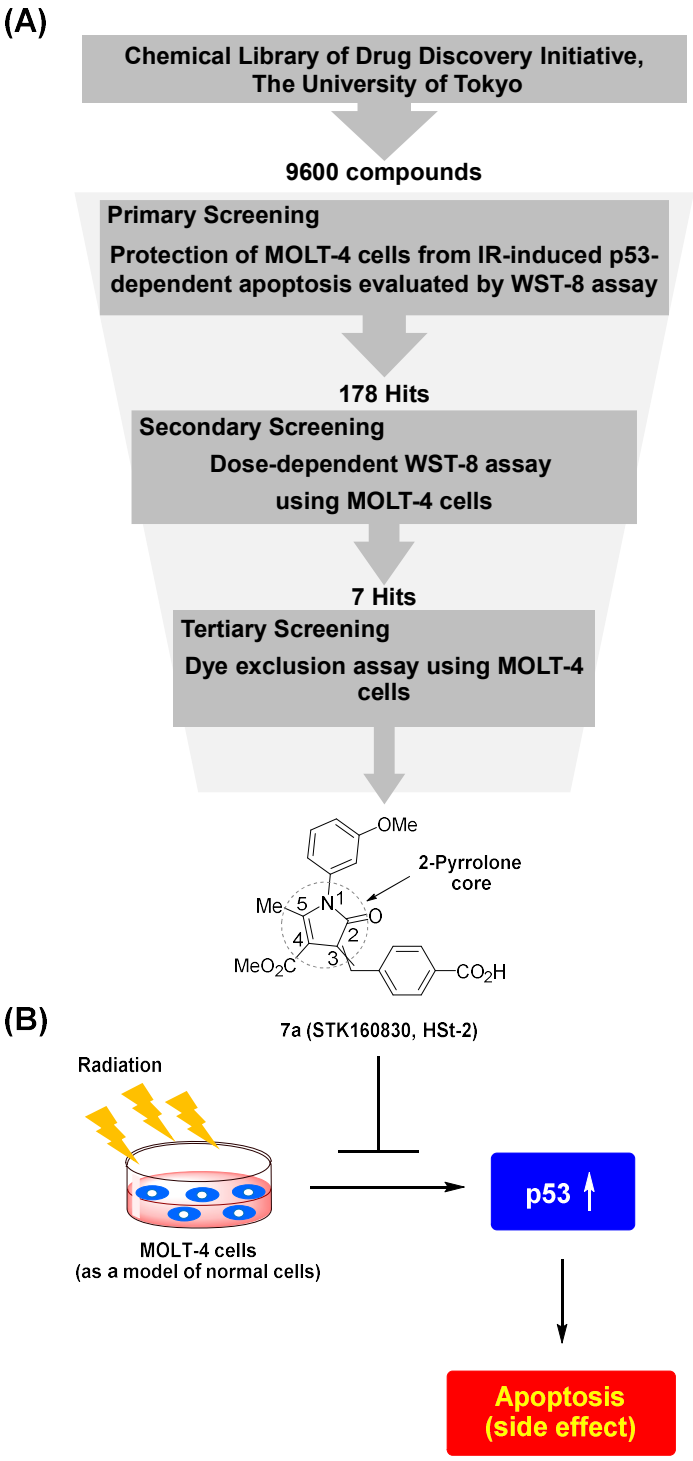

Scheme 2-1. (A) Screening workflow for the discovery of new radioprotectors from a chemical library of the Drug Discovery of Initiative at The University of Tokyo to discover STK160830 (**7a**) as a hit compound. (B) Proposed mechanism for the radioprotective activity of **7a**.

The aforementioned results prompted us to design, synthesize and evaluate the radioprotective activity of **7a** and its derivatives **(*Z*)-7b-7ab**, as summarized in Scheme 2-2, for the use in a structure-activity relationship (SAR) study. The radioprotective activity of **7a-7ab** was evaluated by dye exclusion assay using MOLT-4 cells. We purified and isolated **(*Z*)-7a** from an *EZ* mixture of **7a** and confirmed that it has more potent radioprotective activity than **(*E*)-7a**. We also assessed the p53-suppressing activity of several compounds and found that there is a positive relationship between radioprotective activity and their inhibitory effect on the p53 expression levels, suggesting that the radioprotective activity of 2-pyrrolone derivatives is related to the inactivation or suppression of p53 in MOLT-4 cells.

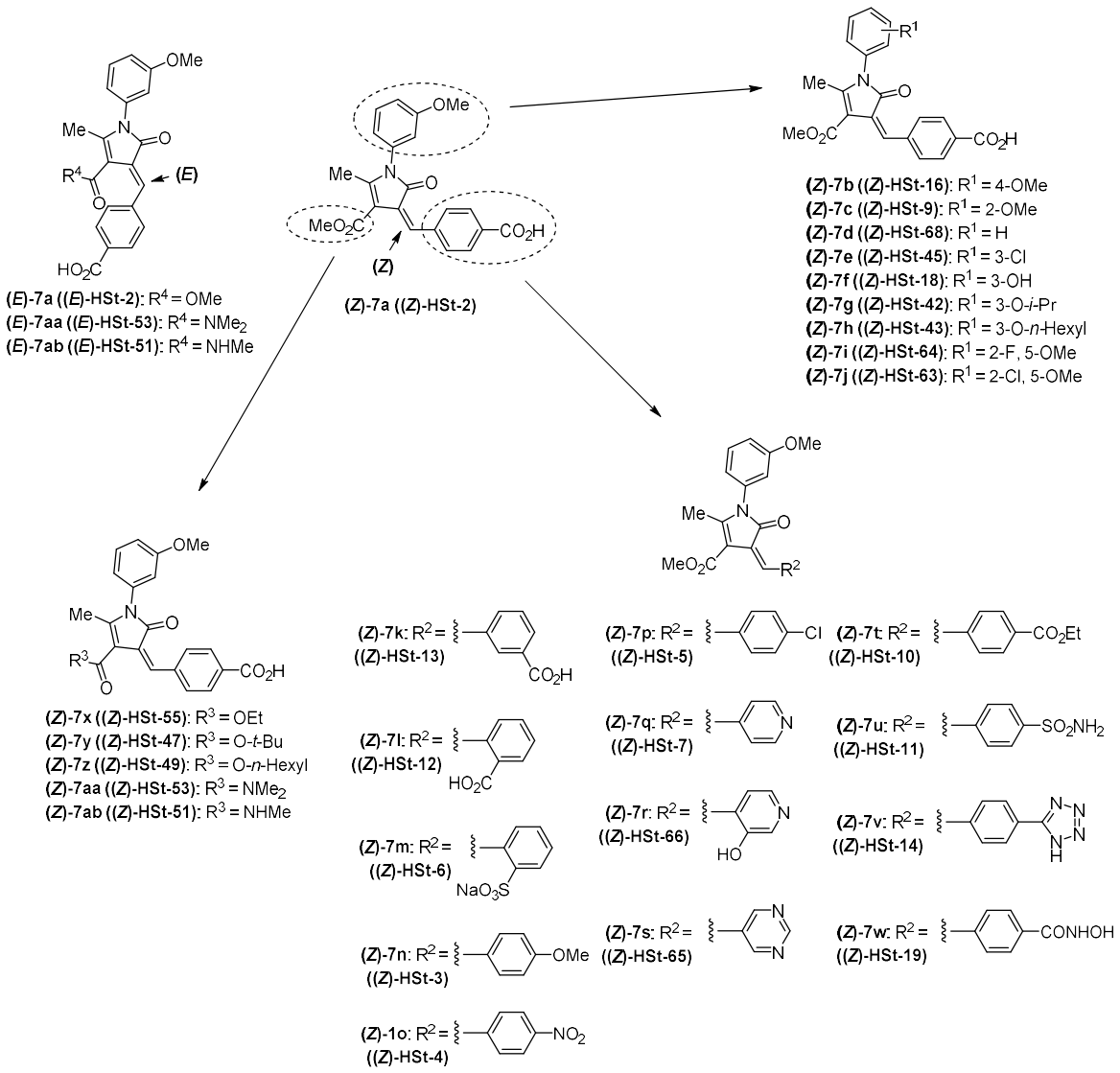

Scheme 2-2. Structures of 2-pyrrolone derivatives synthesized in this work (the compound numbers described in parentheses are named after the author of this Ph. D. thesis)

[2-2] Results and discussion

[2-2-1] Synthesis

The synthesis of **7a** via **8a** is shown in Tables 2-1 and 2-2.[14,15] The synthesis of **8a** from dimethyl acetylsuccinate (**9**) and *m*-anisidine (**10**) in toluene in the presence of *t*-BuOK was not successful (Entry 1 and 2 in Table 2-1) but the use of *p*-TsOH, TFA and AcOH afforded **8a** (Entry 3-5 in Table 2-1).

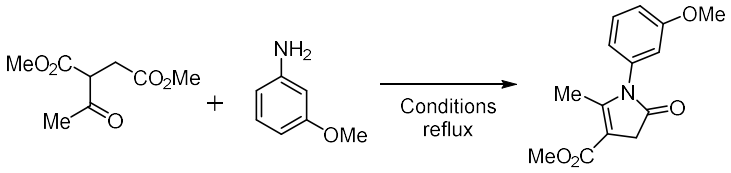

9 (1.0 equiv.) **10** (2.2 equiv.) **8a**

Entry	Additive	Solvent	Time	Yield of **8a** (%)
1	-	Toluene	12 h	not obtained
2	*t*-BuOK (1.0 equiv.)	Toluene	12 h	not obtained
3	*p*-TsOH (1.0 equiv.)	Toluene	12 h	12%
4	-	TFA	12 h	26%
5	-	AcOH	6 h	91%

Table 2-1. Optimization of reaction conditions for **8a**.

Next, an acid-catalyzed Knoevenagel condensation reaction of **8a** with terephthalaldehydic acid (**11**) was carried out (Table 2-2). When the reaction was carried out in MeOH in the presence of a catalytic amount of hydrochloric acid (Entry 1 in Table 2-2), it failed to reach completion in 24 h and the *E/Z* mixture of **7a** with respect to the *exo*-olefin part was obtained in 23% yield with **12** as a by-product, which was possibly

generated by esterification with MeOH. The condensation reaction in the presence of 3.0 equiv. of hydrochloric acid reached completion within 2 h and the chemical yields of **7a** and **12** were improved, although the esterification with MeOH was not suppressed (Entry 2). In Entry 3, the reaction in *t*-BuOH in the presence of a catalytic amount of hydrochloric acid reached completion within 2 h to afford **7a** as a major product with an *E*/*Z* ratio of 22/78.

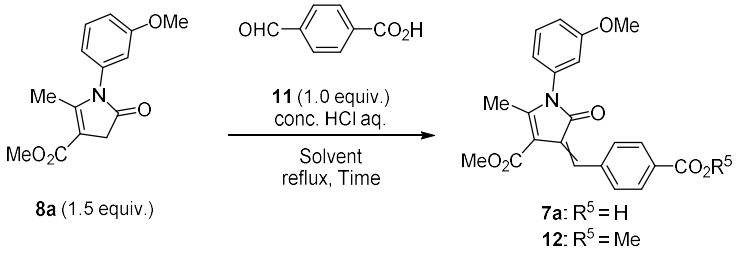

8a (1.5 equiv.)

7a: R^5 = H
12: R^5 = Me

Entry	conc. HCl aq.	Solvent	Time	**7a** (Desired product)	**12** (By-product)
1	0.2 equiv.	MeOH	24 h	23% (*E*/*Z* = 20/80)	32% (*E*/*Z* = 19/81)
2	3.0 equiv.	MeOH	2 h	30% (*E*/*Z* = 25/75)	68% (*E*/*Z* = 26/74)
3	0.2 equiv.	*t*-BuOH	2 h	quant. (*E*/*Z* = 22/78) 42% (*Z* form)[a)]	-

Table 2-2. Optimization of reaction condition for **7a**. [a)] **(*Z*)-7a** was obtained by recrystallization from AcOEt.

The *E*/*Z* mixture of **7a** was purified by recrystallization from AcOEt in a brown glass flask to avoid photochemical isomerization. The resulting single isomer was determined to be the *Z* form by an X-ray crystal structure analysis (Figure 2-1). The isolation of **(*E*)-7a** was not successful even in the dark. For further structure analyses, we carried out NOESY experiments of **(*Z*)-7a** alone and a mixture of **(*E*)-7a** and **(*Z*)-7a** (Figure 2-2). It

is generally accepted that NOE cross-peaks are observed between protons located within 5 Å of each other.[16] In the X-ray crystal structure of **(*Z*)-7a**, the estimated distance between the methyl ester proton (3.82 ppm) and vinyl proton in the benzylidene group (8.14 ppm) was ca. 4-6 Å. On the other hand, the distance between the methyl ester proton (3.82 ppm) and the aromatic proton (7.92 ppm) appears to be greater than 6 Å. The NOESY spectrum of a mixture of **(*E*)-7a** and **(*Z*)-7a** showed a correlation between the methyl ester proton (3.82 ppm) and the benzylidene proton (8.14 ppm) in **(*Z*)-7a**, as displayed in Figure 2-2. A correlation between the methyl ester proton (3.18 ppm) and the aromatic proton (7.96, 7.44 ppm) was also found in **(*E*)-2a**.

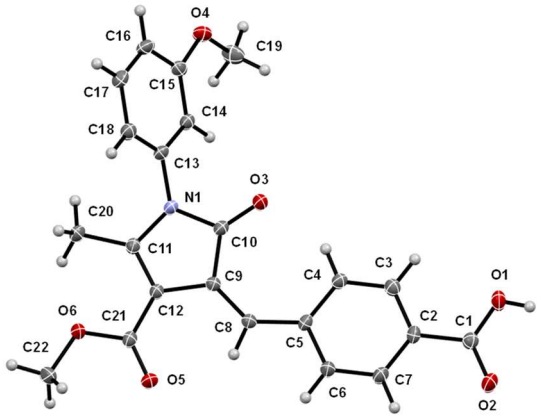

Figure 2-1. ORTEP drawing of the X-ray crystal structure of **(*Z*)-7a** (with 50% probability of ellipsoids) obtained by recrystallization from AcOEt. Each sphere represents an individual atom (gray color: carbon atom; white color: hydrogen atom; blue color: nitrogen atom; red color: oxygen atom).

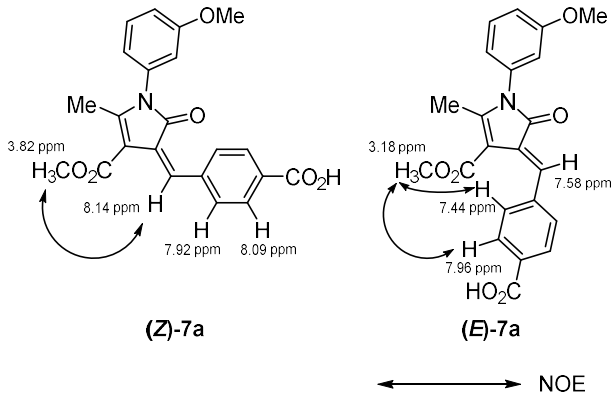

Figure 2-2. NOE observed in the structure of **(*Z*)-7a** and **(*E*)-7a**.

As shown in Figures 2-3 and 2-4, we checked the time-dependent change in the *E*/*Z* ratio of **7a** under the fluorescent light starting from the pure **(*Z*)-7a** and it was found that the photoisomerization of **7a** proceeds in solvents under the fluorescent light.

The photoisomerization was not observed in solvents without photoirradiation nor in solid states with photoirradiation. The effect of the wavelength of the light on the *E*/*Z* ratio was examined using a LED light source with specific wavelengths (365, 425 and 465 nm) and the *E*/*Z* ratio after the photoirradiation was slightly different due to the irradiation wavelength, as shown in Figure 2-4. The UV/Vis spectra of **(*Z*)-7a** and the *E*/*Z* mixture of **7a** (*E*/*Z* = 46/54) are shown in Figure 2-5. Based on these findings, **7a** and its derivatives were treated in the dark to avoid photoisomerization during biological experiments.

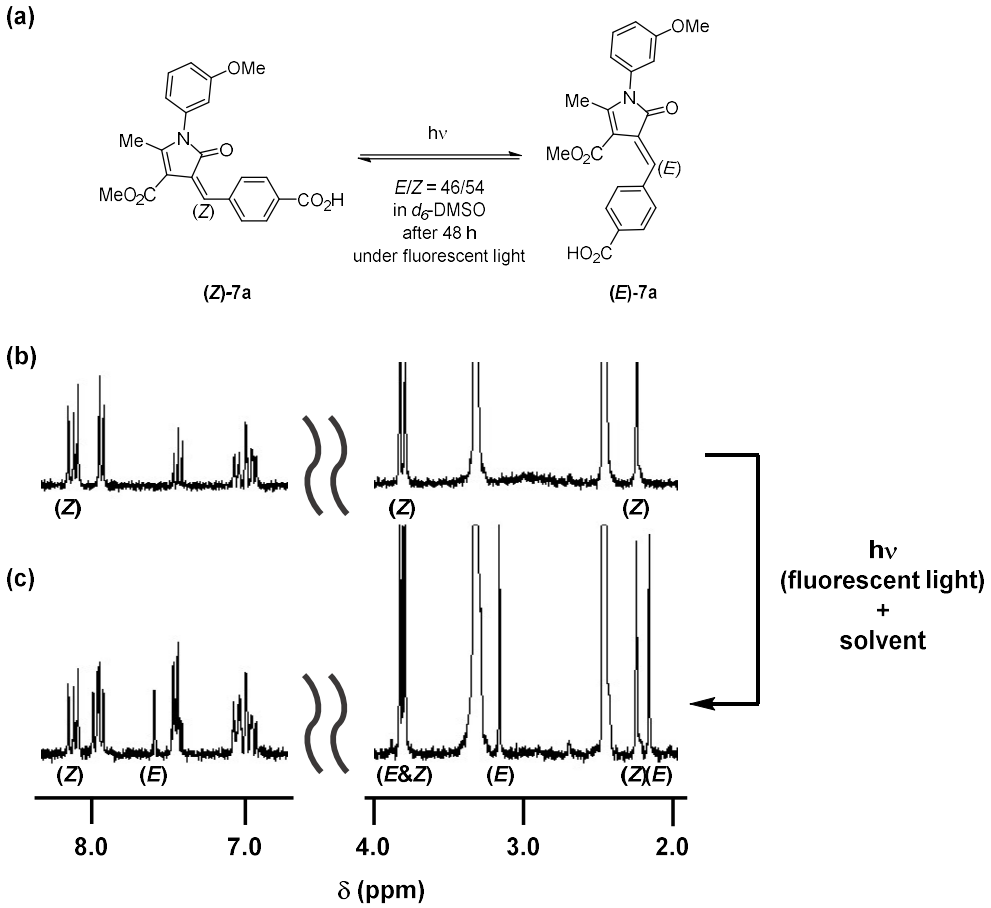

Figure 2-3. (a) The reversible photoisomerization of the exo-olefin part of **7a**. (b, c) The ^{1}H NMR analysis (300 MHz, TMS) for the photoisomerization of **(*Z*)-7a** (14 mM in d_6-DMSO) (b) before and (c) after keeping the solution under a fluorescent light for 48 h (*E*/*Z* = 46/54).

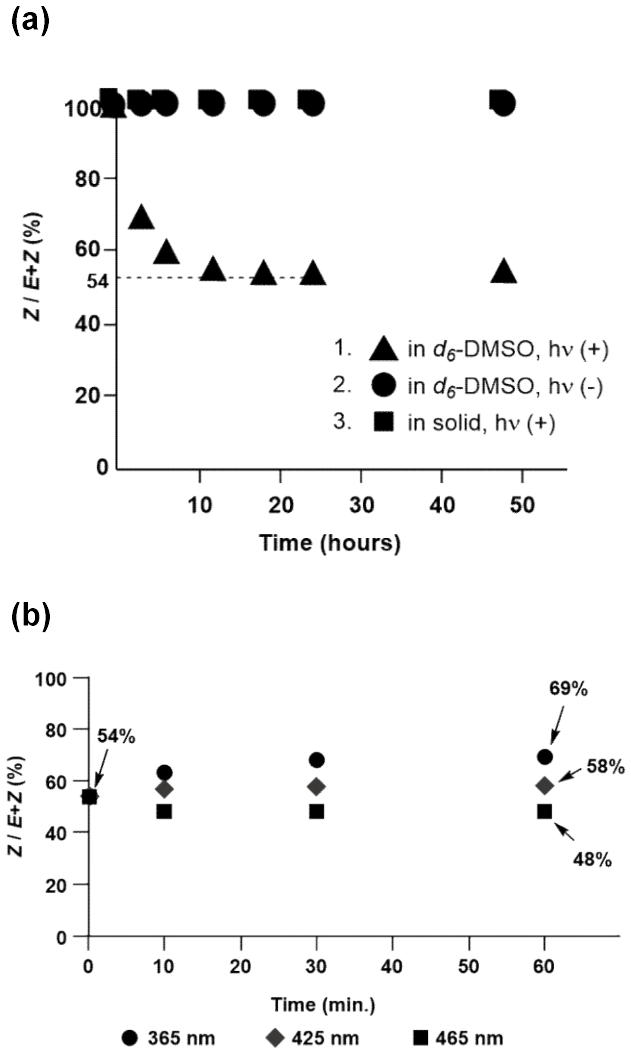

Figure 2-4. (a) Time-course changes in the *E*/*Z* ratio (*Z*/*E*+*Z*) of **7a** (14 mM in *d6*-DMSO). In d_6-DMSO under a fluorescent light (closed triangle), in *d6*-DMSO in the dark (closed circle), and in solid under a fluorescent light (closed sphere). (b) The changes in the *E*/*Z* ratio of **7a** irradiated with LED light with specific wavelengths. The solution of **7a** (14 mM in *d6*-DMSO) in a quartz NMR tube was irradiated with the light at given wavelengths and the *E*/*Z* ratio of **7a** was determined on ^{1}H NMR spectra after photoisomerization at 365 (closed sphere), 425 (closed diamond) and 465 (closed square) nm, respectively.

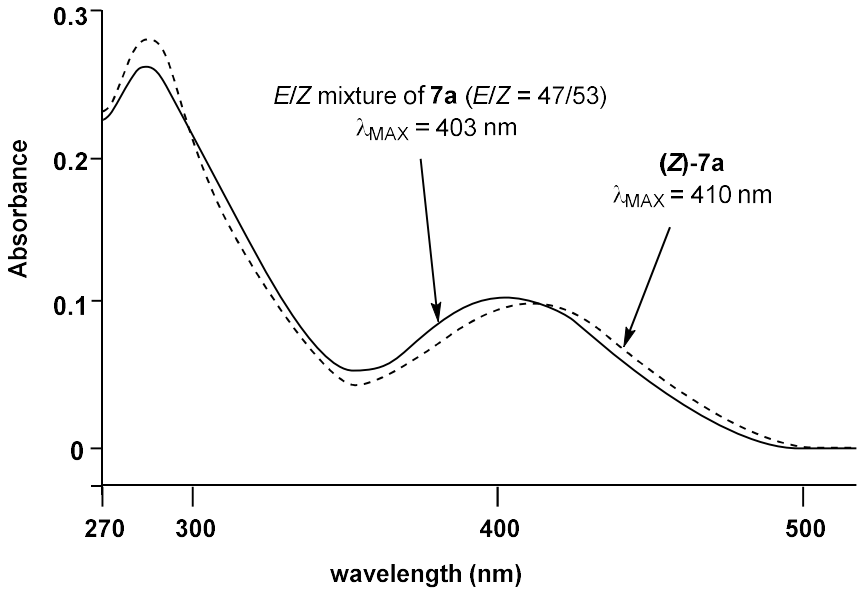

Figure 2-5. UV/vis absorption spectra of an E/Z mixture of **7a** (*E*/*Z* = 46/54) (plain curve) and **(*Z*)-7a** (dashed curve). [Compound] = 10 μM in DMSO at 37°C.

The scheme for the synthesis of **(*Z*)-7b-7j** is described in Scheme 2-3. The intermediates **8b-8e** and **8i-8j** were synthesized from **9** and the aniline derivatives **13-19**. **8g-8h** were obtained from **8f** and *i*-PrOH and *n*-hexanol, respectively, by Mitsunobu reaction using 1,1'-(azodicarbonyl)dipiperidine (ADDP) and triphenylphosphine (PPh_3). The successive condensation of **8b-8j** and **11** afforded **7b-7j**, from which **(*Z*)-7b-7j** could be isolated by recrystallization from appropriate solvent systems. The stereochemistry of each derivative was characterized as the *Z* form by analogy to **(*Z*)-7a**.

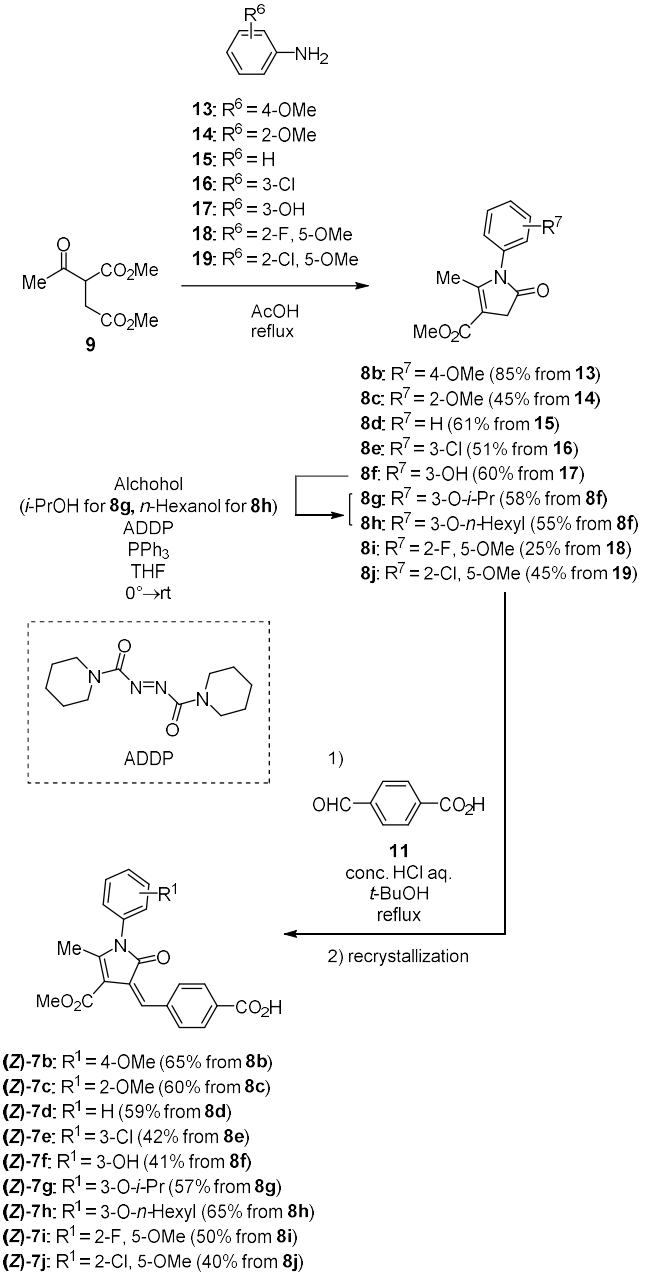

Scheme 2-3. Synthesis of **(*Z*)-7b-7j**.

The synthesis of **(*Z*)-7k-7w** is described in Scheme 2-4. Knoevenagel condensation reactions of **8a** with the benzaldehyde derivatives **20**-**21**, **23**-**33** afforded **(*Z*)-7k-7w**, while only **7l** was obtained as an inseparable mixture. The ^{1}H NMR and mass spectra of a mixture of **7l** suggested that the mixture contains the diastereomeric lactone form **22** (data are not shown).

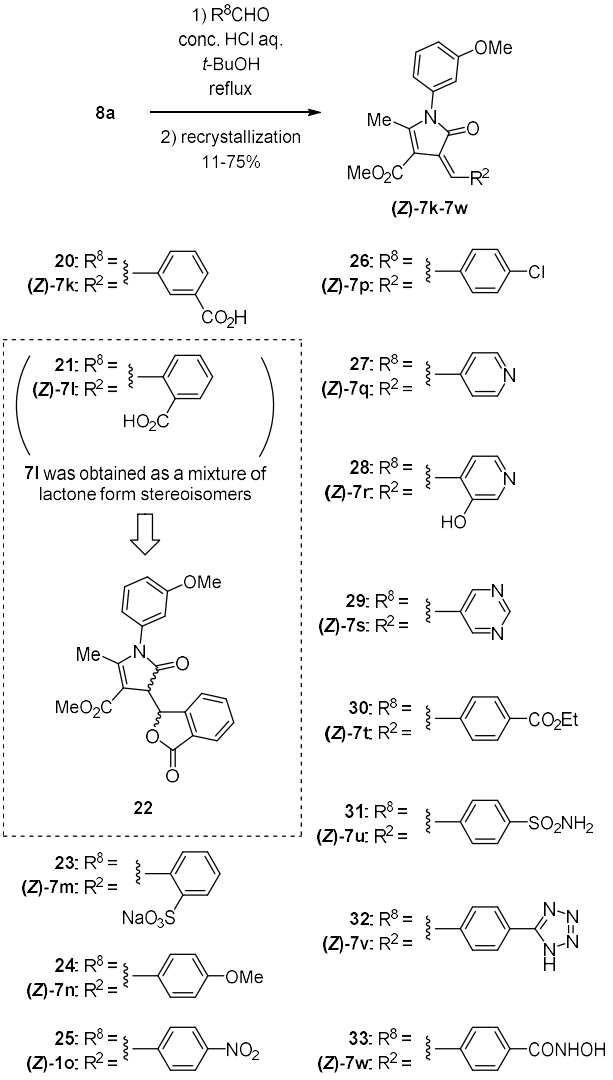

Scheme 2-4. Synthesis of **(*Z*)-7k-7w**.

The synthesis of **(*Z*)-7x-7z** was started from acetoacetic acid esters **34** and **35** (Scheme 2-5). In these reactions, **34** and **35** were reacted with ethyl bromoacetate to furnish **36** and **37**. Deprotection of the *tert*-butyl group of **37** gave **38** and condensation of this derivative with *n*-hexanol provided **39**. Due to the instability of **38**, the synthesis of **39** was performed immediately after the workup of **38**. The synthesized 2-acetylsuccinate derivatives **36**, **37** and **39** were reacted with **10** to afford **8k-8m** and a successive condensation produced **(*Z*)-7x-7z**.

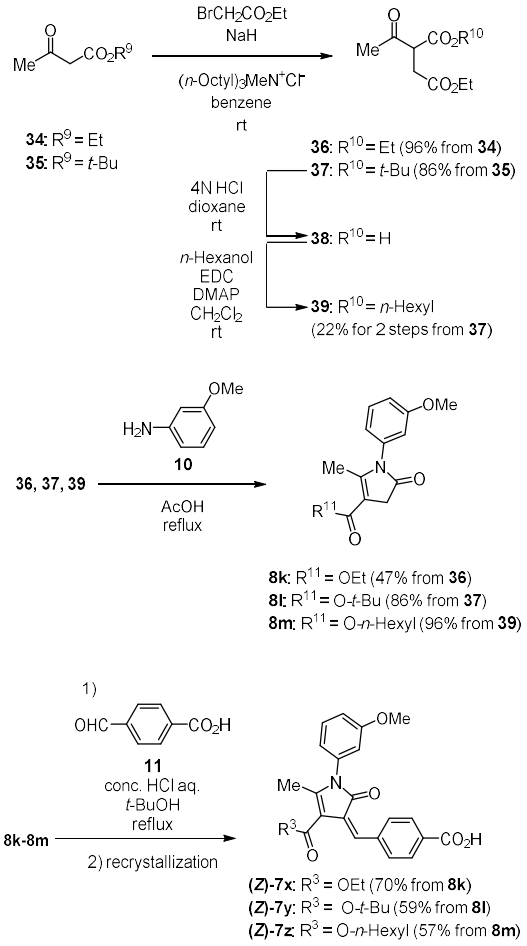

Scheme 2-5. Synthesis of **(*Z*)-7x-7z**.

The synthesis of **7aa** and **7ab** starting from **9** is shown in Scheme 2-6. We examined several conditions for the aminolysis of **9** with dimethylamine (**40**) to give **42** and it was found that the ester group of **9** is relatively unreactive with the amine, even at 120˚C. We therefore conducted the aminolysis reaction of **9** and **40** under the microwave (MW)-irradiation with **42** being produced as the major product, resulting from selective aminolysis reaction at *β*-keto ester in **9**. This selectivity is probably due to the generation of a ketene species with the removal of MeOH from the *β*-keto ester by MW irradiation.[17] Since the aminolysis with the primary amine produced a complex mixture under conditions of MW irradiation, the synthesis of **44** was accomplished via **43**. The reaction of **9** with *N*-(*p*-methoxybenzyl)-*N*-methylamine (**41**) afforded **43**, in which the PMB group was oxidatively cleaved with ammonium cerium(IV) nitrate (CAN) to give the desired **44** in moderate yield. The synthesized 2-acetyl succinate derivatives **42** and **44** were reacted with **10** to afford **8n** and **8o**, respectively. Although the aminolysis reaction of **8a** was attempted, the reaction negligibly proceeded. The condensation of **8n** and **8o** with **11** gave *E*/*Z* mixtures of **7aa** and **7ab**. We attempted to separate **(*Z*)-7aa** and **(*Z*)-7ab** by recrystallization, but only **(*E*)-7aa** was isolated as a single isomer, whose structure was determined by an X-ray crystal structure analysis (Figure 2-6). Because the isolation of **(*Z*)-7aa** was not successful, **(*E*)-7aa** was used for the biological assay, as described

below. In the case of ester-type derivatives for R^3 and R^4 such as **(*E*/*Z*)-7a**, the *E*/*Z* ratio after silica gel column chromatography was 20/80 to 25/75 (Table 2-2). On the other hand, in the case of amide-type derivatives such as **(*E*/*Z*)-1aa** and **(*E*/*Z*)-1ab**, the *E*/*Z* ratio was 86/14 and 78/22 and it was found that the *E*/*Z* ratios had changed to 24/76 and 10/90 as the result of photoirradiation at 365 nm as described in Scheme 2-6. We attempted to recrystallize the *E*/*Z* mixture after the photoisomerization, but only **(*Z*)-1ab** was obtained as a single isomer.

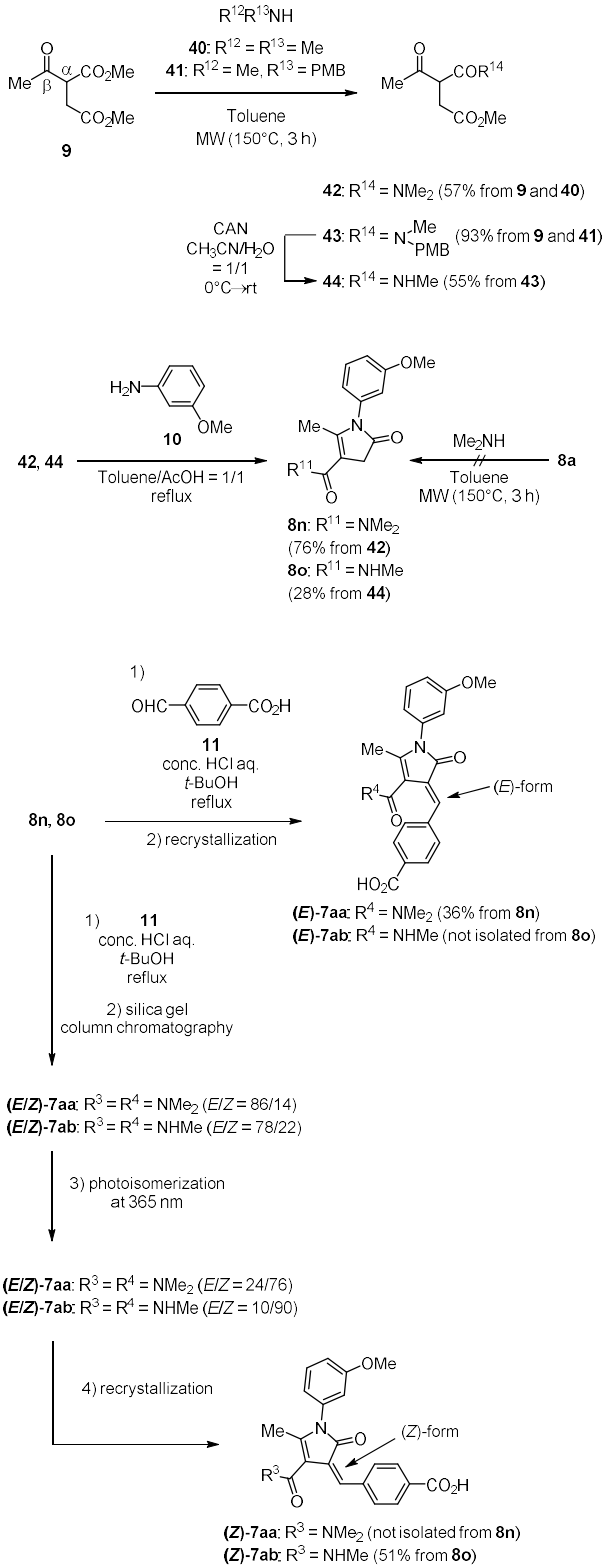

Scheme 2-6. Synthesis of **7aa-7ab**.

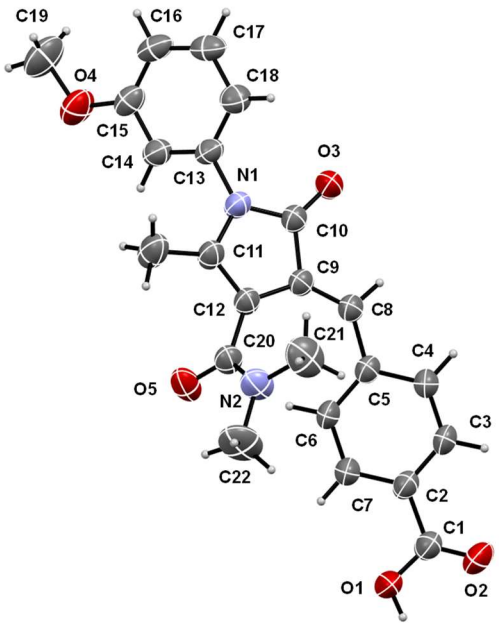

Figure 2-6. ORTEP drawing of the X-ray crystal structure of **(*E*)-7aa** (with 50% probability of ellipsoids) obtained by recrystallization from AcOEt. Each sphere represents an individual atom (gray color: carbon atom; white color: hydrogen atom; blue color: nitrogen atom; red color: oxygen atom).

[2-2-2] Evaluation of radioprotective activity and cytotoxicity

The radioprotective activity and cytotoxicity of **7a** and the derivatives synthesized above were evaluated by dye exclusion assay using a leukemia cell line, MOLT-4 cells as a model of normal cells. The reason for using MOLT-4 cells is that p53 protein in MOLT-4 cells is normally activated and induces apoptosis upon γ-ray irradiation, as described in the Introduction. MOLT-4 cells were incubated in a 96 well plate for 24 h, treated with the synthesized compounds for 1 h, and then subjected to γ-ray irradiation (10 Gy). After

further incubation for 27 h, the dead cells were stained with Erythrosin B, and the number of red-colored cells was counted with a hemocytometer. The cell viability was calculated from the numbers of alive and dead cells. Considering the photoisomerization property of **7a** derivatives, the experiments were conducted in the dark in cell culture containers that were completely covered with aluminum foil.

The SAR results are summarized in Figures 2-7, 2-8 and 2-9. Cell viability without γ-ray irradiation is depicted as black circles and the decrease with increasing concentrations of the compounds is regarded as an index of cytotoxicity. The open circles depict cell viability as a function of γ-ray (10 Gy) irradiation and an increase with increasing concentrations of the drugs serves as an index of their radioprotective activity.

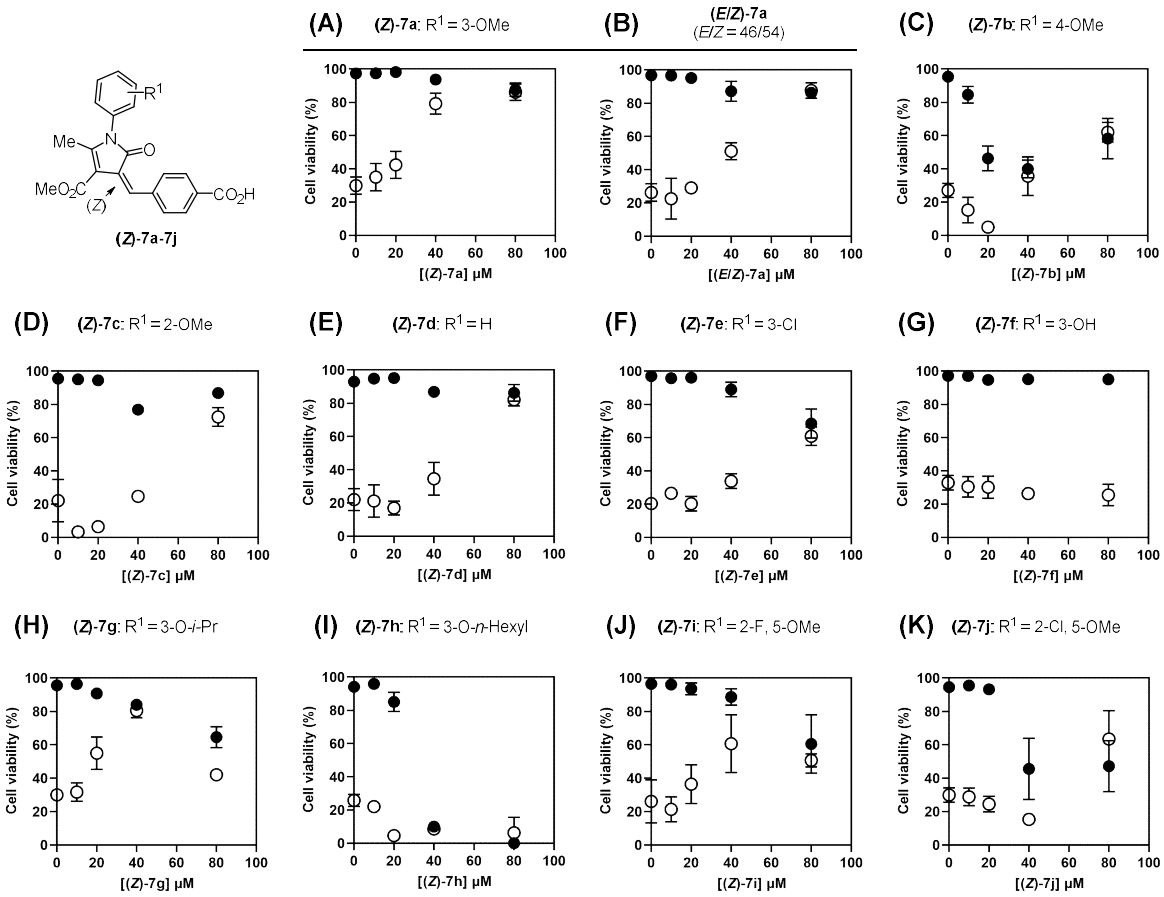

Figure 2-7. SAR study on the R^1 units. Cell viability of MOLT-4 cells treated with **7a-7j** upon γ-ray (10 Gy) irradiation or without irradiation. Black circle (●) depicts the cell viability of MOLT-4 cells without irradiation and open circle (○) depicts the cell viability of MOLT-4 cells with 10 Gy-irradiation.

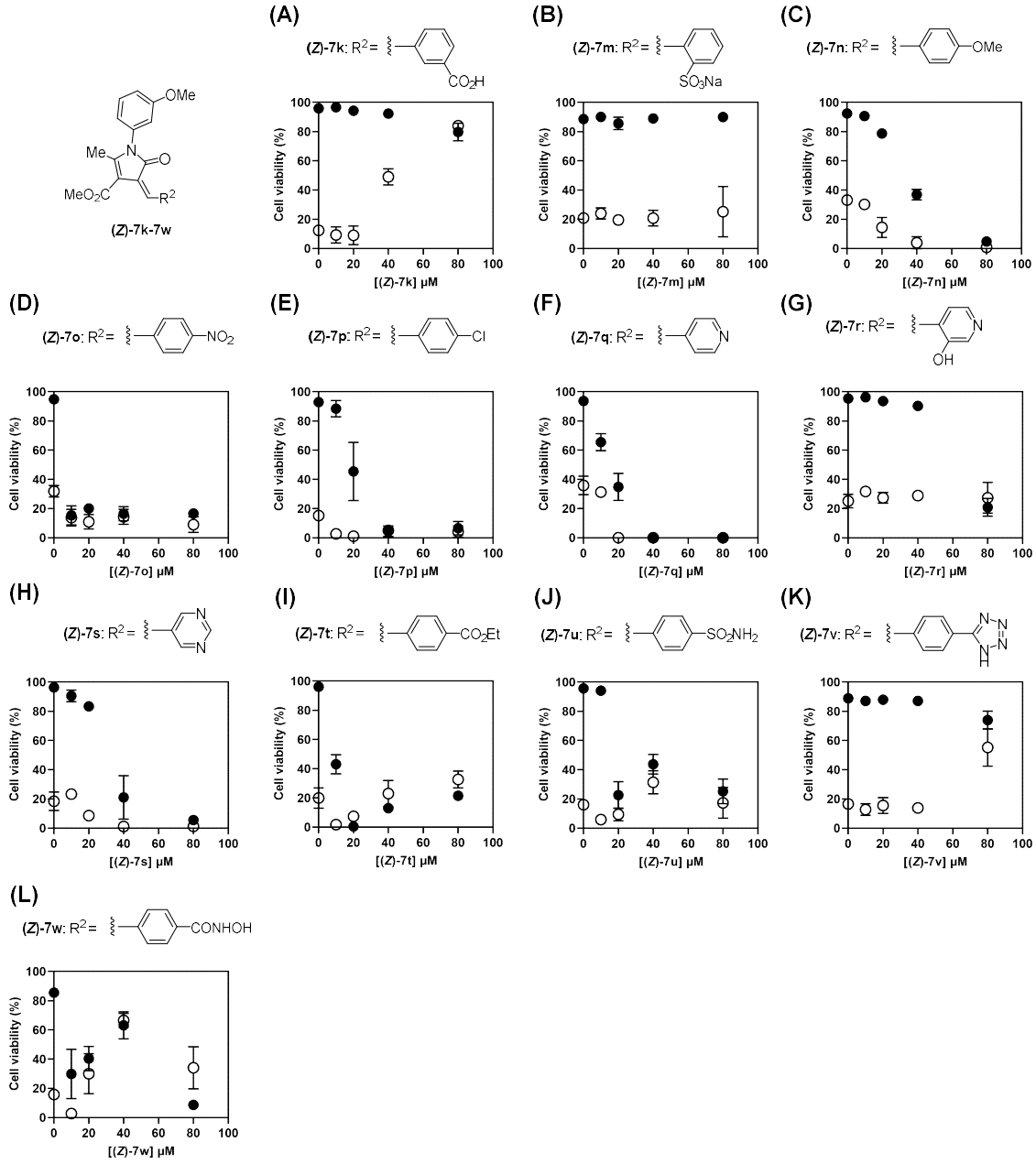

Figure 2-8. SAR study on the R^2 units. Cell viability of MOLT-4 cells treated with **7k-7w** upon γ-ray (10 Gy) irradiation or without irradiation. Black circle (●) depicts the cell viability of MOLT-4 cells without irradiation and open circle (○) depicts the cell viability of MOLT-4 cells with 10 Gy-irradiation.

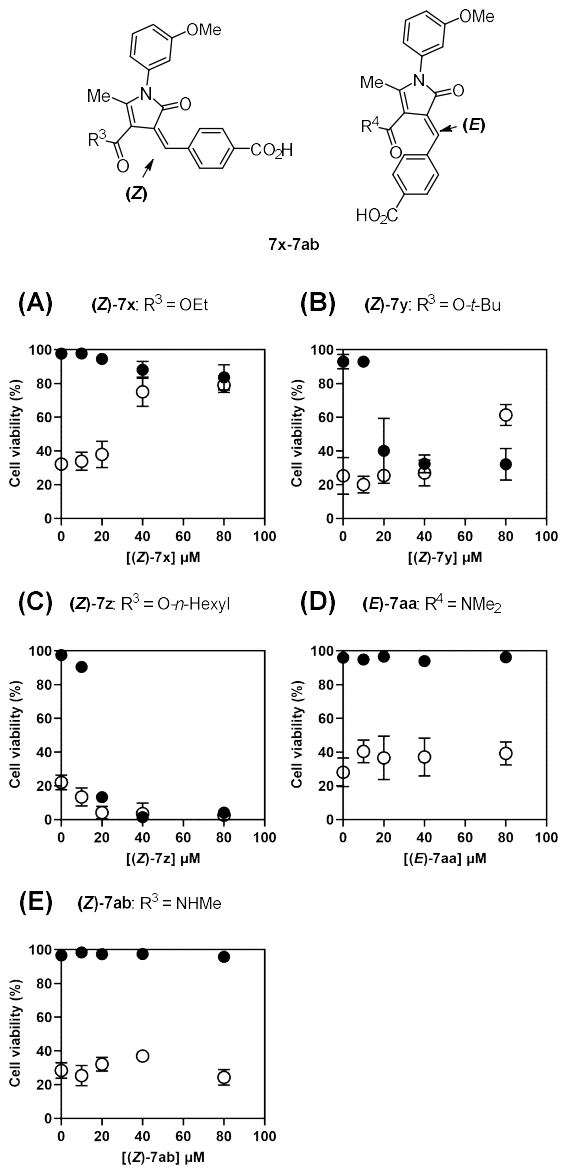

Figure 2-9. SAR study on the R^3 and R^4 units. Cell viability of MOLT-4 cells treated with **7x-7ab** upon γ-ray (10 Gy) irradiation or without irradiation. Black circle (●) depicts the cell viability of MOLT-4 cells without irradiation and open circle (○) depicts the cell viability of MOLT-4 cells with 10 Gy-irradiation.

The results shown in Figures 2-7, 2-8 and 2-9 are summarized below.

1. The radioprotective activity of **(*Z*)-7a** was observed at lower concentrations than that of a mixture of **(*E*)-7a** and **(*Z*)-7a** (*E*/*Z* = 46/54), suggesting that **(*Z*)-7a** exerts a more potent radioprotective activity than that of **(*E*)-7a** (Figure 2-7A-B).
2. The radioprotective activity of **(*Z*)-7a** (Figure 2-7A) is higher than those of **(*Z*)-7b** and **(*Z*)-7c** that have the methoxy group (R^1) at 4- and 2-positions, respectively (Figure 2-7C-D) and that of **(*Z*)-7d** that has no methoxy group (Figure 2-7E).
3. A hydrophilic R^1 group is unpreferable for radioprotective activity (Figure 2-7G), while more hydrophobic groups such as *n*-hexyl group raise cytotoxicity (Figure 2-7I). The **(*Z*)-7g** having an isopropoxy group at *m*eta-position of the phenyl group showed stronger radioprotective activity than **(*Z*)-7a** at 20 μM, although its toxicity was higher than **(*Z*)-7a** at 80 μM (Figure 2-7H).
4. As described in Figure 2-7A and 2-8A, the position of substituents on R^2 were fixed at the *para*-position because *para*-isomer **(*Z*)-7a** had more potent radioprotective activity than the corresponding *meta*-isomer **(*Z*)-7k**. **(*Z*)-7m** with hydrophilic sulfonate (SO_3Na) shows negligible radioprotective activity and toxicity (Figure 2-8B).
5. The findings shown in Figure 2-8 suggest that the substitution of a carboxylic acid (-

CO_2H) group for other functional groups in R^2 site weakens the radioprotective activity and enhances cytotoxicity (Figure 2-8C-I).

6. It is known that functional groups such as sulfonamide ($-SO_2NH_2$), 1*H*-tetrazole, hydroxamic acid (-CONHOH) are functional groups that are biologically similar (bioisosteres) to carboxylic acid.[18] As shown in Figure 2-8J-L, the sulfonamide derivative **(*Z*)-7u** showed higher toxicity than **(*Z*)-7a**. On the other hand, the tetrazole derivative **(*Z*)-7v** showed radioprotective activity, albeit it was somewhat weaker than that of **(*Z*)-7a**. The hydroxamic acid derivative **(*Z*)-7w** showed improved cell viability at 40 μM even in unirradiated groups although it showed cytotoxicity at low concentrations (10-20 μM), suggesting that the suppression of cell death by **(*Z*)-7w** is effective not only for radioprotection but also for its toxicity.
7. The results shown in Figure 2-9 suggest that short alkyl esters such as methyl ester (Figure 2-7A) and ethyl ester (Figure 2-9A) improve radioprotective activity. The introduction of a bulky ester (Figure 2-9B) and a long chain alkyl ester (Figure 2-9C) on R^3 increases toxicity. On the other hand, the loss of radioprotective activity was observed in amide analogs, **(*E*)-7aa** and **(*Z*)-7ab** (Figure 2-9D-E).
8. The results shown in Figures 2-7 to 2-9 indicate that the 2-pyrrolone derivatives having basic or neutral units in R^2 sites (Scheme 2-2) exhibit relatively high toxicity.

The ClogP values of **7a-7ab** were calculated by means of PC software "Chemdraw 20.1.1" as summarized in Table 2-3 to examine the relationship of their hydrophobicity (hydrophilicity) with their biological properties (the ClogP values of the compounds containing acidic CO_2H, SO_3H and tetrazole units were calculated as their corresponding anionic forms). It was suggested that the toxicity of more hydrophobic compounds, whose ClogP values are greater than 2, is relatively high. It was also found that the highly hydrophilic compounds, whose ClogP values are less than zero, exhibit weak radioprotective activity.

	E orZ	R^1	R^2	R^3 or R^4	toxicity at 80 μM	radioprotective activity at 80 μM	ClogP	pKa
7f	Z	3-OH	4-$PhCO_2^-$ (anionic form)	OMe	low	low	-0.550	8.08, 4.10
7ab	Z	3-OMe	4-$PhCO_2^-$ (anionic form)	NHMe	low	low	-0.321	4.10
7aa	E	3-OMe	4-$PhCO_2^-$ (anionic form)	NMe_2	low	low	-0.0290	4.10
7a	Z	3-OMe	4-$PhCO_2^-$ (anionic form)	OMe	low	high	0.0358	4.10
7b	Z	4-OMe	4-$PhCO_2^-$ (anionic form)	OMe	medium	meduim	0.0358	4.10
7c	Z	2-OMe	4-$PhCO_2^-$ (anionic form)	OMe	low	medium	0.0358	4.10
7k	Z	3-OMe	3-$PhCO_2^-$ (anionic form)	OMe	low	high	0.0358	3.60
7d	Z	H	4-$PhCO_2^-$ (anionic form)	OMe	low	high	0.117	4.10
7i	Z	2-F, 5-OMe	4-$PhCO_2^-$ (anionic form)	OMe	medium	medium	0.149	4.10
7j	Z	2-Cl, 5-OMe	4-$PhCO_2^-$ (anionic form)	OMe	medium	medium	0.489	4.10
7x	Z	3-OMe	4-$PhCO_2^-$ (anionic form)	OEt	low	high	0.565	4.10
7e	Z	3-Cl	4-$PhCO_2^-$ (anionic form)	OMe	medium	medium	0.830	4.10
7g	Z	3-O-*i*Pr	4-$PhCO_2^-$ (anionic form)	OMe	medium	low	0.874	4.10
7y	Z	3-OMe	4-$PhCO_2^-$ (anionic form)	O-*t*-Bu	medium	medium	1.27	4.10
7m	Z	3-OMe	2-$PhSO_3H$	OMe	low	low	1.51	not calculated
7s	Z	3-OMe	5-pyrimidinyl	OMe	high	low	1.84	not calculated
7w	Z	3-OMe	4-PhCONHOH	OMe	high	low	2.41	not calculated
7u	Z	3-OMe	4-$PhSO_2NH_2$	OMe	medium	low	2.46	not calculated
7h	Z	3-O-*n*-Hex	4-$PhCO_2^-$ (anionic form)	OMe	high	low	2.68	4.10
7z	Z	3-OMe	4-$PhCO_2^-$ (anionic form)	O-*n*-Hex	high	low	2.68	4.10
7q	Z	3-OMe	4-pyridinyl	OMe	high	low	2.80	not calculated
7r	Z	3-OMe	3-OH-4-pyridinyl	OMe	high	low	3.08	not calculated
7v	Z	3-OMe	4-Ph-(1H-5-tetrazoyl)	OMe	low	medium	3.79	not calculated
7o	Z	3-OMe	4-NO_2	OMe	high	low	4.04	not calculated
7n	Z	3-OMe	4-OMe	OMe	high	low	4.21	not calculated
7t	Z	3-OMe	4-$PhCO_2Et$	OMe	high	low	4.80	not calculated
7p	Z	3-OMe	4-Cl	OMe	high	low	5.01	not calculated

Table 2-3. The ClogP values of **7a-7ab** listed in ascending order of ClogP values (calculated on PC software "Chemdraw 20.1.1"). The ClogP values of the compounds containing acidic CO_2H, SO_3H and tetrazole units were calculated as their corresponding anionic forms (the pKa values for these acidic moieties were also calculated on "Chemdraw 20.1.1"). Note that the ClogP values of neutral forms and anionic forms of **7v** are almost same (3.79 and 3.80). Low toxic compounds (cell viability >80% at 80μM) are shown in blue, moderately toxic compounds (cell viability between 50% and 80% at 80μM) are shown in green, and highly toxic compounds (cell viability 80% at 80μM) are shown in blue, moderately radioprotective compounds (cell viability between 50% and 80% at 80μM) are shown in green, and negligibly radioprotective compounds (cell viability <50% at 80 μM) are shown in red.

[2-2-3] Evaluation of p53-suppressing activity

It was previously reported that negligible radioprotective activity was observed for STK160830 in several p53-mutated cells, suggesting that the radioprotective activity of STK160830 is dependent on p53.[10] For an evaluation of the effect of the synthesized compounds on p53 expression, we conducted Western blot analyses using MOLT-4 cells. Among the **(*Z*)-7a-7ab** derivatives, we selected 5 compounds including **(*Z*)-7a, (*Z*)-7g** and **(*Z*)-7v** that exhibited high radioprotective activity and **(*Z*)-7f** and **(*Z*)-7ab**, whose radioprotective activity was low at 50-100 μM concentrations.

The effects of these compounds on p53 expression are shown in Figure 2-10. In the IR-unirradiated group, the expression level of p53 was low and was increased 6 h after IR-irradiation. The p53 expression level of radioprotective compounds **(*Z*)-(7a, 7g, 7v)** are shown in Figures 2-10A, C and D. These results show that the p53 expression level is decreased in the cells treated by **(*Z*)-7a, (*Z*)-7g** and **(*Z*)-7v** at radioprotective concentrations. On the other hand, **(*Z*)-7f** and **(*Z*)-7ab**, whose radioprotective activity is low, exhibited negligible p53-suppressing activity (Figure 2-10B, E). These results support our previous data that the radioprotective activity of 2-pyrrolone derivatives is dependent on the suppression of p53.

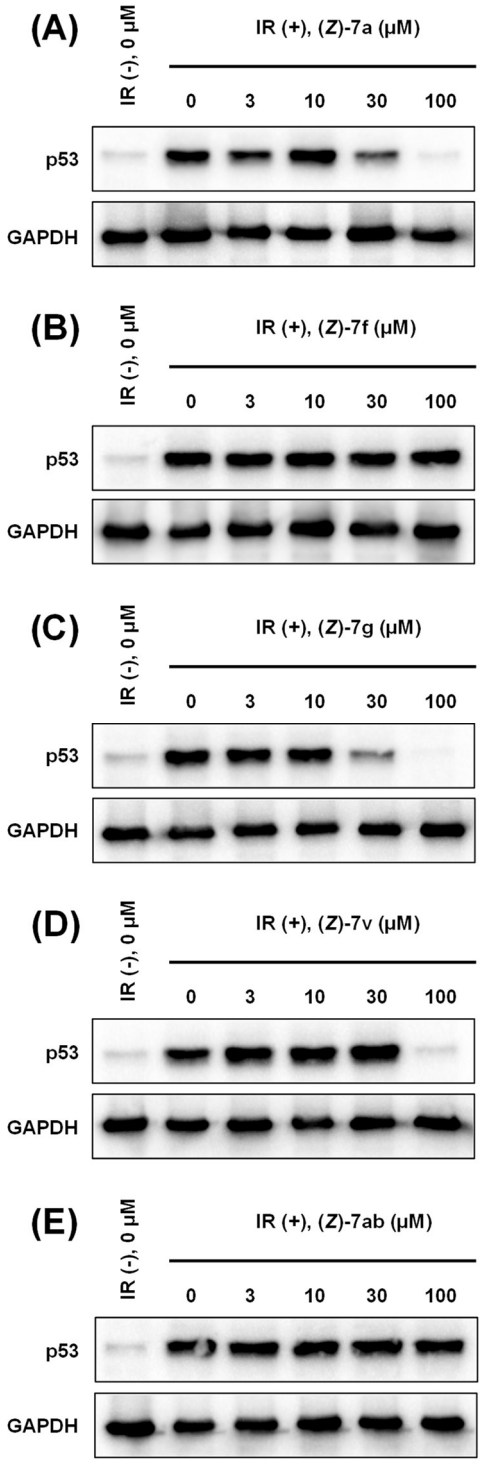

Figure 2-10. The effect of (A) **(*Z*)-7a**, (B) **(*Z*)-7f**, (C) **(*Z*)-7g**, (D) **(*Z*)-7v**, (E) **(*Z*)-7ab** on the expression level of p53 in MOLT-4 cells analyzed by Western blot analysis.

[2-3] Conclusion

In this manuscript, we report on the design, synthesis and biological evaluation of a new radioprotective agent, **7a** (STK160830), that was identified from a chemical library of the Drug Discovery Initiative at the University of Tokyo. The results of SAR study indicate that the following points are important for radioprotective activity: (i) **(*Z*)-7a** is more radioprotective than **(*E*)-7a**, (ii) there is an appropriate hydrophobicity for R^1 to achieve the activity, (iii) a carboxylic acid (-CO_2H) and its bioisosteres are required on R^2 and (iv) short alkyl esters such as methyl ester and ethyl ester are preferred on R^3. The results of Western blot analyses suggest that the radioprotective activity of 2-pyrrolone derivatives has a fairly well relationship with the suppression of p53.

We conclude that the information presented in this report will be helpful for developing and understanding the function of p53 in cellular responses to radiation and for further molecular design of 2-pyrrolone derivatives for use as radioprotectors. The identification of the target biomolecules of these 2-pyrrolone-type radioprotectors and detailed mechanistic studies are currently underway.

Chapter 3.

A Novel RNA Synthesis Inhibitor, STK160830, Has Negligible DNA-Intercalating Activity for Triggering A p53 Response, and Can Inhibit p53-Dependent Apoptosis

（新規 RNA 合成阻害剤 STK160830 は p53 応答を誘発する DNA インターカレート活性を有さず、p53 依存性アポトーシスを抑制する）

[3-1] Introduction

Many biological responses are controlled by up- or down-regulation of genes and gene products through transcription, translation, and post-translational modifications. RNA synthesis inhibitors and protein synthesis inhibitors are useful for investigating whether biological phenomena with unknown mechanisms require transcription or protein synthesis. There are two modes of inhibition of mRNA synthesis by mRNA synthesis inhibitors: direct or indirect inhibition of RNA polymerase II, both of which are known to induce a p53 response. Although the details of the mechanism of induction of the p53 response are unknown, it is thought to be a checkpoint mechanism to prevent the disruption of cellular homeostasis caused by insufficient mRNA synthesis.[19]

Typical RNA synthesis inhibitors have been reported to have the activity to induce the p53 response.[20,21] Actinomycin D (Act. D) is known to cause inhibition of RNA synthesis by its intercalating activity that enters between base pairs of DNA. In response to DNA intercalation by Act. D, cells exhibit a DNA damage response.[22] This activity has also been reported to inhibit DNA topoisomerase I and II, which together with inhibition of RNA synthesis causes a p53-mediated damage response.[23,24] 5,6-dichloro-1-β-D-ribofuranosylbenzimidazole (DRB), is a selective inhibitor of RNA polymerase II-mediated transcriptional elongation and inhibits mRNA synthesis in eukaryotic cells. Its

inhibitory activity is based on its ability to inhibit the kinase activity of P-TEFb[25-27], which phosphorylates the C-terminal domain of the largest subunit of RNA polymerase II, resulting in the induction of the p53 response.[20] Other RNA synthesis inhibitors, such as α-amanitin and H7, have also been reported to trigger the p53 response.[20,21]

The role played by RNA synthesis inhibitors and protein synthesis inhibitors in early studies of apoptosis was important. For example, these drugs have revealed that radiation-induced thymocyte apoptosis requires *de novo* RNA synthesis and protein synthesis.[28-29] After this discovery, it became clear that radiation cell death in thymocytes is p53-dependent, as thymocytes derived from p53 knockout mice were resistant to radiation-induced apoptosis.[30,31] These findings were clearly consistent with the requirement for RNA synthesis and protein synthesis as the mechanism by which p53 executes apoptosis as a transcriptional activator. However, as mentioned earlier, Act. D, a conventional RNA synthesis inhibitor used in these reports, has DNA-damaging effects due to its own DNA-intercalating activity, which alone induces apoptosis in thymocytes and T cell-derived cell lines.[32,33] Although transactivation by p53 should be required for the execution of DNA-damage-induced p53-induced apoptosis, even in Act. D-induced apoptosis, subsequent studies have revealed that p53 itself has an apoptogenic activity that allows it to translocate to mitochondria and induce apoptosis in a transcription-

independent manner.[21, 34-37] The fact that p53 can carry out apoptosis in the absence of transcriptional activation of p53-target genes made it difficult to verify the RNA synthesis requirement of the apoptotic cells under study. For example, we and others have reported that the human T-cell leukemia cell line MOLT-4, which is highly radiosensitive and exhibits p53-dependent radiation apoptosis[13], is not suppressed by radiation-induced apoptosis even in the presence of Act. D, concluding that the contribution of the p53 transcription-independent pathway is dominant in the irradiated cells.[38,39] However, if the induction of the cell death in the presence of Act. D was due not only to radiation but also to the DNA-damaging activity of Act. D, this conclusion had to be revised.

As described in Chapter 1 and Chapter 2, the screening of a library containing core 9600 compounds (Drug Discovery Initiative, The University of Tokyo)[40] using some cell viability assays was conducted and STK160830 was discovered as an anti-apoptotic compound. Besides, many STK160830 analogs were synthesized and their radioprotective activity and toxicity were evaluated. It was strongly suggested that STK160830 has the best properties among the synthesized compounds and it is a novel inhibitor for mRNA synthesis. In addition, unlike Act. D, this inhibitor has a characteristic activity that does not have DNA-intercalating activity and does not induce a p53-mediated damage response. At the same time, it became clear that the previous

conclusion that *de novo* RNA synthesis is not required for radiation cell death of MOLT-4 cells needs to be revised. This finding could not have been found without the RNA synthesis inhibitory activity of STK160830, which does not induce a harmful p53 response. These findings indicate that STK160830 is an effective inhibitor to validate the requirement for transcription.

[3-2] Results

[3-2-1] STK160830 suppresses DNA damage-induced apoptosis in a p53-dependent manner

The effect of STK160830 on mitochondrial membrane potential ($\Delta\psi_m$) in MOLT-4 cells was examined by MitoTracker staining. STK160830 significantly suppressed the loss of $\Delta\psi_m$ in irradiated MOLT-4 cells at 50-100 μM (Figure 3-1A), indicating that it acts upstream of the mitochondria or on the mitochondria themselves.

We then assumed p53 as one of the targets of action and tested the p53-specificity of STK160830 using four cell lines: MOLT-4 (wild-type p53), Nega (mock-transfectant), KD-1 (p53-knockdown cells), and R-p53-1 (p53-revertant) (Figure 3-1B). STK160830 showed significant cell death inhibition in radiation cell death of MOLT-4, Nega, and R-p53-1, in which p53 functions normally. However, no significant cell death inhibitory effect was observed in p53-knockdown cells, KD-1 (p = 0.15), indicating that the protective activity of this compound acts on p53. We also examined the inhibitory effect of STK160830 on DNA damage-induced apoptosis in murine thymocytes, as a typical cell type that exhibits p53-dependent apoptosis. As expected, STK160830 significantly inhibited etoposide- or radiation-induced apoptosis of the thymocytes at 50-100 μM (Figure 3-2A). We also examined the inhibitory effect of STK160830 on etoposide-

induced cell death of MOLT-4 cells and p53-mutated KU812, KY821, Ball-1, CCRF-CEM, and U937 cells by dye exclusion test (Figure 3-2B). STK160830 showed a significant inhibitory effect on etoposide-induced cell death in MOLT-4 cells, whereas it did not show the significant inhibit effect on etoposide-induced cell death in other cells, except for CCRF-CEM cells. These results suggest that the inhibitory effect of STK160830 on DNA damage-induced apoptosis requires p53 in many cases.

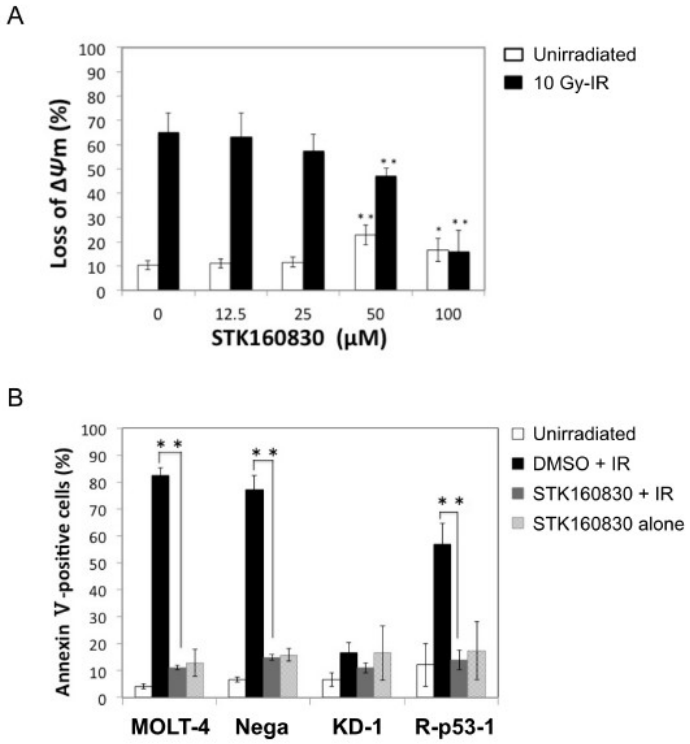

Figure 3-1. STK160830 inhibits p53-dependent mitochondrial-mediated apoptosis in irradiated MOLT4 cells. (A) The percentage of MOLT-4 cells losing Δψm was measured by MitoTracker staining 15 h after 10 Gy-IR. Means and SDs from six independent experiments are shown. (B) The effect of 100 μM STK160830 on parental MOLT-4 cells and various MOLT-4 transfectants 16 h after 10 Gy-IR. Means and SDs from four independent experiments are shown. *, $p < 0.05$; **, $p < 0.01$.

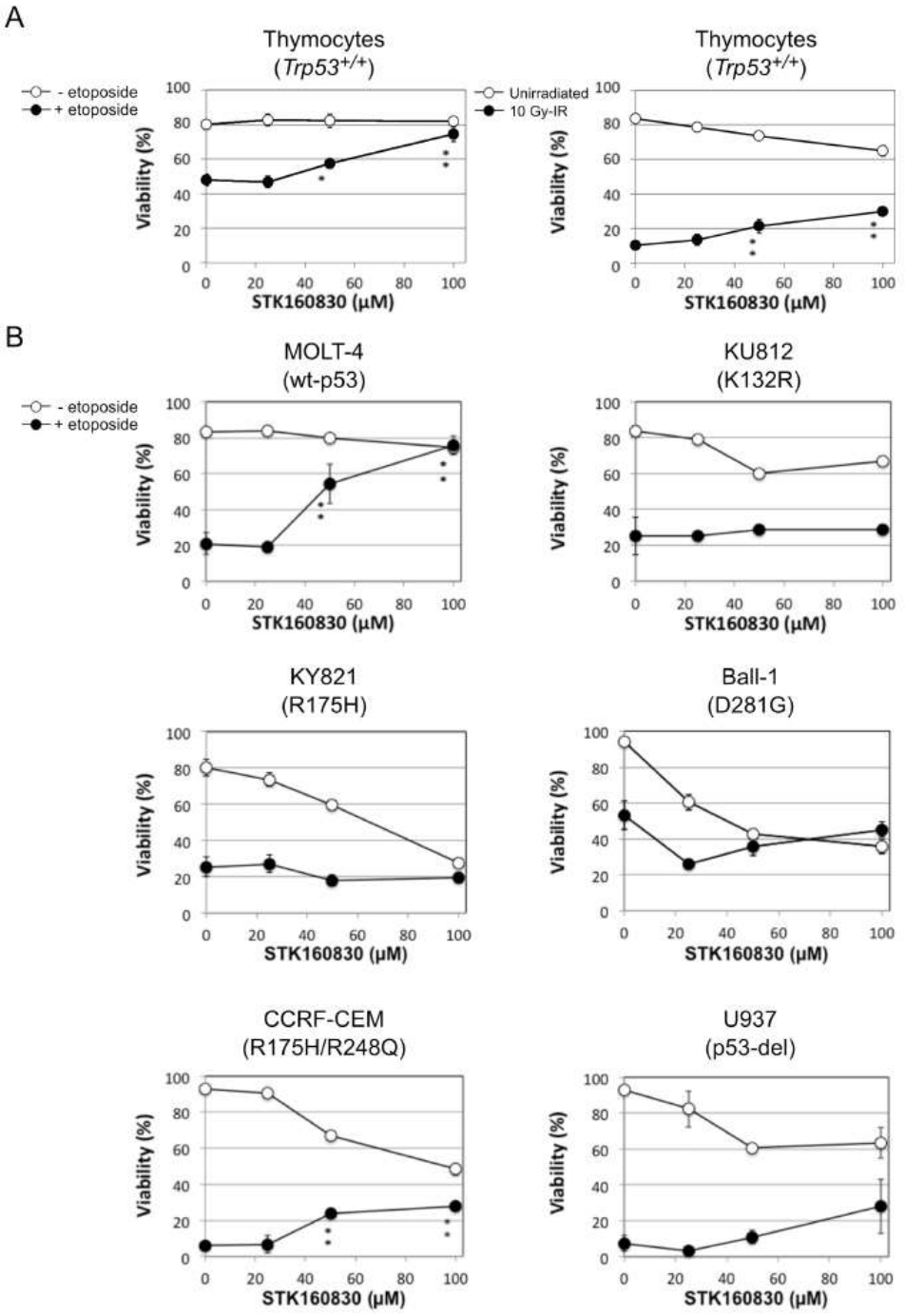

Figure 3-2. Examination of the p53 requirement for the protective effect of STK160830 on DNA damage-induced apoptosis in various cell types. (A) Effect of STK160830 on etoposide- or radiation-induced apoptosis in murine thymocytes. The viability was measured by dye-exclusion test 6 h after 1 μM etoposide-treatment or 8 h after 10 Gy-IR. (B) Effect of STK160830 on etoposide-induced cell death of MOLT-4 cells and p53-mutated KU812, KY821, CCRF-CEM, Ball-1, and U937 cells. The cell lines bearing point mutation(s) in p53 DNA-binding

domain are sorted by the amino acid number. MOLT-4, KU812, KY821, CCRF-CEM, Ball-1, and U937 cells were treated with 5 μM, 50 μM, 50 μM, 2.5 μM, 5 μM, and 5μM etoposide, respectively. The viability was measured by dye-exclusion test 18 h after 10 Gy-IR. Means and SDs from three independent experiments are shown. Asterisks denote statistically significant increases in viabilities of apoptosis-stimulated cells: *, $p < 0.05$; **, $p < 0.01$.

[3-2-2] Correlation between changes in intracellular protein expression and viability by STK160830

To examine the changes in protein expression in irradiated MOLT-4 cells by STK160830, immunoblotting of various proteins was performed (Figure 3-3A). The results showed that STK160830 suppressed protein expression of p53, p21 and PUMA, which are target gene products of p53, GAPDH and β-Actin, which are internal standards, and activated Caspase-3 and -7 (large subunit), which are indicators of apoptotic execution. p53DINP1, a p53 target gene, was exceptionally constitutively expressed and was poorly altered by STK160830.

We then examined the correlation between the protective effect of STK160830 on viability and protein expression (Figure 3-3B). p53, p21, PUMA, GAPDH, and β-Actin showed a high correlation with a coefficient of determination (R^2) of 0.9 or higher. The R^2 between the induction of large subunit of Caspase-3 and Caspase-7 and cell viability was moderate at approximately 0.7. The R^2 for p53DINP1 was exceptionally low, 0.073. Although the degree of repression varies among the proteins, these results suggest that the suppression of p53-dependent apoptosis by STK160830 is due to the repression of a wide range of gene expression.

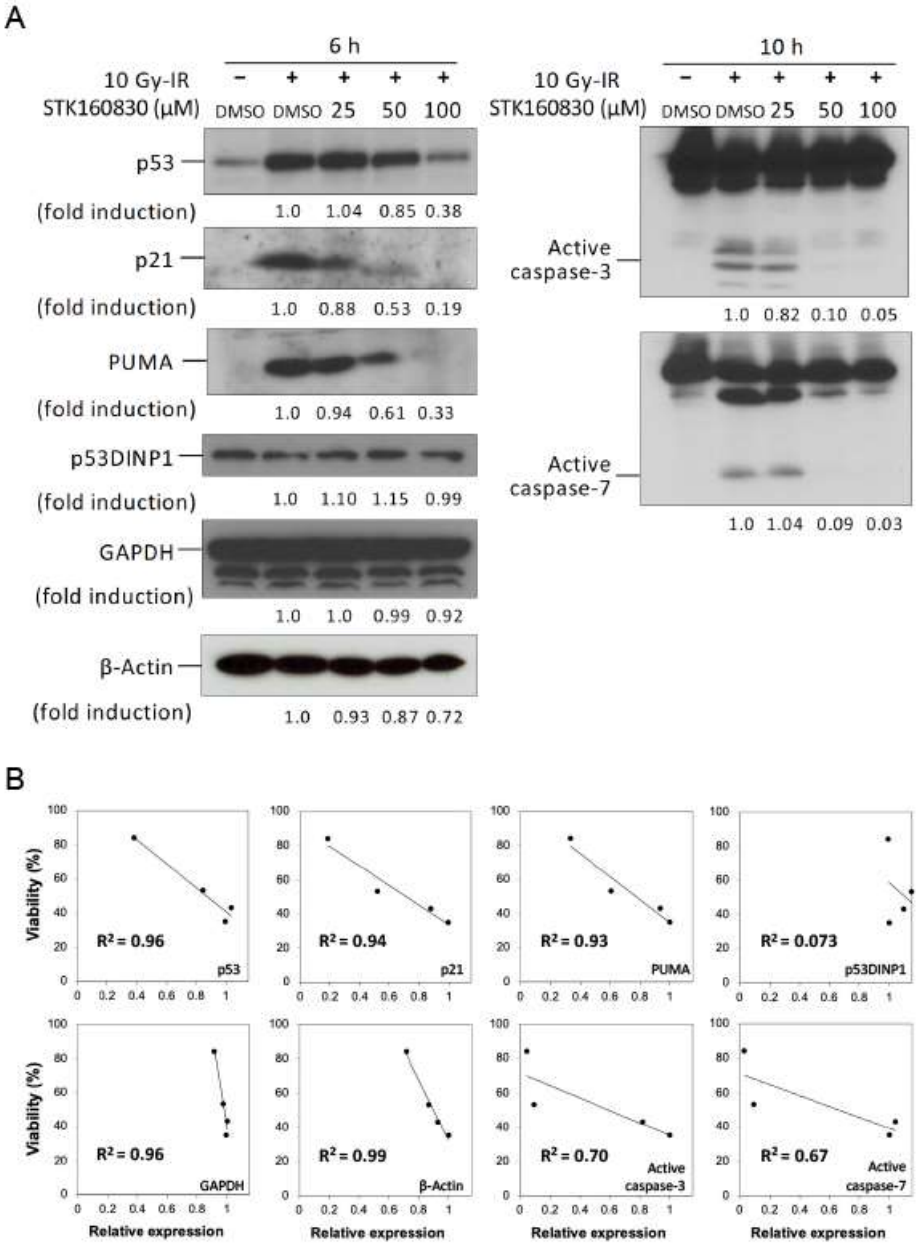

Figure 3-3. The suppressive effect of STK160830 on the MOLT-4 apoptosis was highly correlated with the suppression of various protein expression levels. (A) Dose–response of STK160830 on various protein expression levels. Cells were harvested 6 h after 10 Gy-IR, and the proteins were detected by immunoblotting. –, Unirradiated; +, 10 Gy-IR. (B) Linear regression analyses of the relationship between the irradiated MOLT-4 cell viability obtained from Figure 3-2A, and the relative expression levels of various proteins obtained from (A).

Considering that the decrease of p53 by STK160830 in irradiated MOLT-4 cells might be caused by the enhancement of p53 degradation, we also examined p53 degradation by immunoblotting of ubiquitinated high-molecular-weight p53 (Figure 3-4). The high-molecular-weight p53 was decreased in a concentration-dependent manner by STK160830, suggesting that the p53 degradation pathway was not activated.

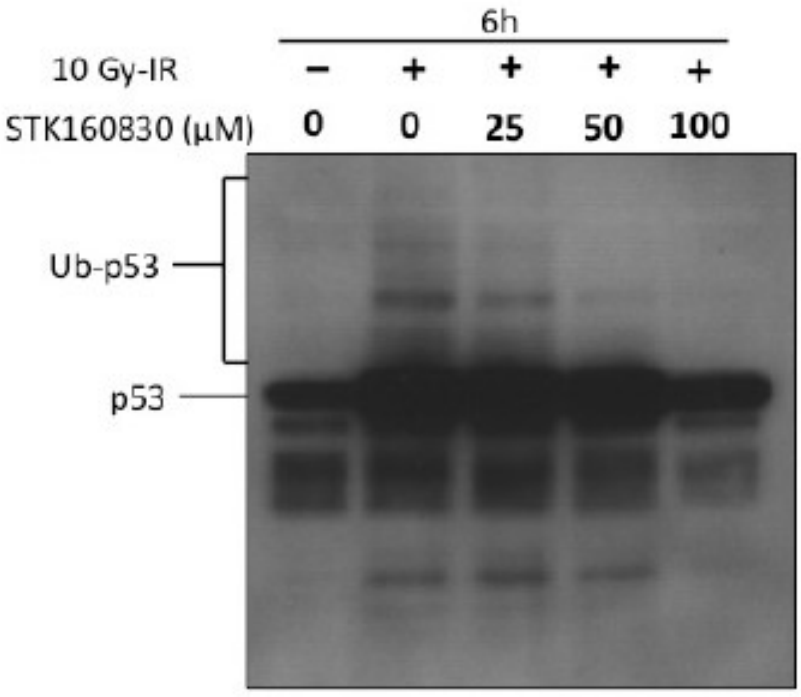

Figure 3-4. Effect of STK160830 on the amount of high-molecular-weight p53 in irradiated MOLT-4 cells. Cells were collected at 6 h after 10 Gy-IR, and the proteins were detected by immunoblotting. The film exposure time for ECL emission was longer than usual to detect high-molecular-weight p53.

[3-2-3] STK160830 is a novel mRNA synthesis inhibitor with a different spectrum of action from Act. D

Since the amount of protein expression depends on the stability of the protein, we examined whether the suppression of gene expression by STK160830 was due to the suppression of mRNA expression. Therefore, the change in mRNA levels in irradiated MOLT-4 cells by STK160830 was examined by qPCR absolute quantification using Act. D as a control compound (Figure 3-5A). In the analysis of constitutively expressed *TP53*, *ACTB*, and *GAPDH*, the three treatments (vehicle DMSO, Act. D, or STK160830) showed a similar decrease in mRNA expression after 10 Gy-IR. In the results for *CDKN1*A (encoding p21), *TP53INP1* (encoding p53DINP1), and *BBC3* (encoding PUMA, 3h post-IR), STK160830 suppressed mRNA expression more strongly than Act. D. In particular, 6 h after IR, Act. D inhibited mRNA expression of *CDKN1A* and *TP53INP1* by 72% and 36%, respectively, while STK160830 highly inhibited both mRNAs by 96%.

Figure 3-5B shows that the treatment dose of 100 μM STK160830 and 80 nM Act. D used in Figure 3-5A is sufficient to inhibit the mRNA expression of *CDKN1A*, while Act. D has a slightly weaker suppressive effect on the mRNA expression of *TP53INP1*. It should be added that tr280 nM Act. D, which is equivalent to 100 ng/mL Act. D, decreases

the viability of non-irradiated MOLT-4 cells by 30%, and increases the viability of 10 Gy-irradiated MOLT-4 cells by only 20%.[39]

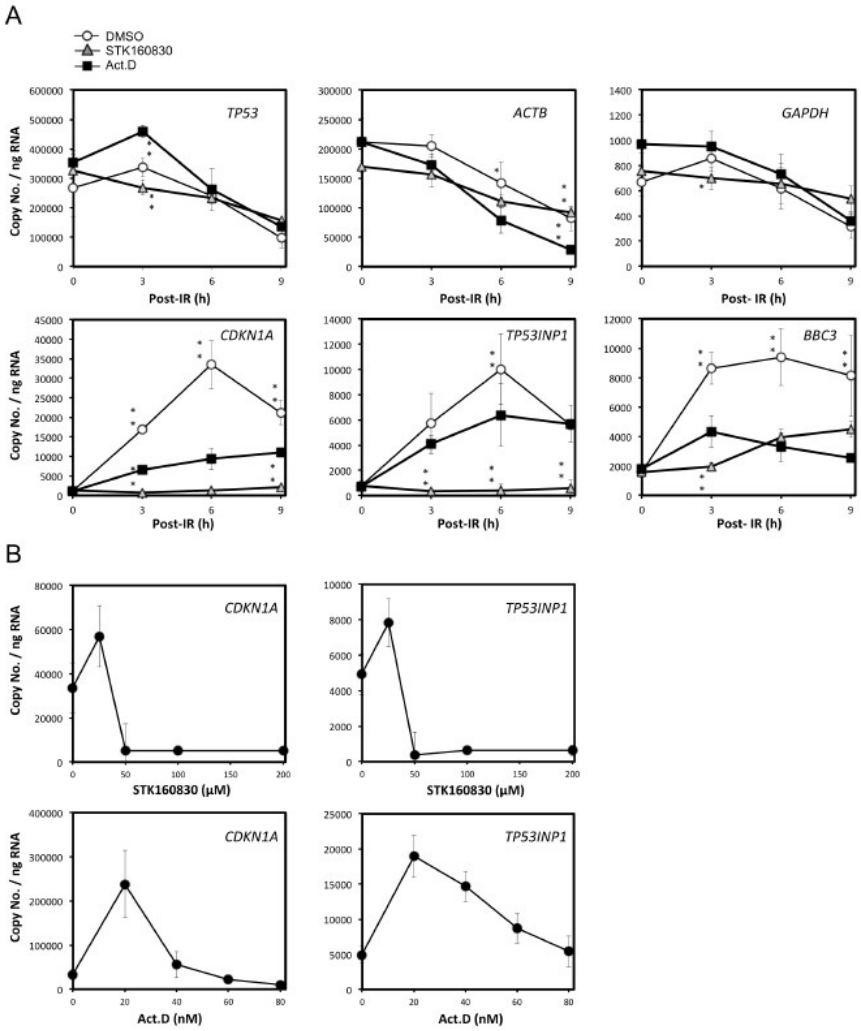

Figure 3-5. Changes in mRNA expression levels by STK160830 or Act. D in irradiated MOLT-4 cells. (A) STK160830 or Act. D were treated at 100 μM or 80 nM. Cells were collected at 3, 6, and 9 h after 10 Gy-IR, and subjected to qPCR absolute quantification. Means and SDs from 4–6 independent experiments are shown. Statistical significance was determined by Dunnett's multiple comparison test using Act. D samples as controls: *, $p < 0.05$; **, $p < 0.01$. (B) Dose-dependent suppression of mRNA expression by STK160830 or Act. D. Cells were collected 6 h after 10 Gy-IR and subjected to qPCR absolute quantification. Means and SDs from 4–6 independent experiments are shown.

We then labeled the nascent mRNA by treating the cells with EU and measured each mRNA by qPCR absolute quantification of the extracted total mRNA and the nascent mRNA obtained with the capture kit (Figure 3-6). In comparison with vehicle DMSO-treated irradiated cells, significant inhibition of nascent mRNA synthesis by STK160830 was observed in *ACTB*, *TP53*, *BBC3*, *TP53INP1*, and *CDKN1A*. The inhibition of nascent mRNA synthesis by Act. D was comparable to that of STK160830 in *ACTB* and *BBC3*, while STK160830 had a higher inhibitory effect than Act. D in *TP53* and *TP53INP1*. For *CDKN1A*, STK160830 showed a high inhibition rate of total mRNA synthesis, whereas the inhibition effect of nascent mRNA synthesis was not remarkable compared with other genes, although it showed a significant difference. On the other hand, in unirradiated cells, the inhibitory effect of Act. D on total mRNA expression of housekeeping genes *ACTB* and *GAPDH* was higher than that of STK160830. These results suggest that STK160830 is an mRNA synthesis inhibitor wia th different inhibition spectrum from Act. D. Of note, in unirradiated cells, nascent mRNA synthesis of *TP53INP1* was induced by Act. D and that of *TP53* was also increased by Act. D treatment, albeit not statistically significant. These results suggested that Act. D activates p53.

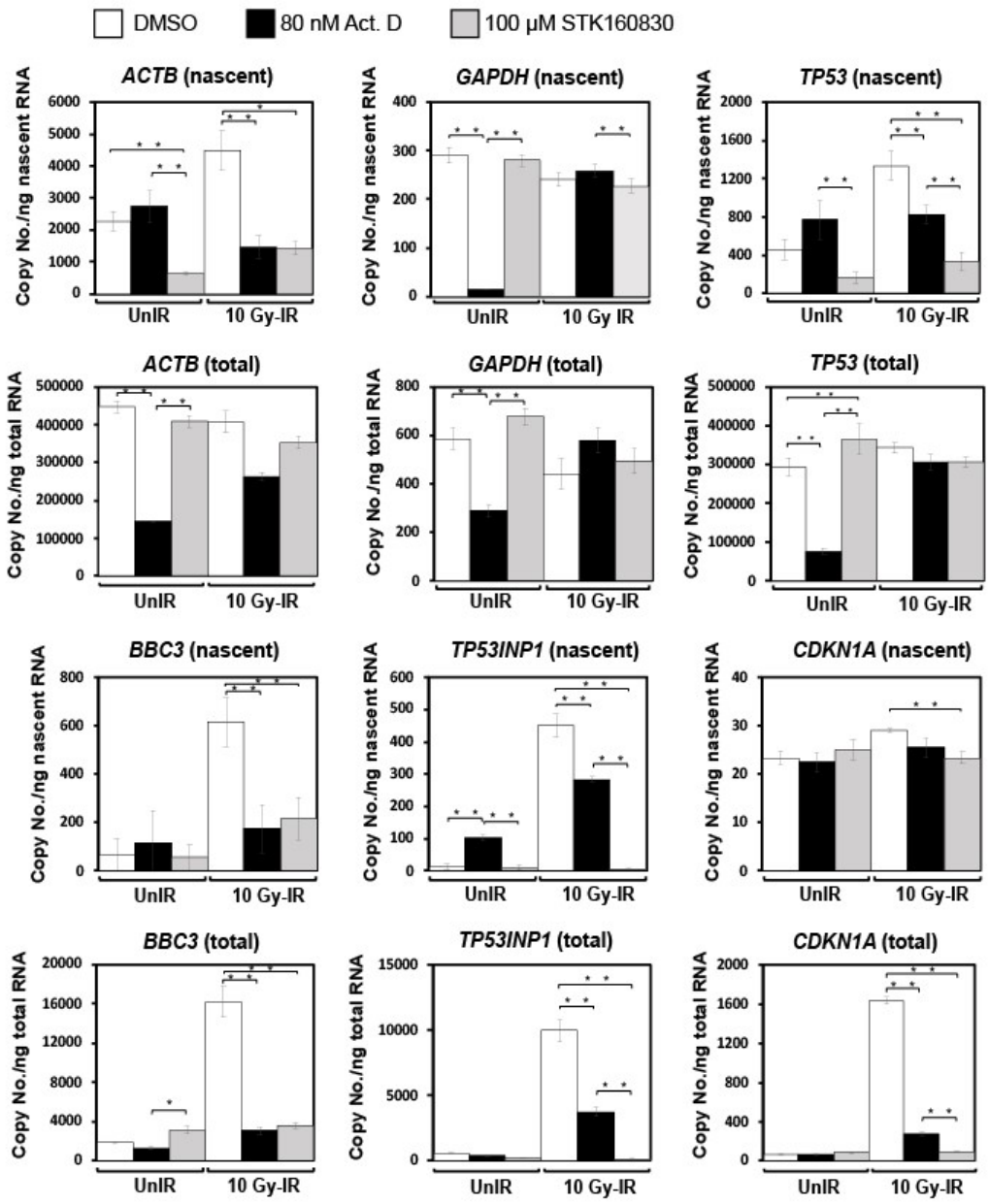

Figure 3-6. Changes in nascent and total mRNA expression by STK160830 or Act. D in irradiated MOLT-4 cells. EU was added to the culture medium immediately after 10 Gy-IR. Six hours later, total RNA was extracted from the harvested cells, and nascent RNA was isolated using the capture kit and absolutely quantified by qPCR. Means and SDs from 4–8 independent experiments are shown. Means were compared using one-way analysis of variance followed by multiple comparisons using the Tukey-Kramer method to examine significant differences: *, $p < 0.05$; **, $p < 0.01$.

[3-2-4] STK160830 has negligible DNA-intercalating activity for triggering a p53 response

We examined the p53-inducing activity of STK160830 by immunoblotting using the conventional RNA synthesis inhibitors Act. D and DRB as controls (Fig. 3-7A and 3-8). Act. D and DRB induced the accumulation of p53, respectively, while STK160830 did not induce the accumulation of p53, suggesting that the inhibition of RNA synthesis is due to a mechanism different from that of the conventional inhibitors. In fact, the DNA-intercalating activity of STK160830 was also examined by measuring the *Tm* value by DNA melting curve analysis. Figure 3-7B shows that the well-known intercalator, ethidium bromide (EtBr) or Act. D, caused an increase in the *Tm* value compared to the control sample, whereas STK160830 did not change the *Tm* value. These results indicate that STK160830 has negligible DNA-intercalating activity and a novel RNA synthesis inhibitory activity that does not trigger the p53 response.

B

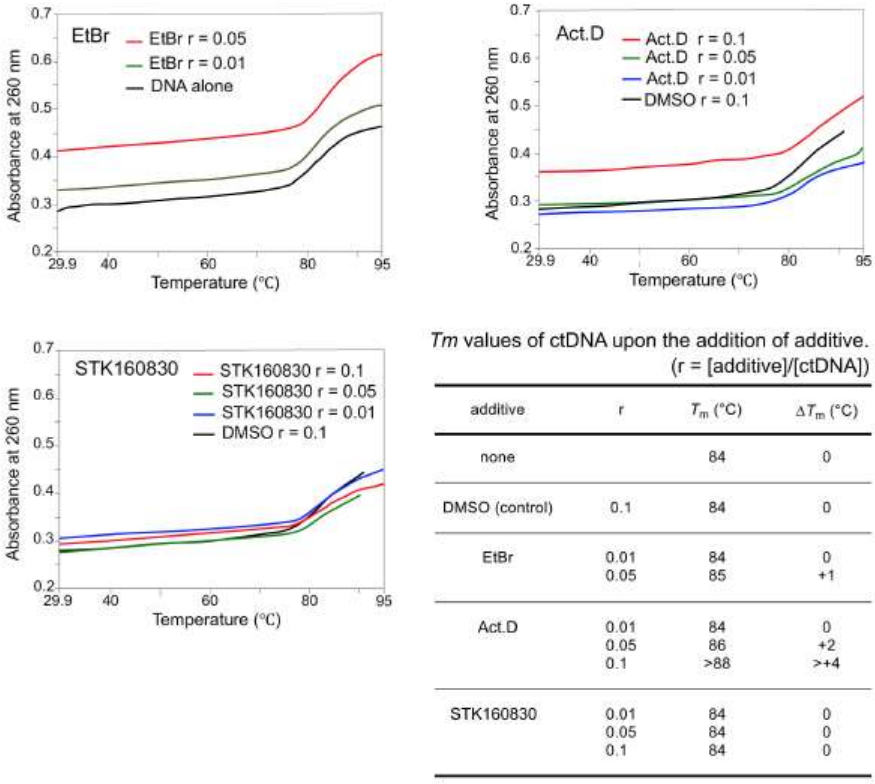

Tm values of ctDNA upon the addition of additive. (r = [additive]/[ctDNA])

additive	r	T_m (°C)	ΔT_m (°C)
none		84	0
DMSO (control)	0.1	84	0
EtBr	0.01	84	0
	0.05	85	+1
Act.D	0.01	84	0
	0.05	86	+2
	0.1	>88	>+4
STK160830	0.01	84	0
	0.05	84	0
	0.1	84	0

Figure 3-7. STK160830 alone does not induce p53 accumulation and has negligible DNA-intercalating activity. (A) Effect of STK160830, Act. D, or DRB on the induction of p53 accumulation. STK160830, Act. D, and DRB were treated at 100 μM, 80 nM, and 40 μM, respectively. Cells were collected at 1, 2, and 4 h after 10 Gy-IR, and the proteins were detected by immunoblotting. (B) Thermal melting curves for calf thymus DNA (ctDNA) in the presence of additives were obtained by following the absorption change at 260 nm as an effect of the raising temperature. The Tm value was graphically determined from the spectral data. r = [additive]/[ctDNA].

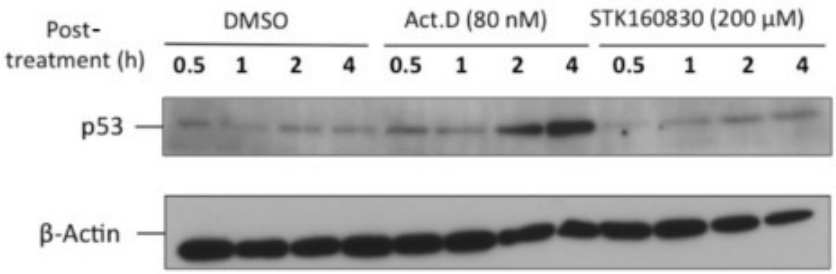

Figure 3-8. Effect of 200 μM STK160830 on the induction of p53 accumulation in irradiated MOLT-4 cells. Cells were collected at 0.5, 1, 2, 4 h after 10 Gy-IR, and the proteins were detected by immunoblotting. Even when the concentration of STK160830 was increased to 200 μM, the accumulation of p53 was slight.

[3-3] Discussion

In this study, STK160830 was selected from the core library consisting of 9600 compounds provided from The University of Tokyo's Drug Discovery Initiative, mainly based on its inhibitory effect on radiation-induced apoptosis of MOLT-4 cells. Of the 9600 compounds with various active compounds, the most effective compound was STK160830, which is an RNA synthesis inhibitor that has negligible DNA-intercalating activity. This indicates that *de novo* RNA synthesis is necessary for the MOLT-4 cell death, but these findings are inconsistent with our and others' conclusions that *de novo* protein synthesis, but not *de novo* RNA synthesis, is required for this cell death.[38,39] The main reason for these conclusions was that the RNA inhibitor Act. D, which was available at that time, did not block the cell death. On the other hand, cycloheximide, a protein synthesis inhibitor, effectively suppressed the accumulation of p53 in irradiated MOLT-4 cells, and we speculated that the contribution of the p53 transcription-dependent pathway was probably small, because the cells had Arg72-p53, which tends to activate the transcription-independent pathway.[41,42] However, STK160830 showed the same mRNA expression inhibition at 50 μM treatment as at 100 μM (Figure 3-5B), and showed high radiation cell death inhibition, unlike Act. D[39], even though 50 μM STK160830 showed only a slight p53 inhibition of about 15% (Figure 3-4A). These results suggest that the

fate of the cell death is not solely dependent on the amount of p53.

In addition, in MOLT-4 cells, Act. D alone induced the p53 accumulation (Figure 3-7A) and had strong cytotoxicity,[39] whereas STK160830 did not induce the p53 accumulation and showed almost no cytotoxicity. It is suggested that the reason why Act. D showed only a small inhibitory effect on radiation-induced apoptosis in our previous study was not because the contribution of the p53 transcription-dependent pathway was small, but because the strong cytotoxicity of Act. D prevented us from observing the inhibitory effect on the MOLT-4 apoptosis. Alternatively, the inhibition of RNA synthesis by DNA-intercalation may activate the transcription-independent pathway by Arg72-p53 as a bypass pathway. We present a proposed scheme for the mechanism of action of STK160830 in Scheme 3-1. In any case, the discovery of the RNA synthesis requirement for the MOLT-4 apoptosis would not have been possible without the RNA synthesis inhibitory activity of STK160830, which does not induce a marked adverse response. STK160830 will be a useful RNA synthesis inhibitor, especially when investigating the transcriptional dependence of cell-death-related responses.

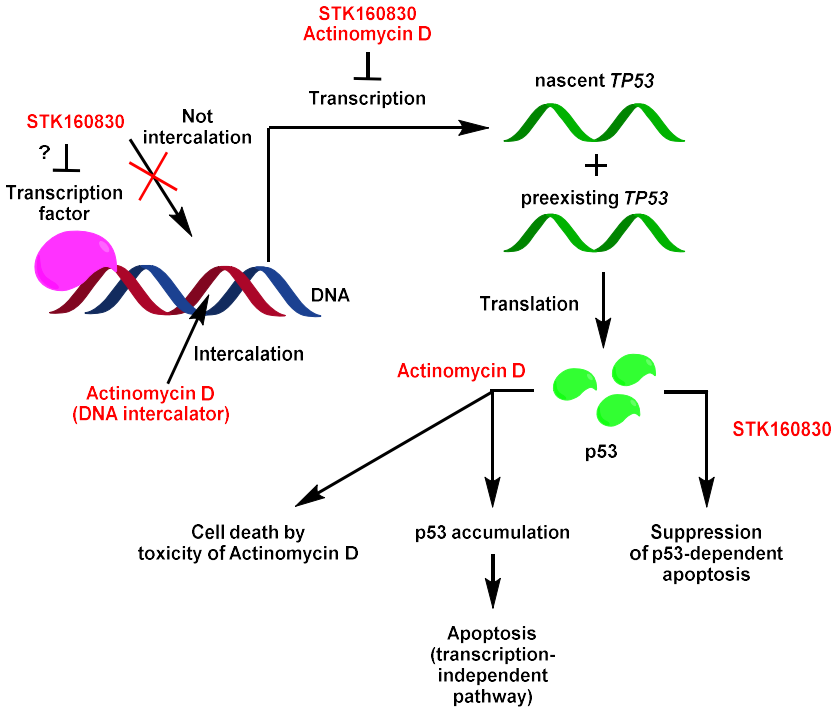

Scheme 3-1. Proposed scheme of the inhibition of mRNA synthesis by STK160830 and Act. D and p53 accumulation.

The known RNA synthesis inhibitors DRB and α-amanitin, which also lack intercalating activity, inhibit the activity of RNA polymerase II but induce a p53 response,[20,21] so the target of STK160830 is presumably different from that of these conventional inhibitors. In a recent study, α-amanitin was reported to show high cytotoxic activity in cancer cells hemizygous for deletion of one allele of *POLR2A*, the gene encoding hRBP1, one of the subunits of RNA polymerase II.[41] However, STK160830 did not show potent cytotoxicity against these cell lines (SNU283 and SW837) compared to α-amanitin (data not shown), also indicating that STK160830 has a different mechanism of RNA synthesis inhibition from that of α-amanitin.

In Figure 3-6, we compared the total and nascent mRNA expression levels of various genes between STK160830- and Act. D-treated cells. Although it is clear that STK160830 has a different inhibition spectrum than that of Act. D, these results are complex and difficult to interpret. As for *CDKN1A* in irradiated MOLT-4 cells, STK160830 and Act. D strongly inhibited the total mRNA synthesis. However, in nascent mRNA expression of *CDKN1A*, STK160830 showed a statistically significant inhibition of the expression, but its inhibition was slight, suggesting that it was not the inhibition of the nascent mRNA synthesis that mainly regulated the expression of total mRNA. *CDKN1A* is also a target of several miRNAs involved in T-cell acute lymphoblastic leukemia[43], suggesting that total mRNA expression of *CDKN1A* is regulated by mechanisms other than direct nascent mRNA synthesis inhibition. More interestingly, in unirradiated cells, the suppressive effect on the total mRNA expression of the housekeeping genes, *ACTB* and *GAPDH*, was observed for Act. D but not for STK160830. Since STK160830 inhibits the nascent mRNA synthesis of *ACTB* in non-irradiated cells, there may be some unknown mechanism that prevents the decrease in total mRNA. These effects of STK160830 may also contribute to its low cytotoxicity. We are currently exploring the target proteins of STK160830 using reactive its derivatives, which are expected to label them, and that should be the subject for future research.

Chapter 4.

Concluding Remarks

In this thesis, we report on the design, synthesis and biological evaluation of 2-pyrrolone derivatives as radioprotectors and their mechanistic study.

In Chapter 2, we report on the design, synthesis and biological evaluation of STK160830 and its derivatives. The 2-pyrrolone derivatives synthesized in this study have two stereoisomers for the *exo*-olefin part of the 2-pyrrolone core and we found that the *Z*-form compound was more biologically active than the corresponding *E*-form. The radioprotective activity was evaluated by dye exclusion assays using MOLT-4 cells, which express wild-type p53, as a model of normal cells. The result of a structure-activity relationships (SAR) study revealed several structural requirements for radioprotective activity. Regarding mechanistic studies, the expression level of p53 was confirmed by Western blot analysis and the results indicated that the radioprotective activity is dependent on the suppression of p53.

In Chapter 3, we report on the biological analysis of the mechanism of radioprotection by STK160830. We verified the p53-specificity of radioprotection of STK160830 by checking anti-apoptotic activity using several cell lines having p53-mutation. As we expected, the anti-apoptotic activity of STK160830 was shown in the cell lines bearing wild-type p53. To examine the effect on p53, the expression level was confirmed by western blot analysis and the result suggested that STK160830 suppressed p53

accumulation upon the IR-irradiation. Further mechanistic study revealed that STK160830 inhibited nascent mRNA synthesis of *TP53*, an encoding gene of p53, without DNA-intercalation.

We believe that this information will be helpful for molecular design of the 2-pyrrolone derivatives and other types of derivatives and for the understanding of the function of p53 in cellular response to radiation.

Chapter 5.

Experimental Section

[5-1] Materials and Methods for Chapter 2

Chemistry

General Information. All reagents and solvents were purchased at the highest commercial quality and were used without further purification. Anhydrous CH_2Cl_2 and DMF were prepared by distillation from calcium hydride. Anhydrous CH_3CN was prepared by distillation from phosphorus(V) oxide. All aqueous solutions were prepared using deionized water. Melting points were measured on a Yanaco micro melting point apparatus. ^1H (300 and 400 MHz), ^{13}C (100 MHz) NMR spectra were recorded on a JEOL Always 300 (JEOL, Tokyo, Japan) and a JNM-ECZ400S (JEOL) spectrometer. Tetramethylsilane (TMS) was used as an internal reference for ^1H NMR measurements in $CDCl_3$, CD_3OD, *d*$_6$-acetone and *d*$_6$-DMSO. IR spectra were recorded on a Perkin-Elmer FTIR Spectrum 100 (ATR) (PerkinElmer, Massachusetts, USA). MS measurements were performed on a Sciex X500R QTOF (AB SCIEX, Framingham, Massachusetts, USA) and Varian 910-MS (Varian Medical Systems, California, USA) spectrometer. Elemental analyses were performed on a Perkin-Elmer CHN 2400 analyzer (PerkinElmer). Thin-layer chromatography (TLC) and silica gel column chromatography was performed using Merck Silica gel 60 F_{254} plate (Merck KGaA, Darmstadt, Germany) and Fuji Silica Chemical FL-100D (Fuji Silysia Chemical, Aichi, Japan), respectively.

The microwave irradiation used in the organic reactions was performed in a reaction chamber, Discover (CEM corporation, Stallings, USA). UV-vis spectra were recorded on a JASCO V-630 and V-650 spectrophotometer at 25 ºC. Photoisomerization experiments were performed by Twin LED Light (RELYON, Tokyo, Japan) equipped with 365 nm, 425 nm and 465 nm light sources.

Synthesis

Compounds **31**[44], **32**[44], **33**[45], **37**[46] and **41**[47] were prepared according to previous reports and other starting materials were purchased. For the synthesis and purification of **7a** and its derivatives under fluorescent lights, brown glass instruments such as flasks, column tubes and test tubes were used to avoid the photoisomerization between the *E*-form and *Z*-form with respect to the *exo*-olefin part of their 2-pyrrolone ring.

(*Z*)-3-(4-Carboxybenzylidene)-4-methoxycarbonyl-1-(3-methoxyphenyl)-5-methyl-2-pyrrolone ((*Z*)-7a)

To a solution of **8a** (88.8 mg, 0.34 mmol, 1.4 equiv.) in *t*-BuOH (1 mL) was added conc. HCl (4 μL, 0.05 mmol, 0.2 equiv.). After stirring for 15 min, terephthalaldehydic acid **11** (37.7 mg, 0.25 mmol, 1.0 equiv.) was added and the reaction mixture was refluxed for 2

h. After cooling to room temperature, the reaction mixture was concentrated in vacuo. The residue was purified by silica gel column chromatography (3:1 (v/v) hexanes:AcOEt) to obtain an *E*/*Z* mixture of **7a** (*E*/*Z* = 22/78). The *E*/*Z* mixture was recrystallized from AcOEt to give **(*Z*)-7a** (41.5 mg, 0.11 mmol, 42%) as orange crystals. mp:213-215˚C; ^{1}H NMR (300 MHz, d_6-DMSO): δ = 2.29 (s, 3H), 3.78 (s, 3H), 3.81 (s, 3H), 6.92–7.07 (m, 3H), 7.40–7.45 (m, 1H), 7.92 (d, *J* = 8.4 Hz, 2H), 8.09 (d, *J* = 8.4 Hz, 2H), 8.13 (s, 1H) ppm; ^{13}C NMR (100 MHz, d_6-DMSO): δ = 166.9, 164.5, 163.9, 159.9, 155.0, 138.3, 138.0, 134.8, 131.3, 131.1, 130.0, 128.8, 128.0, 120.8, 114.6, 114.4, 103.1, 55.4, 51.1, 14.5 ppm; IR (ATR): ν = 2954, 2841, 2657, 2542, 1697, 1676, 1604, 1593, 1568, 1496, 1476, 1461, 1430, 1389, 1360, 1319, 1288, 1260, 1207, 1187, 1157, 1106, 1059, 1043, 932, 859, 839, 775, 750, 709, 689, 613, 547, 506, 426, 417 cm^{-1}; HRMS (FAB^{+}): [M+H]$^{+}$ calcd for $C_{22}H_{20}NO_6$, 394.1291; found, 394,1290; Elemental Anal.: calcd for $C_{22}H_{19}NO_6$, C 67.17, H 4.87, N 3.56%; found, C 66.81, H 4.83, N 3.69%.

(*Z*)-3-(4-Carboxybenzylidene)-4-methoxycarbonyl-1-(4-methoxyphenyl)-5-methyl-2-pyrrolone (*Z*)-7b)

To a solution of **8b** (211.6 mg, 0.81 mmol, 1.5 equiv.) in *t*-BuOH (2 mL) was added conc. HCl (9 μL, 0.1 mmol, 0.2 equiv.). After stirring for 15 min, terephthalaldehydic acid **11** (81.1 mg, 0.54 mmol, 1.0 eq.) was added and the reaction mixture was refluxed

for 3 h. After the reaction, the reaction mixture was concentrated in vacuo. The residue was purified by silica gel column chromatography (3:1 to 0:1 (v/v) hexanes/AcOEt) to obtain an *E*/*Z* mixture of **7b** (*E*/*Z* = 7/93). The *E*/*Z* mixture was recrystallized from AcOEt to give **(*Z*)-7b** (137.8 mg, 0.35 mmol, 65%) as yellow powder. mp:253-255 ˚C; ^{1}H NMR (300MHz, d_6-DMSO): δ 2.25 (s, 3H), 3.79 (s, 6H), 7.04 (d, *J* = 8.7 Hz, 2H), 6.77 (d, *J* = 8.7 Hz, 2H), 7.90 (d, *J* = 8.4 Hz, 2H), 8.07 (d, *J* = 8.4 Hz, 1H), 8.11 (s, 1H) ppm; ^{13}C NMR (100MHz, d_6-DMSO): δ 166.9, 164.9, 164.0, 159.3, 155.5, 138.4, 137.8, 131.2, 131.1, 129.9, 128.8, 128.1, 126.2, 114.5, 102.8, 55.5, 51.1, 14.5 ppm; IR (ATR): 2841, 2547, 1727, 1682, 1606, 1513, 1426, 1390, 1376, 1339, 1319, 1295, 1252, 1215, 1188, 1166, 1137, 1112, 1090, 1059, 1029, 1017, 986, 937, 918, 899, 863, 828, 801, 790, 775, 753, 690, 641, 600, 582, 543, 528 cm^{-1}; HRMS (FAB^{+}, m/z): [M+H]$^{+}$ calcd for $C_{22}H_{20}NO_6$, 394.1291; found, 394.1288; Elemental Anal.: calcd for $C_{22}H_{19}NO_6$, C 67.17, H 4.87, N 3.56%; found, C 67.07, H 4.51, N 3.51%.

(*Z*)-3-(4-Carboxybenzylidene)-4-methoxycarbonyl-1-(2-methoxyphenyl)-5-methyl-2-pyrrolone ((*Z*)-7c)

To a solution of **8c** (290 mg, 1.1 mmol, 1.5 equiv.) in *t*-BuOH (1.5 mL) was added conc. HCl (13 μL, 0.15 mmol, 0.2 equiv.). After stirring for 15 min, terephthalaldehydic acid **11** (111.1 mg, 0.74 mmol, 1.0 equiv.) was added and the reaction mixture was

refluxed for 2 h. After cooling to room temperature, the reaction mixture was concentrated in vacuo. The residue was purified by silica gel column chromatography (1:1 (v/v) hexanes:AcOEt) to obtain **7c** (*Z* only). The residue was recrystallized from AcOEt to give **(*Z*)-7c** (174.0 mg, 0.44 mmol, 60%) as a yellow solid. mp:219-221˚C; ^{1}H NMR (300 MHz, d_6-DMSO): δ = 2.19 (s, 3H), 3.78 (s, 3H), 3.81 (s, 3H), 7.05–7.11 (m, 1H), 7.20–7.23 (m, 1H), 7.31–7.34 (m, 1H), 7.46–7.52 (m, 1H), 7.92 (d, *J* = 8.4 Hz, 2H), 8.08 (d, *J* = 8.4 Hz, 2H), 8.13 (s 1H) ppm; ^{13}C NMR (100 MHz, d_6-DMSO): δ = 166.9, 164.6, 163.9, 155.8, 155.4, 138.3, 137.8, 131.3, 131.1, 130.9, 130.7, 128.8, 127.9, 121.9, 120.8, 112.4, 102.9, 55.8, 51.1, 13.9 ppm; IR (ATR): ν = 2949, 2839, 1684, 1604, 1503, 1466, 1440, 1425, 1386, 1362, 1318, 1283, 1253, 1217, 1184, 1167, 1139, 1104, 1060, 1017, 920, 851, 788, 746, 701, 692, 661, 611, 602, 568, 540, 527, 503, 474, 433, 415 cm^{-1}; HRMS (FAB^{+}): $[M+H]^{+}$ calcd for $C_{22}H_{20}NO_6$, 394.1291; found, 394,1292; Elemental Anal.: calcd for $C_{22}H_{19}NO_6 \cdot 0.5H_2O$, C 65.67, H 5.01, N 3.48%; found, C 65.48, H 4.82, N 3.34%.

(*Z*)-3-(4-Carboxybenzylidene)-4-methoxycarbonyl-5-methyl-1-phenyl-2-pyrrolone ((*Z*)-7d)

To a solution of **8d** (277.5 mg, 1.2 mmol, 1.2 equiv.) in *t*-BuOH (4 mL) was added conc. HCl (17 μL, 0.20 mmol, 0.2 equiv.). After stirring for 15 min, terephthalaldehydic

acid (150.1 mg, 1.0 mmol, 1.0 equiv.) was added and the reaction mixture was refluxed for 2 h. After cooling to room temperature, the reaction mixture was concentrated in vacuo. The residue was purified by recrystallization from AcOEt to give **(*Z*)-7d** (213.3 mg, 0.59 mmol, 59%) as a yellow solid. mp:253-255˚C; ^{1}H NMR (300 MHz, d_6-DMSO): δ = 2.29 (s, 3H), 3.82 (s, 3H), 7.36–7.39 (m, 2H), 7.45–7.56 (m, 3H), 7.92 (d, J = 8.4 Hz, 2H), 8.09 (d, J = 8.4 Hz, 2H), 8.14 (s, 1H) ppm; ^{13}C NMR (100 MHz, d_6-DMSO): δ = 166.9, 164.6, 163.9, 155.0, 138.3, 138.0, 133.7, 131.3, 131.1, 129.3, 128.8, 128.0, 103.1, 51.1, 14.5 ppm; IR (ATR): ν = 2949, 2543, 1679, 1594, 1570, 1495, 1424, 1388, 1361, 1318, 1289, 1214, 1188, 1162, 1135, 1108, 1058, 1015, 928, 862, 840, 798, 750, 714, 692, 663, 617, 600, 543, 505, 428, 413 cm^{-1}; HRMS (FAB^{+}): $[M+H]^{+}$ calcd for $C_{21}H_{18}NO_5$, 364.1185; found, 364.1184; Elemental Anal.: calcd for $C_{21}H_{17}NO_5$, C 69.41, H 4.72, N 3.85%; found, C 69.55, H 4.58, N 3.83%.

(*Z*)-3-(4-Carboxybenzylidene)-1-(3-chlorophenyl)-4-methoxycarbonyl-5-methyl-2-pyrrolone ((*Z*)-7e)

To a solution of **8e** (318.8 mg, 1.2 mmol, 1.2 equiv.) in *t*-BuOH (3 mL) was added conc. HCl (17 μL, 0.2 mmol, 0.2 equiv.). After stirring for 15 min, terephthalaldehydic acid **11** (150.1 mg, 1.0 mmol, 1.0 equiv.) was added and the reaction mixture was refluxed for 4 h. After cooling to room temperature, the reaction mixture was concentrated in

vacuo. The resulting residue was purified by recrystallization from AcOEt to give **(*Z*)-7e** (167.7 mg, 0.42 mmol, 42%) as orange crystals. mp:202-204˚C; ^{1}H NMR (300 MHz, *d*$_6$-DMSO): δ = 2.30 (s, 3H), 3.82 (s, 3H), 7.37–7.41 (m, 1H), 7.55–7.59 (m, 3H), 7.92 (d, *J* = 8.4 Hz, 2H), 8.08 (d, *J* = 8.4 Hz, 2H), 8.14 (s, 1H) ppm; ^{13}C NMR (100 MHz, *d*$_6$-DMSO): δ = 166.7, 164.3, 163.8, 154.4, 138.1, 135.0, 133.3, 131.2, 131.0, 130.7, 128.7, 128.6, 127.7, 127.5, 103.3, 51.1, 14.3 ppm; IR (ATR): ν = 2540, 1697, 1676, 1588, 1564, 1481, 1431, 1387, 1360, 1321, 1292, 1215, 1191, 1165, 1141, 1112, 1092, 1057, 1020, 1002, 933, 904, 863, 841, 790, 765, 752, 700, 679, 618, 605, 548, 506, 449, 418 cm^{-1}; HRMS (FAB^{+}): $[M+H]^{+}$ calcd for $C_{21}H_{17}ClNO_5$, 398.0795; found, 398.0793; Elemental Anal.: calcd for $C_{21}H_{16}ClNO_5$, C 63.40, H 4.05, N 3.52%; found, C 63.00, H 3.73, N 3.39%.

(*Z*)-3-(4-Carboxybenzylidene)-1-(3-Hydroxyphenyl)-4-methoxycarbonyl-5-methyl-2-pyrrolone ((*Z*)-7f)

To a solution of **8f** (200.5 mg, 0.81 mmol, 1.5 equiv.) in *t*-BuOH (3 mL) was added conc. HCl (9 μL, 0.1 mmol, 0.2 equiv.). After stirring for 15 min, terephthalaldehydic acid **11** (83.0 mg, 0.55 mmol, 1.0 equiv.) was added and the reaction mixture was refluxed for 4 h. After the reaction, the reaction mixture was concentrated in vacuo. The residue was purified by silica gel column chromatography (50:1 to 1:1 (v/v) $CHCl_3$:MeOH) to

obtain an *E*/*Z* mixture of **7f** (*E*/*Z* = 7/93). The *E*/*Z* mixture was recrystallized from AcOEt to give **(*Z*)-7f** (84.9 mg, 0.22 mmol, 41%) as orange crystals. mp:234-236˚C; ^{1}H NMR (300MHz, d_6-DMSO): δ 2.29 (s, 3H), 3.81 (s, 3H), 6.72–6.77 (m, 2H), 6.85–6.88 (m, 1H), 7.27–7.33 (m, 1H), 7.92 (d, *J* = 8.4 Hz, 2H), 8.08 (d, *J* = 8.4 Hz, 2H), 8.12 (s, 1H), 9.82 (brs, 1H) ppm; ^{13}C NMR (100MHz, d_6-DMSO): δ 166.9, 164.6, 164.0, 158.1, 155.1, 138.3, 137.9, 134.6, 131.3, 131.1, 130.0, 128.8, 128.0, 119.1, 115.9, 115.7, 103.0, 51.1, 14.5 ppm; IR (ATR): 3334, 2947, 2814, 2540, 1711, 1667, 1604, 1591, 1561, 1507, 1492, 1460, 1440, 1419, 1387, 1364, 1320, 1280, 1212, 1191, 1161, 1106, 1062, 1017, 1000, 933, 897, 865, 840, 822, 789, 752, 714, 692, 613, 546, 505, 480, 462, 416 cm^{-1}; HRMS (FAB^{+}, m/z): [M+H]$^{+}$ calcd for $C_{21}H_{18}NO_6$, 380.1134; found, 380.1129; Elemental Anal.: calcd for $C_{21}H_{17}NO_6 \cdot 0.1H_2O$, C 66.17, H 4.55, N 3.67%; found, C 65.97, H 4.27, N 3.62%.

(*Z*)-3-(4-Carboxybenzylidene)-1-(3-isopropoxyphenyl)-4-methoxycarbonyl-5-methyl-2-pyrrolone ((*Z*)-7g)

To a solution of **8g** (456.5 mg, 1.6 mmol, 1.2 equiv.) in *t*-BuOH (3 mL) was added conc. HCl (22 μL, 0.3 mmol, 0.2 equiv.). After stirring for 15 min, terephthalaldehydic acid **11** (197.4 mg, 1.3 mmol, 1.0 equiv.) was added and the reaction mixture was refluxed for 4 h. After cooling to room temperature, the reaction mixture was concentrated in

vacuo. The residue was purified by recrystallization from AcOEt to give **(*Z*)-7g** (314.7 mg, 0.75 mmol, 57%) as a yellow solid. mp:167-169˚C; ^{1}H NMR (300 MHz, d_6-DMSO): δ = 1.27 (d, J = 6.3 Hz, 6H), 2.30 (s, 3H), 3.81 (s, 3H), 4.60–4.68 (m, 1H), 6.88–7.02 (m, 3H), 7.37–7.42 (m, 1H), 7.92 (d, J = 8.4 Hz, 2H), 8.08 (d, J = 8.4 Hz, 2H), 8.13 (s, 1H) ppm; ^{13}C NMR (100 MHz, d_6-DMSO): δ = 166.9, 164.6, 163.9, 158.0, 155.2, 138.3, 137.9, 134.8, 131.2, 131.1, 130.0, 128.8, 128.0, 120.5, 116.1, 115.8, 103.1, 69.5, 51.1, 21.7 ppm; IR (ATR): ν = 2984, 1692, 1593, 1570, 1495, 1432, 1395, 1366, 1318, 1292, 1257, 1228, 1209, 1192, 1159, 1141, 1110, 1064, 1020, 1003, 978, 936, 895, 849, 840, 796, 784, 751, 712, 693, 662, 614, 595, 581, 547, 507, 463, 447, 416 cm^{-1}; HRMS (FAB^{+}): $[M+H]^{+}$ calcd for $C_{24}H_{24}NO_6$, 422.1604; found, 422.1604; Elemental Anal.: calcd for $C_{24}H_{23}NO_6$, C 68.40, H 5.50, N 3.32%; found, C 68.24, H 5.45, N 3.35%.

(*Z*)-3-(4-Carboxybenzylidene)-1-(3-(hexyloxy)phenyl)-4-methoxycarbonyl-5-methyl-2-pyrrolone ((*Z*)-7h)

To a solution of **8h** (486.0 mg, 1.5 mmol, 1.2 equiv.) in *t*-BuOH (3 mL) was added conc. HCl (21 μL, 0.2 mmol, 0.2 equiv.). After stirring for 15 min, terephthalaldehydic acid **11** (183.4 mg, 1.2 mmol, 1.0 equiv.) was added and the reaction mixture was refluxed for 5 h. After cooling to room temperature, the reaction mixture was concentrated in vacuo. The residue was purified by recrystallization from a solution of 2:1 (v/v)

hexanes:AcOEt to give **(*Z*)-7h** (364.8 mg, 0.79 mmol, 65%) as an orange solid. mp:149-150°C; ^{1}H NMR (300 MHz, d_6-DMSO): δ = 0.87 (t, *J* = 7.2 Hz, 3H), 1.28–1.41 (m, 6H), 1.68–1.73 (m, 2H), 2.29 (s, 3H), 3.81 (s, 3H), 3.98 (t, *J* = 6.3 Hz, 2H), 6.90–7.05 (m, 3H), 7.38–7.43 (m, 1H), 7.92 (d, *J* = 8.4 Hz, 2H), 8.08 (d, *J* = 8.4 Hz, 2H), 8.13 (s, 1H) ppm; ^{13}C NMR (100 MHz, d_6-DMSO): δ = 166.8, 164.4, 163.8, 159.1, 155.0, 138.2, 137.8, 134.7, 131.1, 131.0, 129.9, 128.6, 127.9, 120.5, 115.0, 114.7, 102.9, 67.7, 51.0, 30.9, 28.4, 25.0, 22.0, 14.4, 13.8 ppm; IR (ATR): ν = 2924, 1703, 1676, 1608, 1595, 1570, 1495, 1434, 1389, 1365, 1319, 1292, 1256, 1229, 1207, 1189, 1165, 1134, 1111, 1061, 1015, 971, 933, 898, 862, 840, 798, 781, 762, 751, 711, 690, 619, 545, 505, 460, 418 cm^{-1}; HRMS (FAB^{+}): $[M+H]^{+}$ calcd for $C_{27}H_{30}NO_6$, 464.2073; found, 464.2076; Elemental Anal.: calcd for $C_{27}H_{29}NO_6$, C 69.96, H 6.31, N 3.02%; found, C 69.61, H 6.29, N 2.98%.

(*Z*)-3-(4-Carboxybenzylidene)-1-(2-fluoro-5-methoxyphenyl)-4-methoxycarbonyl-5-methyl-2-pyrrolone ((*Z*)-7i)

To a solution of **8i** (78.8 mg, 0.28 mmol, 1.2 equiv.) in *t*-BuOH (1 mL) was added conc. HCl (4 μL, 0.05 mmol, 0.2 equiv.). After stirring for 15 min, terephthalaldehydic acid **11** (35.3 mg, 0.24 mmol, 1.0 equiv.) was added and the reaction mixture was refluxed for 5 h. After cooling to room temperature, the reaction mixture was concentrated in vacuo. The residue was purified by recrystallization from a solution of 1:2 (v/v) hexanes:AcOEt

to give **(*Z*)-7i** (48.2 mg, 0.12 mmol, 50%) as a yellow solid. mp:234-236˚C; ^{1}H NMR (399 MHz, d_6-DMSO): δ = 2.23 (s, 3H), 3.77 (s, 3H), 3.82 (s, 3H), 7.09–7.13 (m, 1H), 7.16 (dd, J = 6.4, 3.2 Hz, 1H), 7.36–7.41 (m, 1H), 7.93 (d, J = 8.4 Hz, 1H), 8.08 (d, J = 8.4 Hz, 2H), 8.17 (s, 1H) ppm; ^{13}C NMR (100 MHz, d_6-DMSO): δ = 166.7, 163.9, 163.6, 155.6, 154.1, 152.1 (d, $J_{C,F}$ = 239.6 Hz), 138.7, 137.9, 131.4, 131.0, 128.7, 127.2, 121.4 (d, $J_{C,F}$ = 14.4 Hz), 116.8 (d, $J_{C,F}$ = 21.1 Hz), 116.4 (d, $J_{C,F}$ = 6.7 Hz), 115.9, 103.7, 55.8, 51.1, 13.8 ppm; IR (ATR): ν = 2949, 1686, 1604, 1506, 1443, 1421, 1391, 1364, 1290, 1264, 1215, 1162, 1127, 1115, 1095, 1066, 1020, 952, 934, 895, 862, 842, 815, 795, 764, 752, 716, 693, 625, 544, 497, 469, 450, 437, 417 cm^{-1}; HRMS (FAB^{+}): $[M+H]^{+}$ calcd for $C_{22}H_{19}FNO_6$, 412.1196; found, 412.1196; Elemental Anal.: calcd for $C_{22}H_{18}FNO_6$, C 64.23, H 4.41, N 3.40%; found, C 64.26, H 4.19, N 3.50%.

(*Z*)-3-(4-Carboxybenzylidene)-1-(2-chloro-5-methoxyphenyl)-4-methoxycarbonyl-5-methyl-2-pyrrolone ((*Z*)-7j)

To a solution of **8j** (200.0 mg, 0.68 mmol, 1.2 equiv.) in *t*-BuOH (3 mL) was added conc. HCl (10 μL, 0.11 mmol, 0.2 equiv.). After stirring for 15 min, terephthalaldehydic acid **11** (84.6 mg, 0.56 mmol, 1.0 equiv.) was added and the reaction mixture was refluxed for 4 h. After cooling to room temperature, the reaction mixture was concentrated in vacuo. The residue was purified by recrystallization from a solution of 1:2 (v/v)

hexanes:AcOEt to give **(*Z*)-7j** (95.8 mg, 0.22 mmol, 40%) as a yellow solid. mp:248-250˚C; ^{1}H NMR (300 MHz, d_6-DMSO): δ = 2.23 (s, 3H), 3.80 (s, 3H), 3.82 (s, 3H), 7.14 (dd, *J* = 9.0, 3.0 Hz, 1H), 7.25 (d, *J* = 3.0 Hz, 1H), 7.59 (d, *J* = 9.0 Hz, 1H), 7.93 (d, *J* = 8.4 Hz, 2H), 8.09 (d, *J* = 8.4 Hz, 2H), 8.17 (s 1H) ppm; ^{13}C NMR (100 MHz, d_6-DMSO): δ = 166.8, 164.0, 163.8, 158.8, 154.3, 138.6, 138.0, 132.1, 131.5, 131.1, 130.4, 128.8, 127.5, 123.6, 117.1, 117.1, 103.5, 55.9, 51.2, 13.9 ppm; IR (ATR): ν = 2954, 2548, 1696, 1680, 1606, 1509, 1488, 1465, 1438, 1423, 1392, 1380, 1360, 1321, 1291, 1265, 1244, 1191, 1162, 1140, 1110, 1066, 1020, 933, 892, 859, 840, 829, 816, 793, 759, 749, 719, 692, 654, 619, 584, 542, 519, 504, 463 cm^{-1}; HRMS (FAB^{+}): $[M+H]^{+}$ calcd for $C_{22}H_{19}ClNO_6$, 428.0901; found, 428.0900; Elemental Anal.: calcd for $C_{22}H_{18}ClNO_6$, C 61.76, H 4.24, N 3.27%; found, C 61.72, H 4.09, N 3.38%.

(*Z*)-3-(3-Carboxybenzylidene)-4-methoxycarbonyl-1-(3-methoxyphenyl)-5-methyl-2-pyrrolone ((*Z*)-7k)

To a solution of **8a** (289.9 mg, 1.1 mmol, 1.5 equiv.) in *t*-BuOH (1.5 mL) was added conc. HCl (13 μL, 0.2 mmol, 0.2 equiv.). After stirring for 15 min, isophthalaldehydic acid **20** (110.7 mg, 0.74 mmol, 1.0 equiv.) was added and the reaction mixture was refluxed for 3 h. After cooling to room temperature, the reaction mixture was concentrated in vacuo. The residue was purified by silica gel column chromatography

(3:1 to 0:1 (v/v) hexanes:AcOEt) to obtain an *E*/*Z* mixture of **7k** (*E*/*Z* = 37/63). The *E*/*Z* mixture was recrystallized from AcOEt to give (***Z*)-7k** (121.9 mg, 0.31 mmol, 42%) as a yellow solid. mp:211-213˚C; ^{1}H NMR (300 MHz, d_6-DMSO): δ = 2.27 (s, 3H), 3.77 (s, 3H), 3.80 (s, 3H), 6.90–7.06 (m, 3H), 7.39–7.54 (m, 2H), 7.93 (d, *J* = 8.1Hz, 2H), 8.14 (s, 1H), 8.18 (d, *J* = 7.8 Hz, 1H), 8.62 (s, 1H) ppm; ^{13}C NMR (100 MHz, d_6-DMSO): δ = 167.1, 164.6, 164.0, 159.9, 154.6, 138.5, 135.4, 134.9, 134.4, 131.9, 130.6, 130.5, 130.1, 128.3, 127.3, 120.8, 114.6, 114.5, 103.1, 55.5, 51.1, 14.5 ppm; IR (ATR): ν = 2950, 2836, 2542, 1686, 1602, 1495, 1469, 1438, 1397, 1361, 1342, 1311, 1287, 1261, 1227, 1210, 1178, 1168, 1127, 1064, 1044, 1031, 1010, 995, 938, 906, 876, 866, 833, 811, 793, 784, 752, 709, 685, 661, 649, 622, 614, 596, 582, 551, 525, 490, 460, 431, 414 cm^{-1}; HRMS (FAB^{+}, m/z): [M+H]$^{+}$ calcd for $C_{22}H_{20}NO_6$, 394.1291; found, 394,1287; Elemental Anal.: calcd for $C_{22}H_{19}NO_6 \cdot 0.2$AcOEt, C 66.63, H 5.05, N 3.41%; found, C 66.68, H 4.85, N 3.39%.

Sodium (Z)-2-((3-(4-methoxycarbonyl-1-(3-methoxyphenyl)-5-methyl-2-pyrrolone)ylidene)methyl)benzenesulfonate ((*Z*)-7m)

To a solution of **8a** (193.6 mg, 0.74 mmol, 1.4 equiv.) in *t*-BuOH (1 mL) was added conc. HCl aq. (8 μL, 0.09 mmol, 0.2 equiv.). After stirring for 15 min, 2-formylbenzenesulfonic acid sodium salt **23** (106.5 mg, 0.51 mmol, 1.0 equiv.) was added

and the reaction mixture was refluxed for 2 h. After cooling to room temperature, the reaction mixture was concentrated in vacuo. The residue was purified by silica gel column chromatography (7:1 (v/v) $CHCl_3$:MeOH) to obtain **7m** (*Z* only). The residue was recrystallized from a solution of 1:4 (v/v) $CHCl_3$:AcOEt to give **(*Z*)-7m** (97.6 mg, 0.22 mmol, 42%) as yellow powder. mp:224-226˚C; ^{1}H NMR (300 MHz, DMSO-d_6): δ = 2.27 (s, 3H), 3.77 (s, 6H), 6.88–7.03 (m, 3H), 7.21–7.40 (m, 2H), 7.37–7.43 (m, 1H), 7.75–7.80 (m, 1H), 8.86 (s, 1H) ppm; ^{13}C NMR (100 MHz, DMSO- d_6): δ = 164.6, 163.8, 159.7, 152.8, 146.7, 141.6, 135.0, 131.2, 131.1, 129.8, 128.4, 127.2, 126.1, 124.5, 120.6, 114.3, 114.2, 103.6, 55.3, 50.8, 13.9 ppm; IR (ATR): ν = 3511, 3105, 2955, 2837, 1693, 1654, 1600, 1587, 1567, 1492, 1446, 1370, 1316, 1286, 1263, 1242, 1213, 1193, 1171, 1114, 1065, 1022, 994, 941, 922, 894, 832, 810, 782, 758, 720, 688, 614, 594, 572, 557, 547, 514, 466, 459, 451, 446, 439, 421, 414 cm^{-1}; HRMS (FAB$^+$, m/z): $[M+H]^+$ calcd for $C_{21}H_{19}NO_7SNa$, 452.0780; found, 452.0783; Elemental Anal.: calcd for $C_{21}H_{18}NNaO_7S \cdot 0.1CHCl_3$, C 55.43, H 4.08, N 3.08%; found, C 55.49, H 3.74, N 2.76%.

(*Z*)-3-(4-Methoxybenzylidene)-4-methoxycarbonyl-1-(3-methoxyphenyl)-5-methyl-2-pyrrolone ((*Z*)-7n)

To a solution of **8a** (192.1 mg, 0.74 mmol, 1.5 equiv.) in *t*-BuOH (1 mL) was added conc. HCl (24 μL, 0.28 mmol, 0.6 equiv.). After stirring for 15 min, *p*-anisaldehyde **24**

(60 μL, 0.50 mmol, 1.0 equiv.) was added and the reaction mixture was refluxed for 5 h. After cooling to room temperature, the reaction mixture was concentrated in vacuo. The residue was purified by silica gel column chromatography (6:1 (v/v) hexanes:AcOEt) to obtain an *E*/*Z* mixture of **7n** (*E*/*Z* = 4/96). The *E*/*Z* mixture was recrystallized from a solution of 4:3 (v/v) hexanes:AcOEt to give **(*Z*)-7n** (88.5 mg, 0.23 mmol, 47%) as yellow crystals. mp:148-150˚C; ^{1}H NMR (300 MHz, d_6-DMSO): δ = 2.27 (s, 3H), 3.79 (s, 3H), 3.80 (s, 3H), 3.82 (s, 3H), 6.91–7.06 (m, 5H), 7.40–7.46 (m, 1H), 8.12 (s, 1H), 8.23 (d, *J* = 8.7 Hz, 2H), 7.36–7.41 (m, 1H), 8.21 (d, *J* = 9.0 Hz, 2H) ppm; ^{13}C NMR (100 MHz, $CDCl_3$): δ = 165.7, 165.0, 161.4, 160.4, 151.0, 142.1, 135.4, 134.5, 130.1, 127.5, 123.9, 120.7, 114.6, 114.1, 113.4, 104.6, 55.4, 55.3, 51.0, 14.6 ppm; IR (ATR): ν = 3078, 2995, 2950, 2835, 1682, 1588, 1508, 1495, 1467, 1449, 1434, 1394, 1364, 1316, 1308, 1283, 1261, 1233, 1212, 1176, 1163, 1156, 1129, 1109, 1064, 1023, 956, 932, 891, 834, 809, 778, 759, 744, 702, 687, 658, 613, 582, 534, 524, 454, 409 cm^{-1}; HRMS (FAB^{+}): $[M]^{+}$ calcd for $C_{22}H_{21}NO_5$, 379.1420; found, 379.1422; Elemental Anal.: calcd for $C_{22}H_{21}NO_5 \cdot 0.2H_2O$, C 68.99, H 5.63, N 3.66%; found, C 68.99, H 5.39, N 3.62%.

(*Z*)-4-Methoxycarbonyl-1-(3-methoxyphenyl)-5-methyl-3-(4-nitrobenzylidene)-2-pyrrolone ((*Z*)-7o)

To a solution of **7a** (195.6 mg, 0.75 mmol, 1.5 equiv.) in *t*-BuOH (1 mL) was added conc. HCl (8 μL, 0.09 mmol, 0.2 equiv.). After stirring for 15 min, 4-nitrobenzaldehyde **25** (75.6 mg, 0.50 mmol, 1.0 equiv.) was added and the reaction mixture was refluxed for 2 h. After cooling to room temperature, the resulting orange solid was filtered and washed with *t*-BuOH. The residue was purified by recrystallization from AcOEt to give **(*Z*)-7o** (147.9 mg, 0.38 mmol, 75%) as orange powder. mp:166-168˚C; ^{1}H NMR (300 MHz, *d*$_6$-DMSO): δ = 2.31 (s, 3H), 3.78 (s, 3H), 3.82 (s, 3H), 6.92–7.06 (m, 3H), 7.40–7.46 (m, 1H), 8.13–8.23 (m, 5H) ppm; ^{13}C NMR (100 MHz, *d*$_6$-DMSO): δ = 164.5, 163.8, 159.8, 156.3, 147.2, 140.8, 136.1, 134.6, 131.9, 130.0, 129.2, 122.9, 120.8, 114.7, 114.4, 102.9, 55.4, 51.2, 14.53 ppm; IR (ATR): ν = 3096, 3004, 2954, 2840, 1692, 1589, 1514, 1497, 1437, 1379, 1359, 1341, 1256, 1199, 1160, 1126, 1106, 1061, 923, 887, 851, 819, 809, 777, 744, 708, 686, 610, 583, 557, 528, 491, 466, 452, 440, 425, 413 cm^{-1}; HRMS (FAB^{+}): [M+H]$^{+}$ calcd for $C_{21}H_{19}N_2O_6$, 395.1243; found, 395.1245; Elemental Anal.: calcd for $C_{21}H_{18}N_2O_6$, C 63.96, H 4.60, N 7.10%; found, C 63.63, H 4.42, N 7.02%.

(*Z*)-3-(4-Chlorobenzylidene)-4-methoxycarbonyl-1-(3-methoxyphenyl)-5-methyl-2-pyrrolone ((*Z*)-7p)

To a solution of **8a** (195.6 mg, 0.74 mmol, 1.5 equiv.) in *t*-BuOH (1 mL) was added conc. HCl (8 μL, 0.09 mmol, 0.2 equiv.). After stirring for 15 min, 4-chlorobenzaldehyde

26 (69.1 mg, 0.49 mmol, 1.0 equiv.) was added and the reaction mixture was refluxed for 3 h. After cooling to room temperature, the reaction mixture was concentrated in vacuo. The residue was purified by silica gel column chromatography (6:1 (v/v) hexanes:AcOEt) to obtain an *E*/*Z* mixture of **7p** (*E*/*Z* = 21/79). The *E*/*Z* mixture was recrystallized from a solution of 2:1 (v/v) hexanes:AcOEt to give **(*Z*)-7p** (120.7 mg, 0.31 mmol, 64%) as a yellow solid. mp:126-128˚C; ^{1}H NMR (300 MHz, d_6-DMSO): δ = 2.28 (s, 3H), 3.78 (s, 3H), 3.80 (s, 3H), 6.91–7.06 (m, 3H), 7.40–7.47 (m, 3H), 8.07–8.10 (m, 3H) ppm; ^{13}C NMR (100 MHz, d_6-DMSO): δ = 164.6, 164.0, 159.8, 154.2, 138.1, 134.9, 134.5, 133.1, 133.0, 130.0, 128.0, 126.9, 120.8, 114.6, 114.4, 103.1, 55.4, 51.1, 14.4 ppm; IR (ATR): ν = 3074, 3010, 2948, 2839, 1933, 1850, 1693, 1601, 1595, 1570, 1490, 1467, 1433, 1416, 1382, 1361, 1319, 1290, 1261, 1231, 1210, 1190, 1163, 1132, 1102, 1092, 1064, 1027, 1012, 996, 926, 891, 879, 830, 810, 783, 769, 753, 714, 688, 646, 612, 582, 558, 510, 470, 460, 454, 435, 424, 417, 404 cm^{-1}; HRMS (FAB^{+}): $[M+H]^{+}$ calcd for $C_{21}H_{19}ClNO_4$, 384.1003; found, 384.0997; Elemental Anal.: calcd for $C_{21}H_{18}ClNO_4$, C 65.71, H 4.73, N 3.65%; found, C 65.68, H 4.65, N 3.65%.

(*Z*)-4-Methoxycarbonyl-1-(3-methoxyphenyl)-5-methyl-3-(pyridin-4-ylmethylene)-2-pyrrolone ((*Z*)-7q)

To a solution of **8a** (391.3 mg, 1.5 mmol, 1.5 equiv.) in *t*-BuOH (3 mL) was added conc.

HCl aq. (105 μL, 1.2 mmol, 1.2 equiv.). After stirring for 15 min, 4-pyridinecarboxaldehyde **27** (95 μL, 1.0 mmol, 1.0 equiv.) was added and the reaction mixture was refluxed for 30 min. After cooling to room temperature, the reaction mixture was diluted in $CHCl_3$ and 1M HCl aq. and extracted with 1M HCl aq. three times. The pH value of the combined aqueous layer was adjusted to 7 with sat. $NaHCO_3$ aq. and the resulting aqueous layer was extracted with $CHCl_3$ three times. The organic layer was dried over Na_2SO_4, filtered and concentrated in vacuo. The residue was purified by recrystallization from a solution of 1:1 (v/v) hexanes:AcOEt to give **(*Z*)-7q** (72.2 mg, 0.21 mmol, 20%) as brown crystals. mp:138-142˚C; ^{1}H NMR (300 MHz, DMSO-d_6): δ = 2.30 (s, 3H), 3.78 (s, 3H), 3.81 (s, 3H), 6.91–7.06 (m, 3H), 7.43 (t, J = 8.0 Hz, 1H), 7.79 (d, J = 5.1 Hz, 2H), 8.00 (s, 1H), 8.59 (d, J = 5.1 Hz, 2H) ppm; ^{13}C NMR (100 MHz, DMSO- d_6): δ = 164.4, 163.7, 159.7, 156.3, 149.3, 141.3, 135.5, 134.5, 129.9, 129.5, 124.1, 120.6, 114.6, 114.3, 102.6, 55.3, 51.0, 14.4 ppm; IR (ATR): ν = 3078, 3011, 2953, 2836, 1704, 1682, 1603, 1591, 1568, 1494, 1464, 1437, 1418, 1393, 1362, 1324, 1287, 1260, 1246, 1206, 1186, 1160, 1121, 1086, 1063, 1044, 1034, 990, 932, 891, 866, 825, 808, 788, 757, 709, 591, 569, 527, 492 cm^{-1}; HRMS (FAB$^+$, m/z): $[M+H]^+$ calcd for $C_{20}H_{18}N_2O_4$, 351.1345; found, 351.1344; Elemental Anal.: calcd for $C_{20}H_{18}N_2O_4$, C 68.56, H 5.18, N 8.00%; found, C 68.18, H 5.00, N 7.82%.

(*Z*)-3-(3-Hydroxypyridin-4-ylmethylene)-1-(3-methoxyphenyl)-4-methoxycarbonyl-5-methyl-2-pyrrolone ((*Z*)-7r)

To a solution of **8a** (261.3 mg, 1.0 mmol, 1.2 equiv.) in *t*-BuOH (2 mL) was added conc. HCl (86 μL, 1.2 mmol, 1.2 equiv.). After stirring for 15 min, 3-hydroxy-4-pyridinecarbaldehyde **28** (102.6 mg, 0.83 mmol, 1.0 equiv.) was added and the reaction mixture was refluxed for 2 h. After cooling to room temperature, the reaction mixture was diluted with $CHCl_3$ and sat. $NaHCO_3$ aq. and the aqueous layer was extracted with $CHCl_3$ three times. The combined organic layer was washed with brine, dried over Na_2SO_4, filtered and concentrated in vacuo. The residue was purified by silica gel column chromatography (1:1 to 1:3 (v/v) hexanes:AcOEt) to obtain **7r** (*Z* only). The residue was recrystallized from a solution of 1:5 (v/v) hexanes:$CHCl_3$ to give **(*Z*)-7r** (202.3 mg, 0.55 mmol, 66%) as a yellow solid. mp:198-199˚C; ^{1}H NMR (300 MHz, d_6-DMSO): δ = 2.29 (s, 3H), 3.77 (s, 3H), 3.80 (s, 3H), 6.90–7.05 (m, 3H), 7.39–7.44 (m, 1H), 7.87 (d, J = 5.1 Hz, 1H), 7.98 (d, J = 5.1 Hz, 1H), 8.16 (s, 1H), 8.24 (s, 1H), 10.37 (brs, 1H) ppm; ^{13}C NMR (100 MHz, d_6-DMSO): δ = 164.6, 163.9, 159.8, 155.4, 151.7, 139.4, 138.2, 134.8, 131.9, 130.0, 128.2, 127.6, 123.9, 120.8, 114.6, 114.4, 102.8, 55.4, 51.1, 14.4 ppm; IR (ATR): ν = 2478, 1714, 1688, 1604, 1593, 1564, 1495, 1458, 1429, 1384, 1360, 1344, 1319, 1310, 1286, 1274, 1237, 1210, 1189, 1177, 1145, 1117, 1071, 1058, 1032, 995, 950,

929, 887, 849, 837, 817, 808, 781, 761, 742, 708, 685, 651, 620, 608, 589, 576, 544, 480, 455, 422, 407 cm^{-1}; HRMS (FAB^+): $[M+H]^+$ calcd for $C_{20}H_{19}N_2O_5$, 367.1294; found, 367.1294; Elemental Anal.: calcd for $C_{20}H_{18}N_2O_5 \cdot 0.1H_2O$, C 65.57, H 4.95, N 7.65%; found, C 65.25, H 4.98, N 7.61%.

(*Z*)-4-Methoxycarbonyl-1-(3-methoxyphenyl)-5-methyl-3-(pyrimidin-5-ylmethylene)-2-pyrrolone ((*Z*)-7s)

To a solution of **8a** (313.5 mg, 1.2 mmol, 1.2 equiv.) in *t*-BuOH (3 mL) was added conc. HCl (206 μL, 2.4 mmol, 2.4 equiv.). After stirring for 15 min, 5-pyrimidinecarbaldehyde **29** (108.1 mg, 1.0 mmol, 1.0 equiv.) was added and the reaction mixture was refluxed for 4 h. After cooling to room temperature, the reaction mixture was concentrated in vacuo. The residue was purified by silica gel column chromatography (1% Et_3N in 3:1 to 3:2 (v/v) hexanes:AcOEt) to obtain an *E*/*Z* mixture of **7s** (*E*/*Z* = 16/84). The *E*/*Z* mixture was recrystallized from a solution of 3:1 (v/v) hexanes:AcOEt to give **(*Z*)-7s** (37.8 mg, 0.11 mmol, 11%) as red crystals. mp:183-184°C; ^1H NMR (399 MHz, d_6-DMSO): δ = 2.31 (s, 3H), 3.78 (s, 3H), 3.82 (s, 3H), 6.93–7.06 (m, 3H), 7.41–7.45 (m, 1H), 7.99 (s, 1H), 9.10 (s, 1H), 9.10 (s, 1H), 9.23 (s, 2H) ppm; ^{13}C NMR (100 MHz, d_6-DMSO): δ = 164.7, 163.7, 159.7, 157.6, 157.6, 156.3, 134.4, 131.1, 130.0, 129.3, 128.4, 120.6, 114.6, 114.3, 102.7, 55.3, 51.1, 14.3 ppm; IR (ATR): ν = 2951, 1688, 1602, 1589, 1575, 1543, 1489,

1440, 1412, 1387, 1361, 1341, 1313, 1287, 1249, 1216, 1197, 1169, 1150, 1126, 1104, 1061, 1042, 996, 936, 881, 834, 804, 776, 754, 712, 690, 659, 627, 609, 569, 488, 460 cm^{-1}; HRMS (FAB^+): $[M+H]^+$ calcd for $C_{19}H_{18}N_3O_4$, 352.1297; found, 352.1296; Elemental Anal.: calcd for $C_{19}H_{17}N_3O_4$, C 64.95, H 4.88, N 11.96%; found, C 64.68, H 4.65, N 11.74%.

(*Z*)-3-(4-Ethoxycarbonylbenzylidene)-4-methoxycarbonyl-1-(3-methoxyphenyl)-5-methyl-2-pyrrolone ((*Z*)-7t)

To a solution of **8a** (287.6 mg, 1.1 mmol, 1.5 equiv.) in *t*-BuOH (1.5 mL) was added conc. HCl (13 μL, 0.2 mmol, 0.2 equiv.). After stirring for 15 min, 4-ethoxycarbonylbenzaldehyde **30** (134.8 mg, 0.76 mmol, 1.0 equiv.) was added and the reaction mixture was refluxed for 1 h. After cooling to room temperature, the reaction mixture was concentrated in vacuo. The residue was purified by silica gel column chromatography (7:1 (v/v) hexanes:AcOEt) to obtain an *E*/*Z* mixture of **7t** (*E*/*Z* = 20/80). The *E*/*Z* mixture was recrystallized from a solution of 5:1 (v/v) hexanes:AcOEt to give **(*Z*)-7t** (139.5 mg, 0.33 mmol, 44%) as orange powder. mp:125-130˚C; ^{1}H NMR (300 MHz, $CDCl_3$): δ = 1.39 (t, *J* = 7.2 Hz, 3H), 2.36 (s, 3H), 3.82 (s, 3H), 3.89 (s, 3H), 4.37 (q, *J* = 7.2 Hz, 2H), 6.73–6.78 (m, 2H), 6.96–6.99 (m, 1H), 7.36–7.42 (m, 1H), 8.01 (d, *J* = 8.4 Hz, 2H), 8.09 (d, *J* = 8.4 Hz, 2H), 8.25 (s, 3H) ppm; ^{13}C NMR (100 MHz, $CDCl_3$):

δ = 166.2, 165.4, 164.6, 160.4, 154.1, 140.0, 138.7, 134.9, 131.2, 131.0, 130.2, 129.0, 127.8, 120.6, 114.8, 114.1, 104.3, 61.0, 55.5, 51.2 ppm; IR (ATR): ν = 3080, 2997, 2980, 2951, 2838, 1711, 1690, 1601, 1593, 1569, 1493, 1466, 1437, 1419, 1384, 1360, 1319, 1302, 1258, 1209, 1190, 1162, 1134, 1102, 1061, 1018, 1005, 934, 888, 869, 857, 825, 812, 805, 778, 752, 709, 688, 611, 584, 555, 510, 501, 482, 473, 437, 425, 409 cm^{-1}; HRMS (FAB^+): $[M+H]^+$ calcd for $C_{24}H_{24}NO_6$, 422.1604; found, 422.1599; Elemental Anal.: calcd for $C_{24}H_{23}NO_6$, C 68.40, H 5.50, N 3.32%; found, C 68.03, H 5.30, N 2.93%.

(*Z*)-4-Methoxycarbonyl-1-(3-methoxyphenyl)-5-methyl-3-(4-sulfamoylbenzylidene)-2-pyrrolone ((*Z*)-7u)

To a solution of **8a** (210.1 mg, 0.80 mmol, 1.5 equiv.) in *t*-BuOH (2 mL) was added conc. HCl (9 μL, 0.1 mmol, 0.2 equiv.). After stirring for 15 min, 4-formylbenzenesulfonamide **31** (96.3 mg, 0.52 mmol, 1.0 eq.) was added and the reaction mixture was refluxed for 4 h. After the reaction, the reaction mixture was concentrated in vacuo. The residue was purified by silica gel column chromatography (1:0 to 10:1 (v/v) $CHCl_3$:MeOH) to obtain an *E*/*Z* mixture of **7u** (*E*/*Z* = 14/86). The *E*/*Z* mixture was recrystallized from acetone to give **(*Z*)-7u** (144.9 mg, 0.39 mmol, 65%) as a yellow solid. mp:211-215˚C; ^{1}H NMR (300 MHz, d_6-DMSO): δ = 2.30 (s, 3H), 3.78 (s, 3H), 3.81 (s, 3H), 6.92–7.07 (m, 3H), 7.40–7.46 (m, 3H), 7.80 (d, *J* = 8.7 Hz, 2H), 8.12 (s, 1H), 8.13

(d, J = 8.7 Hz, 2H) ppm; ^{13}C NMR (100 MHz, d_6-DMSO): δ = 164.6, 164.0, 159.9, 155.3, 144.4, 137.4, 137.3, 134.8, 131.3, 130.1, 128.2, 125.1, 120.8, 114.7, 114.5, 103.0, 55.5, 51.2, 14.5 ppm; IR (ATR): ν = 3306, 3218, 3089, 2948, 2841, 1699, 1688, 1603, 1589, 1567, 1490, 1440, 1415, 1391, 1361, 1334, 1244, 1226, 1166, 1107, 1063, 1046, 947, 927, 890, 838, 822, 802, 783, 770, 756, 718, 685, 652, 627, 609, 592, 578, 545, 531, 491, 461, 407 cm^{-1}; HRMS (FAB$^+$): $[M+H]^+$ calcd for $C_{21}H_{21}N_2O_6S$, 429.1120; found, 429.1121; Elemental Anal.: calcd for $C_{21}H_{20}N_2O_6S \cdot 0.5H_2O \cdot 0.5C_3H_6O$, C 57.93, H 5.19, N 6.01%; found, C 58.08, H 5.13, N 5.74%.

(*Z*)-4-Methoxycarbonyl-1-(3-methoxyphenyl)-5-methyl-3-(4-(1*H*-tetrazol-5-yl)benzylidene)-2-pyrrolone ((*Z*)-7v)

To a solution of **8a** (327.7 mg, 1.3 mmol, 1.5 equiv.) in *t*-BuOH (3 mL) was added conc. HCl (14.5 μL, 0.2 mmol, 0.2 equiv.). After stirring for 15 min, 4-(1*H*-tetrazol-5-yl)benzaldehyde **32** (146.7 mg, 0.84 mmol, 1.0 eq.) was added and the reaction mixture was refluxed for 3 h. After cooling to room temperature, the reaction mixture was concentrated in vacuo. The residue was purified by silica gel column chromatography (100:1 to 50:1 (v/v) $CHCl_3$:MeOH) to obtain an *E*/*Z* mixture of **7v** (*E*/*Z* = 33/67). The *E*/*Z* mixture was recrystallized from AcOEt to give **(*Z*)-7v** (150.7 mg, 0.36 mmol, 43%) as orange crystals. mp:173-175˚C; ^{1}H NMR (300MHz, d_6-DMSO): δ = 2.30 (s, 3H), 3.79

(s, 3H), 3.82 (s, 3H), 6.94–7.08 (m, 3H), 7.41–7.46 (m, 1H), 8.05 (d, J = 8.4 Hz, 2H), 8.16 (s, 1H), 8.25 (d, J = 8.4 Hz, 2H), ppm; ^{13}C NMR (100 MHz, d_6-DMSO): δ = 164.5, 163.9, 159.7, 154.7, 137.9, 136.6, 132.0, 129.9, 127.7, 126.3, 120.7, 114.5, 114.3, 103.0, 55.3, 51.0, 14.4, 14.0 ppm; IR (ATR): ν = 3037, 2951, 1732, 1685, 1661, 1598, 1588, 1550, 1489, 1439, 1401, 1365, 1353, 1312, 1287, 1260, 1233, 1216, 1196, 1184, 1159, 1133, 1112, 1061, 1044, 1035, 1009, 996, 945, 936, 887, 855, 833, 805, 779, 769, 761, 743, 717, 692, 618, 584, 567, 530 cm^{-1}; HRMS (FAB$^+$): $[M+H]^+$ calcd for $C_{22}H_{19}N_5O_4$, 418.1515; found, 418.1514; Elemental Anal.: calcd for $C_{22}H_{19}N_5O_4 \cdot 0.5$AcOEt, C 62.47, H 5.02, N 15.18%; found, C 62.31, H 4.76, N 15.23%.

(*Z*)-3-(4-(Hydroxycarbamoyl)benzylidene)-4-methoxycarbonyl-1-(3-methoxyphenyl)-5-methyl-2-pyrrolone ((*Z*)-7w)

To a solution of **8a** (328.9 mg, 1.3 mmol, 1.5 equiv.) in *t*-BuOH (3 mL) was added conc. HCl aq. (14 μL, 0.16 mmol, 0.2 equiv.). After stirring for 15 min, 4-formyl-*N*-hydroxybenzamide **33** (139.4 mg, 0.84 mmol, 1.0 equiv.) was added and the reaction mixture was refluxed for 3 h. After the reaction, the reaction mixture was concentrated in vacuo. The residue was purified by silica gel column chromatography (1:0 to 50:1 (v/v) $CHCl_3$:MeOH) to obtain an *E*/*Z* mixture of **7w** (*E*/*Z* = 24/76). The *E*/*Z* mixture was recrystallized from AcOEt to give **(*Z*)-7w** (178.8 mg, 0.44 mmol, 52%) as a yellow solid.

mp:183-185˚C; ^{1}H NMR (300MHz, DMSO-d_6): δ 2.28 (s, 3H), 3.77 (s, 3H), 3.80 (s, 3H), 6.91–7.06 (m, 3H), 7.39–7.44 (m, 1H), 7.74 (d, J = 8.4 Hz, 2H), 8.07 (d, J = 8.4 Hz, 2H), 811 (s, 1H), 9.08 (brs, 1H), ppm; ^{13}C NMR (100MHz, DMSO-d_6): δ 164.5, 163.8, 159.7, 154.5, 138.2, 136.6, 134.8, 133.3, 131.0, 129.9, 127.4, 126.3, 120.7, 114.5, 114.3, 102.9, 55.3, 51.0, 14.4 ppm; IR (ATR): 3318, 3299, 3163, 3002, 2962, 2897, 1713, 1653, 1602, 1588, 1554, 1521, 1494, 1446, 1388, 1365, 1342, 1313, 1291, 1260, 1227, 1208, 1175, 1164, 1103, 1088, 1052, 1027, 1017, 996, 939, 916, 900, 887, 848, 826, 804, 774, 751, 710, 686, 643, 619, 607, 590, 566, 542, 491, 475, 451, 423, 413 cm^{-1}; HRMS (FAB^{+}, m/z): $[M+H]^{+}$ calcd for $C_{22}H_{21}N_2O_6$, 409.1400; found, 409.1399; Elemental Anal.: calcd for $C_{22}H_{20}N_2O_6$, C 64.70, H 4.94, N 6.86%; found, C 64.65, H 4.73, N 6.66%.

(*Z*)-3-(4-Carboxybenzylidene)-4-ethoxycarbonyl-1-(3-methoxyphenyl)-5-methyl-2-pyrrolone ((*Z*)-7x)

To a solution of **8k** (200.0 mg, 0.73 mmol, 1.2 equiv.) in *t*-BuOH (4 mL) was added conc. HCl (10 μL, 0.12 mmol, 0.2 equiv.). After stirring for 15 min, terephthalaldehydic acid **11** (90.9 mg, 0.61 mmol, 1.0 equiv.) was added and the reaction mixture was refluxed for 5 h. After cooling to room temperature, the reaction mixture was concentrated in vacuo. The residue was purified by recrystallization from AcOEt to give **(*Z*)-7x** (173.5 mg, 0.43 mmol, 70%) as an orange solid. mp:234-236˚C; ^{1}H NMR (300 MHz, d_6-

DMSO): δ = 1.32 (t, *J* = 7.2 Hz, 3H), 2.30 (s, 3H), 3.78 (s, 3H), 4.29 (q, *J* = 7.2 Hz, 2H), 6.92–7.06 (m, 3H), 7.40–7.45 (m, 1H), 7.92 (d, *J* = 8.4 Hz, 2H), 8.09 (d, *J* = 8.4 Hz, 2H), 8.15 (s, 1H) ppm; ^{13}C NMR (100 MHz, *d*$_6$-DMSO): δ = 166.8, 164.4, 163.4, 159.7, 154.8, 138.2, 137.7, 134.7, 131.1, 131.0, 129.9, 128.7, 128.0, 120.7, 114.5, 114.3, 103.0, 59.6, 55.3, 14.4, 14.2 ppm; IR (ATR): ν = 2978, 2542, 1677, 1601, 1591, 1569, 1493, 1464, 1424, 1402, 1375, 1346, 1318, 1287, 1255, 1228, 1205, 1187, 1157, 1126, 1107, 1077, 1057, 1023, 997, 967, 933, 862, 845, 817, 782, 750, 713, 690, 624, 607, 582, 542, 505, 458, 420, 407 cm^{-1}; HRMS (FAB$^+$): $[M+H]^+$ calcd for $C_{23}H_{22}NO_6$, 408.1447; found, 408.1448; Elemental Anal.: calcd for $C_{23}H_{21}NO_6$, C 67.81, H 5.20, N 3.44%; found, C 67.85, H 5.01, N 3.46%.

(*Z*)-4-(*tert*-Butoxycarbonyl)-3-(4-carboxybenzylidene)-1-(3-methoxyphenyl)-5-methyl-2-pyrrolone ((*Z*)-7y)

To a solution of **8l** (300.2 mg, 0.99 mmol, 1.2 equiv.) in AcOH (4 mL) was added terephthalaldehydic acid **11** (123.8 mg, 0.825 mmol, 1.0 equiv.) and the reaction mixture was refluxed for 3 h. After cooling to room temperature, the reaction mixture was concentrated in vacuo. The residue was purified by recrystallization from a solution of 3:1 (v/v) hexanes:AcOEt to give **(*Z*)-7y** (213.2 mg, 0.49 mmol, 59%) as an orange solid. mp:216-217˚C ˚C; ^{1}H NMR (300 MHz, *d*$_6$-DMSO): δ = 1.56 (s, 9H), 2.27 (s, 3H), 3.77

(s, 3H), 6.91–7.05 (m, 3H), 7.39–7.44 (m, 1H), 7.91 (d, J = 8.1 Hz, 2H), 8.08 (d, J = 8.1 Hz, 2H), 8.14 (s, 1H) ppm; ^{13}C NMR (100 MHz, d_6-DMSO): δ = 166.8, 164.4, 162.7, 159.7, 154.4, 138.2, 137.6, 134.8, 130.9, 129.9, 128.6, 128.1, 120.7, 114.5, 114.3, 104.0, 102.6, 80.4, 55.3, 28.0, 14.3 ppm; IR (ATR): ν =2976, 2548, 1708, 1684, 1673, 1604, 1593, 1550, 1495, 1469, 1452, 1427, 1391, 1363, 1320, 1308, 1295, 1260, 1215, 1189, 1172, 1154, 1129, 1108, 1082, 1061, 1046, 1014, 997, 967, 935, 855, 819, 803, 780, 751, 720, 707, 688, 642, 622, 611, 581, 550, 505, 463, 453, 432, 413 cm^{-1}; HRMS (FAB$^+$): [M+H]$^+$ calcd for $C_{25}H_{26}NO_6$, 436.1760; found, 436.1760; Elemental Anal.: calcd for $C_{25}H_{25}NO_6$, C 68.95, H 5.79, N 3.22%; found, C 68.70, H 5.67, N 3.16%.

(*Z*)-3-(4-Carboxybenzylidene)-4-((hexyloxy)carbonyl)-1-(3-methoxyphenyl)-5-methyl-2-pyrrolone ((*Z*)-7z)

To a solution of **8m** (308.2 mg, 0.93 mmol, 1.2 equiv.) in *t*-BuOH (4 mL) was added conc. HCl aq. (13 μL, 0.15 mmol, 0.2 equiv.) and terephthalaldehydic acid **11** (116.3 mg, 0.775 mmol, 1.0 equiv.). The reaction mixture was refluxed for 4 h. After cooling to room temperature, the reaction mixture was concentrated in vacuo. The residue was purified by recrystallization from a solution of 1:1 (v/v) hexanes:AcOEt to give **(*Z*)-7z** (188.5 mg, 0.43 mmol, 57%) as a yellow solid. mp:169-170˚C; ^{1}H NMR (300 MHz, d_6-DMSO): δ = 0.86 (t, J = 6.9 Hz, 3H), 1.28–1.41 (m, 6H), 1.66–1.73 (m, 2H), 2.23 (s, 3H),

3.78 (s, 3H), 4.24 (t, J = 6.6 Hz, 2H), 6.93–7.06 (m, 3H), 7.40–7.45 (m, 1H), 7.92 (d, J = 8.4 Hz, 2H), 8.08 (d, J = 8.4 Hz, 2H), 8.14 (s, 1H) ppm; ^{13}C NMR (100 MHz, d_6-DMSO): δ = 166.7, 166.4, 163.4, 159.7, 154.9, 138.2, 137.7, 134.7, 131.2, 131.0, 129.9, 128.7, 128.0, 120.7, 114.5, 114.3, 103.0, 63.6, 55.3, 30.8, 28.1, 25.3, 21.9, 14.3, 13.8 ppm; IR (ATR): ν = 2929, 1686, 1602, 1494, 1454, 1403, 1379, 1348, 1316, 1286, 1260, 1227, 1207, 1183, 1164, 1128, 1109, 1064, 988, 967, 928, 878, 856, 846, 817, 795, 769, 754, 726, 711, 689, 611, 583, 540, 519, 505, 488, 465, 418, 403 cm^{-1}; HRMS (FAB$^+$): $[M+H]^+$ calcd for $C_{27}H_{30}NO_6$, 464.2073; found, 464.2072; Elemental Anal.: calcd for $C_{27}H_{29}NO_6$, C 69.96, H 6.31, N 3.02%; found, C 69.80, H 6.28, N 3.17%.

(*E*)-3-(4-Carboxybenzylidene)-4-dimethylcarbamoyl-1-(3-methoxyphenyl)-5-methyl-2-pyrrolone ((*E*)-7aa)

To a solution of **8n** (202.8 mg, 0.74 mmol, 1.2 equiv.) in *t*-BuOH (1 mL) was added conc. HCl (11 μL, 0.13 mmol, 0.2 equiv.). After stirring for 15 min, terephthalaldehydic acid **11** (92.5 mg, 0.62 mmol, 1.0 equiv.) was added and the reaction mixture was refluxed for 3 h. After cooling to room temperature, the reaction mixture was concentrated in vacuo. The residue was purified by recrystallization from AcOEt to give **(*E*)-7aa** (91.2 mg, 0.22 mmol, 36%) as an orange solid. mp:208-210˚C; ^{1}H NMR (300 MHz, d_6-DMSO): δ = 1.94 (s, 3H), 2.59 (s, 6H), 3.80 (s, 3H), 6.95–7.03 (m, 3H), 7.40–7.48 (m, 4H), 7.93

(d, J = 8.1 Hz, 2H) ppm; ^{13}C NMR (100 MHz, d_6-DMSO): δ = 166.7, 166.6, 165.0, 159.7, 147.5, 138.6, 135.2, 130.8, 130.7, 129.8, 129.4, 128.7, 120.2, 114.0, 113.8, 107.8, 55.3, 37.1, 33.8, 12.7 ppm; IR (ATR): ν = 2927, 1703, 1599, 1490, 1452, 1414, 1369, 1309, 1244, 1175, 1105, 1046, 1020, 1005, 906, 871, 841, 792, 770, 755, 730, 715, 687, 663, 643, 600, 559, 514, 503, 457, 421 cm^{-1}; HRMS (FAB$^+$): $[M+H]^+$ calcd for $C_{23}H_{23}N_2O_5$, 407.1607; found, 407.1607; Elemental Anal.: calcd for $C_{23}H_{22}N_2O_5$, C 67.97, H 5.46, N 6.89%; found, C 67.80, H 5.30, N 6.79%.

(*Z*)-3-(4-Carboxybenzylidene)-1-(3-methoxyphenyl)-5-methyl-4-methylcarbamoyl-2-pyrrolone ((*Z*)-7ab)

To a solution of **8o** (200.0 mg, 0.77 mmol, 1.2 equiv.) in *t*-BuOH (1 mL) was added conc. HCl (11 μL, 0.13 mmol, 0.2 equiv.). After stirring for 15 min, terephthalaldehydic acid **5** (96.1 mg, 0.64 mmol, 1.0 equiv.) was added and the reaction mixture was refluxed for 2 h. After cooling to room temperature, the reaction mixture was concentrated in vacuo. The residue was purified by silica gel column chromatography (1:0 to 10:1 (v/v) AcOEt:MeOH). The purified *E*/*Z* mixture (174.1 mg, 0.444 mol, *E*/*Z* = 78/22) was dissolved in MeOH (40 mL) and irradiated by 365 nm LED light for 8 h. Then, isomerized *E*/*Z* mixture (*E*/*Z* =10/90) was purified by recrystallization from a solution of 1:1 (v/v) AcOEt:EtOH to give **(*Z*)-7ab** (129.2 mg, 0.329 mmol, 51%) as an orange solid.

mp:265-268˚C; ^{1}H NMR (300 MHz, d_6-DMSO): δ = 2.06 (s, 3H), 2.77 (d, J = 4.2 Hz, 3H), 3.79 (s, 3H), 6.86–7.05 (m, 3H), 7.40–7.47 (m, 2H), 7.91–7.97 (m, 3H), 8.18 (d, J = 8.4 Hz, 2H) ppm; ^{13}C NMR (100 MHz, d_6-DMSO): δ = 166.9, 164.5, 163.7, 159.8, 144.6, 138.1, 136.2, 135.4, 131.3, 130.0, 129.3, 128.9, 120.6, 114.2, 111.1, 55.4, 25.9, 13.4 ppm; IR (ATR): ν = 3276, 2940, 1689, 1627, 1605, 1588, 1532, 1488, 1424, 1383, 1341, 1317, 1289, 1241, 1187, 1112, 1049, 995, 960, 909, 877, 858, 803, 772, 723, 697, 606, 539, 499, 463, 412 cm^{-1}; HRMS (FAB^{+}): $[M+H]^{+}$ calcd for $C_{22}H_{21}N_2O_5$, 393.1450; found, 393.1451; Elemental Anal.: calcd for $C_{22}H_{20}N_2O_5 \cdot 0.1EtOH \cdot 0.3H_2O$, C 66.42, H 5.22, N 7.04%; found, C 66.30, H 4.95, N 7.02%.

3-Hydro-4-methoxycarbonyl-1-(3-methoxyphenyl)-5-methyl-2-pyrrolone (8a)

To a solution of dimethyl acetylsuccinate **9** (2.3 mL, 14 mmol, 1.0 equiv.) in acetic acid (20 mL) was added *m*-anisidine **10** (3.5 mL, 31 mmol, 2.2 equiv.) and the mixture was refluxed for 6 h. After cooling to room temperature, the reaction mixture was concentrated in vacuo. The residue was diluted with $CHCl_3$ and the organic layer was washed with 1M HCl aq., H_2O and brine, successively. The organic layer was dried over Na_2SO_4, filtered and concentrated in vacuo. The resulting residue was purified by silica gel column chromatography (6:1 to 5:1 (v/v) hexanes:AcOEt) and then recrystallized from a solution of 10:1 (v/v) hexanes:AcOEt to give **8a** (3.4 g, 13 mmol, 91%) as colorless

crystals. mp:84-86˚C; ^{1}H NMR (300 MHz, $CDCl_3$): δ = 2.25 (t, *J* = 2.4 Hz, 3H), 3.45 (m, 2H), 3.77 (s, 3H), 3.82 (s, 3H), 6.71–6.77 (m, 2H), 6.95–6.98 (m, 1H), 7.36–7.41 (m, 1H) ppm; ^{13}C NMR (100 MHz, $CDCl_3$): δ = 175.3, 164.6, 160.4, 154.5, 134.9, 130.3, 120.2, 114.6, 113.9, 103.7, 55.4, 51.2, 36.8, 13.5 ppm; IR (ATR): ν =□3059, 3012, 2949, 2916, 2842, 1728, 1688, 1636, 1604, 1589, 1492, 1435, 1396, 1375, 1335, 1313, 1297, 1264, 1237, 1189, 1162, 1131, 1092, 1069, 1048, 997, 977, 937, 891, 878, 844, 815, 781, 754, 735, 695, 625, 609, 579, 566, 526, 460, 437, 424, 413 cm^{-1}; HRMS (FAB^+, m/z): $[M+H]^+$ calcd for $C_{14}H_{16}NO_4$, 262.1079; found, 262.1080; Elemental Anal.: calcd for $C_{14}H_{15}NO_4$, C 64.36, H 5.79, N 5.36%; found, C 64.33, H 5.75, N 5.43%.

3-Hydro-4-methoxycarbonyl-1-(4-methoxyphenyl)-5-methyl-2-pyrrolone (8b)

To a solution of dimethyl acetylsuccinate **9** (430 μL, 2.7 mmol, 1.0 equiv.) in acetic acid (10 mL) was added *p*-anisidine **10** (720.5 mg, 5.9 mmol, 2.2 equiv.). The reaction mixture was refluxed for 4 h. After cooling to room temperature, the reaction mixture was concentrated in vacuo. The residue was diluted with $CHCl_3$ and the organic layer was washed with 1M HCl aq., H_2O and brine, successively. The organic layer was dried over Na_2SO_4, filtered and concentrated in vacuo. The resulting residue was purified by silica gel column chromatography (5:1 (v/v) hexanes:AcOEt) and recrystallized from a solution of 4:1 (v/v) hexanes:AcOEt to give **8b** (591.2 mg, 2.3 mmol, 85%) as a colorless

solid. mp:94-95˚C; ^{1}H NMR (300MHz, $CDCl_3$): δ 2.23 (t, *J* = 2.1 Hz, 3H), 3.43 (m, 2H), 3.77 (s, 3H), 3.84 (s, 3H), 6.98 (t, *J* = 8.7 Hz, 1H), 7.40 (t, *J* = 8.7 Hz, 2H) ppm; ^{13}C NMR (100MHz, $CDCl_3$): δ 175.8, 164.6, 159.7, 154.9, 129.2, 126.4, 114.8, 103.4, 55.5, 51.1, 36.7, 13.4 ppm; IR (ATR): 3056, 3021, 2997, 2971, 2945, 2906, 2842, 1724, 1689, 1626, 1513, 1459, 1435, 1397, 1382, 1333, 1302, 1238, 1207, 1188, 1172, 1138, 1127, 1112, 1065, 1024, 969, 955, 935, 842, 831, 819, 796, 756, 736, 717, 664, 645, 627, 609, 576, 532, 521 cm^{-1}; HRMS (FAB^+, m/z): $[M+H]^+$ calcd for $C_{14}H_{16}NO_4$, 262.1079; found, 262.1078; Elemental Anal.: calcd for $C_{14}H_{15}NO_4$, C 64.36, H 5.79, N 5.36%; found, C 64.41, H 5.59, N 5.34%.

3-Hydro-4-methoxycarbonyl-1-(2-methoxyphenyl)-5-methyl-2-pyrrolone (8c)

To a solution of dimethyl acetylsuccinate **9** (3.2 mL, 20 mmol, 1.0 equiv.) in AcOH (12 mL) was added *o*-anisidine **14** (4.4 mL, 39 mmol, 2.0 equiv.) and the mixture was refluxed for 3 h. After cooling to room temperature, the reaction mixture was concentrated in vacuo. The residue was diluted with $CHCl_3$ and the organic layer was washed with 1M HCl aq., water and brine, successively. The organic layer was dried over Na_2SO_4, and concentrated in vacuo. The resulting residue was purified by silica gel column chromatography (4:1 (v/v) hexanes:AcOEt) and then recrystallized from a solution of 5:3 (v/v) hexanes:AcOEt to give **8c** (2.3g, 8.7 mmol, 45%) as a colorless solid.

mp:116-118˚C; ^{1}H NMR (300MHz, $CDCl_3$): δ 2.15– 2.17 (t, *J* = 2.4 Hz, 3H), 3.43–3.45 (q, *J* = 2.4 Hz, 2H), 3.76 (s, 3H), 3.81 (s, 3H), 7.00–7.07 (m, 2H), 7.13–7.16 (m, 1H), 7.38–7.41 (m, 1H) ppm; ^{13}C NMR (400MHz, $CDCl_3$): δ 175.6, 164.8, 155.7, 155.5, 130.7, 130.2, 122.5, 121.0, 112.0, 103.2, 55.7, 51.0, 36.7, 12.8 ppm; IR (ATR): 3044, 3005, 2947, 2845, 1729, 1691, 1625, 1598, 1504, 1465, 1438, 1378, 1339, 1305, 1289, 1262, 1239, 1218, 1190, 1178, 1133, 1117, 1065, 1045, 1024, 943, 859, 830, 791, 754, 747, 726, 693, 632, 623, 604, 568, 524, 513, 477, 460, 438, 417 cm^{-1}; HRMS (FAB^{+}): $[M+H]^{+}$ calcd for $C_{14}H_{16}NO_4$, 262.1079; found, 262.1080; Elemental Anal.: calcd for $C_{14}H_{15}NO_4$, C 64.36, H 5.79, N 5.36%; found, C 64.14, H 5.68, N 5.26%.

3-Hydro-4-methoxycarbonyl-5-methyl-1-phenyl-2-pyrrolone (8d)

To a solution of dimethyl acetylsuccinate **9** (649 μL, 4.0 mmol, 1.0 equiv.) in acetic acid (20 mL) was added aniline **15** (804 μL, 8.8 mmol, 2.2 equiv.) and the mixture was refluxed for 4 h. After cooling to room temperature, the reaction mixture was poured into a mixture of sat. $NaHCO_3$ aq. and $CHCl_3$. The organic layer was washed with sat. $NaHCO_3$ aq., 1M HCl aq., H_2O and brine, successively. The organic layer was dried over Na_2SO_4, filtered and concentrated in vacuo. The resulting residue was purified by silica gel column chromatography (5:1 (v/v) hexanes:AcOEt) and recrystallized from a solution of 5:1 (v/v) hexanes:AcOEt to give **8d** (562.1 mg, 2.4 mmol, 61%) as a colorless solid.

mp:121-122˚C; ^{1}H NMR (300 MHz, $CDCl_3$): δ = 2.24 (t, *J* = 2.2 Hz, 3H), 3.45 (q, *J* = 2.2 Hz, 2H), 3.77 (s, 3H), 7.16–7.20 (m, 2H), 7.40–7.52 (m, 3H) ppm; ^{13}C NMR (100 MHz, $CDCl_3$): δ = 175.4, 164.6, 154.4, 133.9, 129.6, 128.9, 128.1, 103.8, 51.2, 36.8, 13.5 ppm; IR (ATR): ν = 3050, 2962, 1682, 1620, 1596, 1500, 1443, 1393, 1357, 1285, 1252, 1216, 1172, 1119, 1060, 950, 924, 832, 765, 750, 730, 695, 633, 601, 500, 488, 419 cm^{-1}; HRMS (FAB^+, m/z): $[M+H]^+$ calcd for $C_{13}H_{14}NO_3$, 232.0974; found, 232.0973; Elemental Anal.: calcd for $C_{13}H_{13}NO_3$, C 67.52, H 5.67, N 6.06%; found, C 67.47, H 5.44, N 6.09%.

1-(3-Chlorophenyl)-3-hydro-4-methoxycarbonyl-5-methyl-2-pyrrolone (8e)

To a solution of dimethyl acetylsuccinate **9** (811 μL, 5.0 mmol, 1.0 equiv.) in acetic acid (10 mL) was added 3-chloroaniline **16** (1150 μL, 11 mmol, 2.2 equiv.) and the mixture was refluxed for 1.5 h. After cooling to room temperature, the reaction mixture was concentrated in vacuo. The residue was diluted with $CHCl_3$ and the organic layer was washed with 1M HCl aq., H_2O and brine, successively. The organic layer was dried over Na_2SO_4, filtered and concentrated in vacuo. The resulting residue was purified by silica gel column chromatography (4:1 (v/v) hexanes:AcOEt) and recrystallized from a solution of 4:1 (v/v) hexanes:AcOEt to give **8e** (672.6 mg, 2.5 mmol, 51%) as colorless crystals. mp:109-110˚C; ^{1}H NMR (300 MHz, $CDCl_3$): δ = 2.26 (t, *J* = 2.4 Hz, 3H), 3.45 (m, 2H), 3.77 (s, 3H), 7.07–7.11 (m, 1H), 7.21–7.22 (m, 1H), 7.39–7.43 (m, 2H) ppm;

^{13}C NMR (100 MHz, $CDCl_3$): δ = 175.1, 164.5, 153.6, 135.2, 135.0, 130.5, 129.2, 128.4, 126.3, 104.3, 51.3, 36.7, 13.5 ppm; IR (ATR): ν = 3066, 2959, 1723, 1683, 1625, 1592, 1479, 1440, 1392, 1373, 1357, 1252, 1218, 1180, 1122, 1064, 972, 950, 920, 838, 790, 770, 753, 729, 692, 673, 639, 615, 606, 548, 520, 489, 443, 417 cm^{-1}; HRMS (FAB^+, m/z): $[M+H]^+$ calcd for $C_{13}H_{13}ClNO_3$, 266.0584; found, 266.0585; Elemental Anal.: calcd for $C_{13}H_{12}ClNO_3$, C 58.77, H 4.55, N 5.27%; found, C 58.66, H 4.20, N 5.26%.

3-Hydro-1-(3-hydroxyphenyl)-4-methoxycarbonyl-5-methyl-2-pyrrolone (8f)

To a solution of dimethyl acetylsuccinate **9** (1.6 mL, 10 mmol, 1.0 equiv.) in a mixture of acetic acid (20 mL) and anhydrous MeOH (5 mL) was added *m*-aminophenol **17** (2.2 g, 20 mmol, 2.0 equiv.). The reaction mixture was refluxed for 4 h. After cooling to room temperature, the reaction mixture was concentrated in vacuo. The resulting residue was diluted with AcOEt and the organic layer was washed with 1M HCl aq., H_2O and brine, successively. The organic layer was dried over Na_2SO_4, filtered and concentrated in vacuo. The resulting residue was recrystallized from a solution of 2:1 (v/v) hexanes:AcOEt to give **8f** (1493 mg, 6.0 mmol, 60%) as a colorless solid. mp:234-236˚C; ^{1}H NMR (300MHz, $CDCl_3$): δ 2.23–2.24 (m, 3H), 3.47 (m, 2H), 3.78 (s, 3H), 6.16–6.21 (m, 1H), 6.61 (s, 1H), 6.67–6.69 (m, 1H), 6.80–6.83 (s, 1H), 7.29–7.32 (m, 1H) ppm; ^{13}C NMR (100MHz, $CDCl_3$): δ 176.2, 164.6, 157.2, 154.4, 134.4, 130.5, 119.6, 116.5, 115.5,

104.2, 51.3, 37.0, 13.4 ppm; IR (ATR): 3301, 3060, 2962, 1677, 1608, 1593, 1496, 1484, 1440, 1391, 1359, 1311, 1279, 1221, 1184, 1170, 1150, 1122, 1067, 1002, 954, 928, 894, 868, 823, 791, 749, 733, 698, 613, 568, 529 cm^{-1} ; HRMS (FAB^+, m/z): $[M+H]^+$ calcd for $C_{13}H_{14}NO_4$, 248.0923; found, 248.0924; Elemental Anal.: calcd for $C_{13}H_{13}NO_4$, C 63.15, H 5.30, N 5.67%; found, C 63.05, H 5.03, N 5.64%.

3-Hydro-1-(3-isopropoxyphenyl)-4-methoxycarbonyl-5-methyl-2-pyrrolone (8g)

To a solution of **8f** (494.5 mg, 2.0 mmol, 1.0 equiv.) in THF (9.5 mL) was added *i*-PrOH (500 μL) and the mixture was stirred at 0 ˚C for 15 min. Then, 1,1′-(Azodicarbonyl)dipiperidine (ADDP) (757.0 mg, 3.0 mmol, 1.5 equiv.) and triphenylphosphine (PPh_3) (786.9 mg, 3.0 mmol, 1.5 equiv.) were added and the reaction temperature was allowed to warm to room temperature and stirred for 36 h. After the reaction, a solution of 1:1 (v/v) hexanes:Et_2O was added to the reaction solution and resulting precipitate was removed by filtration. The filtrate was washed with H_2O and brine, successively. The organic layer was dried over Na_2SO_4, filtered and concentrated in vacuo. The resulting residue was purified by silica gel column chromatography (4:1 (v/v) hexanes:AcOEt) to give **8g** (334.0 mg, 1.2 mmol, 58%) as pale yellow oil. ^1H NMR (300 MHz, $CDCl_3$): δ = 1.34 (d, *J* = 6.0 Hz, 2H), 2.26 (t, *J* = 2.4 Hz, 3H), 3.43–3.45 (m, 2H), 3.77 (s, 3H), 4.50–4.58 (m, 1H), 6.68–6.74 (m, 2H), 6.92–6.95 (m, 1H), 7.33–7.38

(m, 1H) ppm; ^{13}C NMR (100 MHz, $CDCl_3$): δ = 175.3, 164.7, 158.8, 154.6, 134.9, 130.3, 119.9, 116.2, 115.5, 103.7, 70.2, 51.2, 36.8, 22.0, 13.5 ppm; IR (ATR): ν = 3072, 2978, 2951, 1734, 1693, 1632, 1599, 1588, 1490, 1437, 1374, 1357, 1334, 1286, 1262, 1227, 1208, 1188, 1154, 1138, 1113, 1062, 1010, 996, 944, 871, 831, 811, 784, 753, 734, 694, 667, 650, 608, 597, 574, 521, 491, 462, 432, 422, 414 cm^{-1}; HRMS (FAB^+, m/z): $[M+H]^+$ calcd for $C_{16}H_{20}NO_4$, 290.1392; found, 290.1392.

1-(3-(Hexyloxy)phenyl)-3-hydro-4-methoxycarbonyl-5-methyl-2-pyrrolone (8h)

To a solution of **8f** (494.5 mg, 2.0 mmol, 1.0 equiv.) in THF (9.5 mL) was added *n*-hexanol (500 μL) and the mixture was stirred at 0 ˚C for 15 min. Then, 1,1′-(Azodicarbonyl)dipiperidine (ADDP) (757.0 mg, 3.0 mmol, 1.5 equiv.) and triphenylphosphine (PPh_3) (786.9 mg, 3.0 mmol, 1.5 equiv.) was added and the reaction temperature was allowed to warm to room temperature and stirred for 20 h. After the reaction, a solution of 1:1 (v/v) hexanes:Et_2O was added to the reaction solution and resulting precipitate was removed by filtration. The filtrate was washed with H_2O and brine, successively. The organic layer was dried over Na_2SO_4, filtered and concentrated in vacuo. The resulting residue was purified by silica gel column chromatography (6:1 (v/v) hexanes:AcOEt) to give **8h** (364.6 mg, 1.1 mmol, 55%) as pale yellow oil. ^{1}H NMR (300 MHz, $CDCl_3$): δ = 0.90 (t, *J* = 6.9 Hz, 3H), 1.33–1.44 (m, 6H), 1.73–1.82 (m, 2H),

2.25 (t, J = 2.4 Hz, 3H), 3.43–3.44 (m, 2H), 3.77 (s, 3H), 3.95 (t, J = 6.6 Hz, 2H), 6.70–6.74 (m, 2H), 6.93–6.96 (m, 1H), 7.33–7.39 (m, 1H) ppm; ^{13}C NMR (100 MHz, $CDCl_3$): δ = 175.4, 164.7, 160.0, 154.6, 134.8, 130.2, 120.0, 115.2, 114.4, 103.7, 68.3, 51.2, 36.8, 31.5, 29.1, 25.7, 22.6, 14.0, 13.5 ppm; IR (ATR): ν = 2932, 2860, 1736, 1695, 1633, 1602, 1591, 1492, 1437, 1376, 1357, 1334, 1288, 1263, 1227, 1208, 1156, 1127, 1063, 996, 935, 868, 823, 752, 734, 694, 667, 608, 574, 521, 491, 461, 413 cm^{-1}; HRMS (FAB^+, m/z): $[M+H]^+$ calcd for $C_{19}H_{26}NO_4$, 332.1862; found, 332.1863.

1-(2-Fluoro-5-methoxyphenyl)-3-hydro-4-(methoxycarbonyl)-5-methyl-2-pyrrolone (8i)

To a solution of dimethyl acetylsuccinate **9** (243 μL, 1.5 mmol, 1.0 equiv.) in acetic acid (3 mL) was added 2-fluoro-5-methoxyaniline **18** (423.4 mg, 3.0 mmol, 2.0 equiv.) in acetic acid (2 mL) and the mixture was refluxed for 8 h. After cooling to room temperature, the reaction mixture was diluted with AcOEt and the organic layer was washed with sat. $NaHCO_3$ aq., 1M HCl aq., H_2O and brine, successively. The organic layer was dried over Na_2SO_4, filtered and concentrated in vacuo. The resulting residue was purified by silica gel column chromatography (100:10:1 (v/v) hexanes:AcOEt:toluene) to give **8i** (104.7 mg, 0.38 mmol, 25%) as pale yellow oil. ^{1}H NMR (300 MHz, $CDCl_3$): δ = 2.24–2.25 (m, 3H), 3.44–3.48 (m, 2H), 3.77 (s, 3H), 3.80

(s, 3H), 6.73 (dd, J = 6.0, 3.0 Hz, 1H), 6.91–6.97 (m, 1H), 7.12–7.18 (m, 1H) ppm; ^{13}C NMR (100 MHz, $CDCl_3$): δ = 174.9, 164.5, 156.0, 154.1, 152.5 (d, $J_{C,F}$ = 242.4 Hz), 121.8 (d, $J_{C,F}$ = 14.4 Hz), 117.1 (d, $J_{C,F}$ = 22.0 Hz), 116.19 (d, $J_{C,F}$ = 7.7 Hz), 115.2, 104.2, 55.9, 51.2, 36.6, 12.8 ppm; IR (ATR): ν = 3016, 2952, 1738, 1696, 1635, 1607, 1507, 1436, 1383, 1357, 1335, 1301, 1261, 1234, 1210, 1188, 1160, 1129, 1062, 1029, 978, 956, 916, 861, 824, 751, 734, 690, 666, 647, 611, 578, 545, 502, 466, 405 cm^{-1}; HRMS (FAB^+, m/z): $[M+H]^+$ calcd for $C_{14}H_{15}FNO_4$, 280.0985; found, 280.0985.

1-(2-Chloro-5-methoxyphenyl)-3-hydro-4-(methoxycarbonyl)-5-methyl-2-pyrrolone (8j)

To a solution of dimethyl acetylsuccinate **9** (405 μL, 2.5 mmol, 1.0 equiv.) in acetic acid (5 mL) was added 2-chloro-5-methoxyaniline **19** (640 μL, 5.0 mmol, 2.0 equiv.) and the mixture was refluxed for 24 h. After cooling to room temperature, the reaction mixture was diluted with $CHCl_3$ and the organic layer was washed with sat. $NaHCO_3$ aq., 1M HCl aq., H_2O and brine, successively. The organic layer was dried over Na_2SO_4, filtered and concentrated in vacuo. The resulting residue was purified by silica gel column chromatography (7:1 (v/v) hexanes:AcOEt) and recrystallized from hexanes to give **8j** (334 mg, 1.1 mmol, 45%) as colorless powder. mp:78-79˚C; ^{1}H NMR (300 MHz, $CDCl_3$): δ = 2.19 (t, J = 2.4 Hz, 3H), 3.45–3.49 (m, 2H), 3.78 (s, 3H), 3.81 (s, 3H), 6.78

(d, J = 3.0 Hz, 1H), 6.95 (dd, J = 8.7, 3.0 Hz, 1H), 7.42 (d, J = 8.7 Hz, 1H) ppm; ^{13}C NMR (100 MHz, $CDCl_3$): δ = 174.8, 164.6, 159.1, 154.2, 132.4, 130.9, 124.6, 116.7, 116.2, 104.1, 55.8, 51.2, 36.6, 12.9 ppm; IR (ATR): ν = 2948, 2844, 1734, 1692, 134, 1598, 1578, 1486, 1435, 1379, 1366, 1334, 1290, 1276, 1250, 1229, 1207, 1190, 1166, 1128, 1077, 1061, 1023, 977, 881, 849, 821, 755, 737, 691, 658, 639, 615, 575, 554, 515, 483, 464, 436, 416 cm^{-1}; HRMS (FAB^+, m/z): $[M+H]^+$ calcd for $C_{14}H_{15}ClNO_4$, 296.0690; found, 296.0689; Elemental Anal.: calcd for $C_{14}H_{14}ClNO_4$, C 56.86, H 4.77, N 4.74%; found, C 56.91, H 4.58, N 4.78%.

4-Ethoxycarbonyl-3-hydro-1-(3-methoxyphenyl)-5-methyl-2-pyrrolone (8k)

To a solution of diethyl acetylsuccinate **36** (600 μL, 3.0 mmol, 1.0 equiv.) in acetic acid (10 mL) was added *m*-anisidine **10** (1.0 mL, 31 mmol, 3.0 equiv.) and the mixture was refluxed for 18 h. After cooling to room temperature, the reaction mixture was concentrated in vacuo. The residue was diluted with $CHCl_3$ and the organic layer was washed with 1M HCl aq., H_2O and brine, successively. The organic layer was dried over Na_2SO_4, filtered and concentrated in vacuo. The resulting residue was purified by silica gel column chromatography (7:1 (v/v) hexanes:AcOEt) and recrystallized from a solution of 4:1 (v/v) hexanes:Et_2O to give **8k** (385.6 mg, 1.4 mmol, 47%) as a colorless solid. mp:66˚C; ^{1}H NMR (300 MHz, $CDCl_3$): δ = 1.32 (t, J = 7.2 Hz, 3H), 2.25 (t, J = 2.4 Hz,

3H), 3.44 (m, 2H), 3.82 (s, 3H), 4.23 (q, J = 7.2 Hz, 2H), 6.70–6.77 (m, 2H), 6.94–6.98 (m, 1H), 7.35–7.41 (m, 1H) ppm; ^{13}C NMR (100 MHz, $CDCl_3$): δ = 175.4, 164.3, 160.4, 154.1, 135.0, 130.3, 120.2, 114.6, 113.9, 104.2, 59.9, 55.5, 36.8, 14.5, 13.5 ppm; IR (ATR): ν = 1721, 1683, 1634, 1594, 1493, 1470, 1432, 1382, 1362, 1332, 1298, 1280, 1267, 1235, 1218, 1192, 1175, 1161, 1128, 1089, 1067, 1035, 998, 856, 832, 789, 754, 728, 690, 611, 572, 479, 458, 418, 407 cm^{-1}; HRMS (FAB^+, m/z): $[M+H]^+$ calcd for $C_{15}H_{18}NO_4$, 276.1236; found, 276.1236; Elemental Anal.: calcd for $C_{15}H_{17}NO_4$, C 65.44, H 6.22, N 5.09%; found, C 65.52, H 6.15, N 5.09%.

4-(*tert*-Butoxycarbonyl)-3-hydro-1-(3-methoxyphenyl)-5-methyl-2-pyrrolone (8l)

To a solution of 1-(*tert*-butyl)-4-ethyl-2-acetylsuccinate **37** (500.0 mg, 2.1 mmol, 1.0 equiv.) in acetic acid (10 mL) was added *m*-anisidine **10** (918 μL, 8.20 mmol, 4.0 equiv.) and the mixture was refluxed for 12 h. After cooling to room temperature, the reaction mixture was poured into a mixture of sat. $NaHCO_3$ aq. and $CHCl_3$. The organic layer was washed with sat. $NaHCO_3$ aq., 1M HCl aq. and brine, successively. The organic layer was dried over Na_2SO_4, filtered and concentrated in vacuo. The resulting residue was purified by silica gel column chromatography (10:1 to 7:1 (v/v) hexanes:AcOEt) to give **8l** (534.3 mg, 1.8 mmol, 86%) as pale yellow oil. ^{1}H NMR (300 MHz, $CDCl_3$): δ = 1.52 (s, 9H), 2.21 (t, J = 2.4 Hz, 3H), 3.40 (m, 2H), 3.82 (s, 3H), 6.70–6.77 (m, 3H), 6.94–6.97

(m, 1H), 7.35–7.40 (m, 1H) ppm; ^{13}C NMR (100 MHz, $CDCl_3$): δ = 175.5, 163.7, 160.4, 152.8, 135.1, 130.2, 120.3, 114.5, 113.9, 105.8, 80.4, 55.4, 37.2, 28.4, 13.4 ppm; IR (ATR): ν = 2975, 1730, 1684, 1632, 1601, 1491, 1455, 1378, 1366, 1356, 1334, 1286, 1236, 1213, 1176, 1149, 1129, 1058, 996, 975, 929, 849, 832, 750, 731, 693, 666, 644, 607, 573, 519, 490, 461, 434, 424, 414 cm^{-1}; HRMS (FAB^+, m/z): $[M+H]^+$ calcd for $C_{17}H_{22}NO_4$, 304.1549; found, 304.1549.

3-Hydro-4-((hexyloxy)carbonyl)-1-(3-methoxyphenyl)-5-methyl-2-pyrrolone (8m)

To a solution of 4-ethyl-1-hexyl-2-acetylsuccinate **39** (431.4 mg, 1.6 mmol, 1.0 equiv.) in acetic acid (8 mL) was added *m*-anisidine **10** (370 μL, 3.5 mmol, 2.2 equiv.) and the mixture was refluxed for 6 h. After cooling to room temperature, the reaction mixture was poured into a mixture of sat. $NaHCO_3$ aq. and $CHCl_3$. The organic layer was washed with sat. $NaHCO_3$ aq., 1M HCl aq. and brine, successively. The organic layer was dried over Na_2SO_4, filtered and concentrated in vacuo. The resulting residue was purified by silica gel column chromatography (10:1 to 7:1 (v/v) hexanes:AcOEt) to give **8m** (501.5 mg, 1.5 mmol, 96%) as pale yellow oil. ^{1}H NMR (300 MHz, $CDCl_3$): δ = 0.90 (t, *J* = 6.9 Hz, 3H), 1.26–1.41 (m, 6H), 1.57–1.70 (m, 2H), 2.25 (t, *J* = 2.1 Hz, 3H), 3.45 (q, *J* = 2.1 Hz, 2H), 3.82 (s, 3H), 4.17 (t, *J* = 6.6 Hz, 2H), 6.70–6.78 (m, 2H), 6.94–6.98 (m, 1H), 7.35–7.41 (m, 1H) ppm; ^{13}C NMR (100 MHz, $CDCl_3$): δ = 175.4, 164.3, 160.4, 154.0,

135.0, 130.3, 120.2, 114.6, 113.9, 104.2, 64.2, 55.4, 36.8, 31.4, 28.7, 25.7, 22.5, 14.0, 13.5 ppm; IR (ATR): ν = 2930, 2858, 1735, 1690, 1632, 1601, 1492, 1456, 1383, 1331, 1286, 1262, 1228, 1207, 1157, 1126, 1060, 996, 975, 845, 826, 781, 752, 734, 693, 666, 607, 576, 518, 491, 458, 410 cm^{-1}; HRMS (FAB^+, m/z): $[M+H]^+$ calcd for $C_{19}H_{26}NO_4$, 332.1862; found, 332.1861.

4-(Dimethylcarbamoyl)-3-hydro-1-(3-methoxyphenyl)-5-methyl-2-pyrrolone (8n)

To a solution of methyl 3-(dimethylcarbamoyl)-4-oxopentanoate **42** (205 mg, 1.0 mmol, 1.0 equiv.) in a mixture of toluene (2.5 mL) and acetic acid (2.5 mL) was added *m*-anisidine **10** (216 µL, 2.0 mmol, 2.0 equiv.) and the mixture was refluxed for 4 h. After cooling to room temperature, the reaction mixture was concentrated in vacuo. The resulting residue was purified by silica gel column chromatography (AcOEt) to give **8n** (213 mg, 0.78 mmol, 76%) as orange oil. ^1H NMR (300 MHz, $CDCl_3$): δ = 1.89 (t, *J* = 2.4 Hz, 3H), 3.07 (s, 6H), 3.49 (q, *J* = 2.4 Hz, 2H), 3.82 (s, 3H), 6.72–6.79 (m, 2H), 6.92–6.96 (m, 1H), 7.34–7.39 (m, 1H) ppm; ^{13}C NMR (100 MHz, $CDCl_3$): δ = 175.4, 166.9, 160.4, 143.0, 135.4, 130.2, 120.2, 114.3, 113.8, 108.2, 55.4, 38.5, 13.5 ppm; IR (ATR): ν = 2926, 2242, 1716, 1600, 1489, 1454, 1389, 1361, 1316, 1286, 1246, 1224, 1202, 1150, 1097, 1051, 996, 975, 912, 839, 766, 752, 724, 694, 669, 644, 600, 558, 522, 489,

462, 446, 424 cm^{-1}; HRMS (FAB^+, m/z): $[M+H]^+$ calcd for $C_{15}H_{19}N_2O_3$, 275.1396; found, 275.1395.

3-Hydro-1-(3-methoxyphenyl)-5-methyl-4-methylcarbamoyl-2-pyrrolone (8o)

To a solution of methyl 3-(methylcarbamoyl)-4-oxopentanoate **44** (524.0 mg, 2.8 mmol, 1.0 equiv.) in a mixture of toluene (7.5 mL) and acetic acid (7.5 mL) was added *m*-anisidine **10** (885 μL, 4.70 mmol, 2.5 equiv.) and the mixture was refluxed for 9 h. After cooling to room temperature, the reaction mixture was concentrated in vacuo. The residue was purified by silica gel column chromatography (1:5 to 1:10 (v/v) hexanes:AcOEt) to give **8o** (202.6 mg, 0.78 mmol, 28%) as pale brown amorphous. ^1H NMR (300 MHz, $CDCl_3$): δ = 2.29 (t, *J* = 2.4 Hz, 3H), 2.91 (d, *J* = 4.5 Hz, 3H), 3.35 (q, *J* = 2.4 Hz, 2H), 3.82 (s, 3H), 5.30 (brs, 1H), 6.70–6.77 (m, 2H), 6.94–6.98 (m, 1H), 7.35–7.40 (m, 1H) ppm; ^{13}C NMR (100 MHz, $CDCl_3$): δ = 174.4, 164.8, 160.4, 150.9, 135.0, 130.2, 120.2, 114.5, 113.9, 105.9, 55.4, 26.4, 26.2, 13.2 ppm; IR (ATR): ν = 3351, 2935, 1714, 1646, 1599, 1531, 1490, 1454, 1410, 1369, 1327, 1284, 1245, 1220, 1190, 1173, 1098, 1036, 995, 974, 851, 822, 782, 732, 694, 608, 571, 516, 460, 414 cm^{-1}; HRMS (FAB^+, m/z): $[M+H]^+$ calcd for $C_{14}H_{17}N_2O_3$, 261.1239; found, 261.1239.

4-Ethyl-1-hexyl 2-acetylsuccinate (39)

To a flask, **37** (1465.7 mg, 6.0 mmol, 1.0 equiv.) and 4N HCl in dioxane were added and the mixture was stirred at room temperature for 12 h. After the reaction, the reaction mixture was diluted with $CHCl_3$ and H_2O and extracted with $CHCl_3$ three times. The combined organic layer was extracted with sat. $NaHCO_3$ aq. three times. The pH value of the combined aqueous layer was adjusted to 1 by adding 3M HCl aq. and the aqueous layer was extracted with $CHCl_3$ three times. The combined organic layer was washed with brine, dried over Na_2SO_4, filtered and concentrated in vacuo. The resulting residue (1050.2 mg) was used for the next reaction without further purification.

To a solution of the residue described in the previous reaction (1050.2 mg) in CH_2Cl_2 (15 mL) was added *n*-hexanol (748 μL, 6.0 mmol), EDC·HCl (1380.2 mg, 7.2 mmol) and DMAP (73.3 mg, 0.60 mmol). The resulting mixture was stirred at room temperature for 2 h. After the reaction, the reaction mixture was diluted with CH_2Cl_2 and washed with 1M HCl aq., H_2O and brine, successively. The organic layer was dried over Na_2SO_4, filtered, concentrated in vacuo. The residue was purified by silica gel column chromatography (10:1 to 5:1 (v/v) hexanes:AcOEt) to give **39** (366.6 mg, 1.4 mmol, 22% for 2 steps) as colorless oil. ^{1}H NMR (300 MHz, $CDCl_3$): δ = 0.89 (t, *J* = 6.6 Hz, 3H), 1.25 (t, *J* = 7.2 Hz, 3H), 1.30 (m, 6H), 1.59–1.66 (m, 2H), 2.36 (s, 3H), 2.97 (dd, *J* = 17.7, 8.4 Hz, 1H), 2.82 (dd, *J* = 17.7, 6.3 Hz, 1H), 3.99 (dd, *J* = 8.4, 6.3 Hz, 1H), 4.09–4.16 (m,

4H) ppm; ^{13}C NMR (100 MHz, $CDCl_3$): δ = 201.8, 171.4, 168.4, 66.0, 61.0, 54.6, 32.4, 31.3, 30.0, 28.4, 25.5, 22.5, 14.1, 14.0 ppm; IR (ATR): ν = 2958, 2933, 2860, 1719, 1467, 1411, 1375, 1355, 1318, 1250, 1157, 1096, 1031, 901, 861, 804, 756, 642, 554, 499, 427 cm^{-1}; HRMS (FAB^+, m/z): $[M+H]^+$ calcd for $C_{14}H_{25}O_5$, 273.1702; found, 273.1703.

Methyl 3-(dimethylcarbamoyl)-4-oxopentanoate (42)

To a reaction tube, dimethyl acetylsuccinate **9** (650 μL, 4.0 mmol, 1.0 equiv.) in toluene (4 mL) was added 2M dimethylamine in THF (4 mL, 8 mmol, 2.0 equiv.) and the mixture was reacted under microwave irradiation (150˚C, 3h). After the reaction, the reaction mixture was concentrated in vacuo. The residue was purified by silica gel column chromatography (1:1 (v/v) hexanes:AcOEt) to give **42** (455.8 mg, 2.3 mmol, 57%) as orange oil. ^{1}H NMR (300 MHz, $CDCl_3$): δ = 2.19 (s, 3H), 2.92 (d, *J* = 6.9 Hz, 2H), 3.01 (s, 3H), 3.17 (s, 3H), 3.69 (s, 3H), 4.14 (t, *J* = 6.9 Hz, 1H) ppm; ^{13}C NMR (100 MHz, $CDCl_3$): δ = 202.3, 172.1, 168.5, 52.8, 52.1, 37.9, 36.1, 32.8, 27.8 ppm; IR (ATR): ν = 2953, 1720, 1636, 1497, 1436, 1399, 1357, 1258, 1198, 1158, 1136, 1059, 1003, 956, 933, 904, 850, 752, 687, 634, 555, 503, 429 cm^{-1}; HRMS (FAB^+, m/z): $[M+H]^+$ calcd for $C_{14}H_{25}O_5$, 202.1079; found, 202.1079.

Methyl 3-(*N*-(4-methoxybenzyl)-*N*-methyl-carbamoyl)-4-oxopentanoate (43)

To a reaction tube, dimethyl acetylsuccinate **9** (1031 μL, 6.4 mmol, 1.0 equiv.) in toluene (16 mL) was added *N*-(4-methoxyphenyl)-*N*-methylamine **41** (1441.1 mg, 9.5 mmol, 1.5 equiv.) and the mixture was reacted under microwave irradiation (150˚C, 3h). After the reaction, the reaction mixture was diluted with AcOEt and washed with 1M HCl aq., H_2O and brine, successively. The organic layer was washed with brine, dried over Na_2SO_4, filtered and concentrated in vacuo. The residue was purified by silica gel column chromatography (2:1 (v/v) hexanes:AcOEt) to give **43** (1459.3 mg, 4.8 mmol, 75%, *E*/*Z* = 2/1) as yellow oil. ^{1}H NMR (300 MHz, $CDCl_3$): δ = 2.13 (s, 3H), 2.18 (s, 6H), 2.86–3.04 (m, 15H), 3.69 (s, 9H), 3.80 (s, 6H), 3.81 (s, 3H), 4.12–4.21 (m, 3H) 4.47–4.71 (m, 6H), 6.85–6.93 (m, 6H), 7.16–7.19 (m, 6H) ppm; ^{13}C NMR (100 MHz, $CDCl_3$): δ = 202.5, 202.3, 172.1, 172.0, 168.6, 159.1, 129.4, 128.8, 128.1, 128.0, 114.4, 114.1, 55.3, 55.3, 53.2, 53.1, 53.0, 52.1, 50.8, 35.2, 34.4, 33.1, 32.9, 27.8, 27.7 ppm; IR (ATR): ν = 3007, 2953, 1721, 1637, 1495, 1452, 1436, 1406, 1357, 1259, 1203, 1172, 1157, 1117, 1078, 1002, 896, 849, 748, 699, 666, 596, 555, 499, 459 cm^{-1}; HRMS (FAB$^+$, m/z): $[M+H]^+$ calcd for $C_{16}H_{22}NO_5$, 308.1498; found, 308.1498.

Methyl 3-(methylcarbamoyl)-4-oxopentanoate (44)

A solution of **43** (1570 mg, 5.1 mmol, 1.0 equiv.) in a mixture of MeCN (10 mL) and H_2O (10 mL) was cooled to 0˚C and ammonium cerium(IV) nitrate (7003.5 mg, 13 mmol, 2.5 equiv.) was added and the reaction temperature was allowed to warm to room temperature. After stirring for 4 h, sodium ascorbate (2531.8 mg, 13 mmol, 2.5 equiv.) was added and the reaction mixture was stirred for 15 min. The reaction mixture was diluted with AcOEt and the aqueous layer was extracted with AcOEt at three times. The combined organic layer was dried over Na_2SO_4, filtered and concentrated in vacuo. The resulting residue was purified by silica gel column chromatography (1:1 to 1:3 (v/v) hexanes:AcOEt) to give **44** (524.7 mg, 2.8 mmol, 55%) as a pale yellow solid. mp:80-81˚C; ^{1}H NMR (300 MHz, $CDCl_3$): δ = 2.29 (s, 3H), 2.81–2.89 (m, 4H), 3.00 (dd, *J* = 17.4, 7.2 Hz, 1H), 3.69 (s, 3H), 3.73 (t, *J* = 7.2 Hz, 1H), 6.16 (brs, 1H) ppm; ^{13}C NMR (100 MHz, $CDCl_3$): δ = 203.9, 172.3, 168.4, 56.5, 52.1, 32.9, 28.8, 26.7 ppm; IR (ATR): ν = 3306, 3098, 2946, 1732, 1715, 1644, 1561, 1435, 1409, 1359, 1343, 1278, 1250, 1201, 1180, 1156, 1025, 996, 977, 955, 916, 868, 851, 749, 713, 679, 601, 504 cm^{-1}; HRMS (FAB^+, m/z): $[M+H]^+$ calcd for $C_8H_{14}NO_4$, 188.0923; found, 188.0923.

X-ray data collection and refinement.

The crystalline sample of **(*Z*)-7a** and **(*E*)-7aa** were obtained by recrystallization from AcOEt. The X-ray diffraction images were obtained by XtaLAB synergy-S (RIGAKU, Tokyo, Japan) and analyzed by Olex2 software Ver. 2-1. 3 (OlexSys, Durham, UK).[48] The crystal structure was solved by the SHELXT program and refined by the SHELXL program.[49,50] The crystal data file for **(*Z*)-7a** and **(*E*)-7z** is deposited with Cambridge Crystallographic Data Centre (CCDC; Deposition numbers: 2156681 and 2156682).

Biology

Cell culture

MOLT-4 cells were cultured in RPMI-1640 medium (WAKO, Osaka, Japan) supplemented with 10% fetal bovine serum (FBS; Gibco, Grand Island, NY) and 100 U/mL penicillin (WAKO) and 0.1 mg/mL streptomycin (Tokyo Chemical Industry, Tokyo, Japan) maintained at 37˚C in a humidified atmosphere containing 5% CO_2.

Dye Exclusion Assay

A suspension of MOLT-4 cells in medium (7.0×10^5 cells/mL, 80 µL) was incubated (37˚C, 5% CO_2) for 24 h in a 96 well plate. The cells were treated with 20 µL of compound solution in a 1% DMSO medium and incubated (37˚C, 5% CO_2) for 1 h. The

cells were then irradiated/unirradiated with 10 Gy of ^{137}Cs γ−ray in Gammacell 40 (Nordion International, Ottawa, Canada) at room temperature. After further 27 h incubation (37˚C, 5% CO_2), the dead cells were stained with 25 μL of 1(w/v)% Erythrosine B (Tokyo Chemical Industry) in PBS and then stained/unstained cells were counted with a hemocytometer for cell viability. Graph creation and statistical analysis were carried out on GraphPad Prism 9 Software (San Diego, CA, USA).

Western Blot Analysis

A suspension of MOLT-4 cells in medium (1.25×10^6 cells/mL, 4 mL) was plated in a 6-well plate. The cells were treated with 8 μL of compound solution in DMSO and incubated (37˚C, 5% CO_2) for 1 h. Then, the cells were irradiated/unirradiated with 10 Gy of ^{137}Cs γ−ray at room temperature and incubated (37˚C, 5% CO_2) for 6 h. After the incubation, the cells were collected by centrifugation (400 g, 3 min, 4 ˚C) and washed twice with ice-cold PBS. The cell pellet was lysed with 50 μL of radioimmunoprecipitation assay (RIPA) buffer containing 50 mM Tris-HCl (pH 7.6), 150 mM NaCl, 1% Nonidet P40, 0.5% Sodium deoxycholate and 0.1% SDS (Nacalai Tesque, Kyoto, Japan). The lysed cells were mixed vigorously with voltex and kept at 4˚C for 30 min. The insoluble material was removed by centrifugation (20,000 g, 10 min, 4 ˚C) and

the supernatant was collected. The concentration of protein extract was quantified by BCA assay (Thermo Fischer Scientific, Massachusetts, USA). To a solution of protein, 1/3 volume of 4x Laemmli sample buffer containing 20% 2-mercaptoethanol, 8% SDS, 40% glycerol, 0.02% bromophenol blue and 250 mM Tris/HCl (pH 6.8) was added and the proteins were denatured by boiling at 100˚C for 5 min. The obtained protein samples were separated by SDS-poly acrylamide gel electrophoresis (PAGE), transferred to a polyvinylidene fluoride (PVDF) transfer membrane (Immobilon-P 0.45 μm, Merck Millipore, Darmstadt, Germany). The membrane was blocked with blocking one (Nacalai Tesque) at room temperature for 30 min and washed with Tris-buffer saline containing 0.1% tween-20 (TBST; Nacalai Tesque). The membrane was then reacted with a solution of anti-p53 antibody (DO-1, mouse mAb, Santa Cruz Biotechnology) or anti-GADPH antibody (14C10, rabbit mAb, Cell Signaling Technology) diluted in TBST (1:1000) at 4℃ overnight. The membrane was washed three times with TBST and reacted with horseradish peroxidase (HRP)-conjugated secondary antibody diluted in TBST (1:5000) at room temperature for 1 h. The membrane was washed three times with TBST and then the blot was developed by Chemi-Lumi One Ultra solution (Nacalai Tesque) and the luminescent image was obtained by ChemiDoc MP system (BioRad, California, USA)

equipped with a CCD camera. The image was analyzed by the Image Lab 6.0 software (BioRad).

[5-2] Materials and Methods for Chapter 3

Cell culture and treatment

Wild-type (wt)-p53-bearing human T-cell leukemia MOLT-4 cells[13,51-55] and their derivative transformed cell lines (Nega, KD-1, and R-p53-1)[11], KU812, KY821, Ball-1, CCRF-CEM, and U937 cells[51, 56-58] were cultured in RPMI 1640 medium (Wako, Japan) supplemented with 10% fetal bovine serum (FBS; Sigma) and antibiotics (100 U/ml penicillin and 0.1 mg/ml streptomycin (Nacalai Tesque, Japan). Thymocytes from ICR female mice aged 5 weeks (SLC, Inc., Japan) were prepared as described in a previous report[59], except for the composition of the medium. The composition of the medium is RPMI-1640 with supplemented with 10% FBS, 1 mM sodium pyruvate, 2 mM L-glutamine, 50 μM β-mercaptoethanol, and antibiotics. Cells were maintained at 37 °C in a humidified atmosphere containing 5% CO_2. Cell density was determined with a cell counter (Z1 Cell and particle counter, Beckman Coulter). Exponentially growing cell cultures (5×10^5 cells/ml) in tissue culture plates or flasks (Greiner) were irradiated at room temperature with an X-ray generator (MBR-1520R-3, Hitachi, Japan) operating at

150 kV–20 mA with a filter of 0.3 mm Cu and 0.5 mm Al at a dose rate of 1.6 Gy/min, or treated with etoposide (Wako). Each compound was added to the culture medium 1 h before irradiation (IR) or the etoposide treatment. The core 9,600 compounds were provided by the Drug Discovery Initiative, University of Tokyo, and primary screening was performed at the Center for Therapeutic Innovation, Graduate School of Biomedical Sciences, Nagasaki University. The experiments after the primary screening were performed at the University of Tokushima or Tokyo University of Science. STK160830 were purchased from Vitas-M Laboratory. It should be noted that STK160830 is a 1:1 mixture of *Z* and *E* forms with respect to the double bond indicated by the arrow in Figure 1A and was used as a mixture of these stereoisomers in this work, because we could not separate them due to the quick isomerization of this double bond (within 1 h) in solutions and in media at room temperature even under weak light. The protein concentrations of all the protein samples were determined using the BCA Protein Assay Reagent (Thermo Fisher Scientific) and equalized.

Apoptosis assay

Cell viability was determined by means of the WST-8 reduction assay (Cell counting kit-8; Dojindo, Japan**),** MitoTracker Red CMXRos (Molecular Probes) staining, or the

erythrosin B dye-exclusion test[11,13,59]. The graphs for the experiments with 3-5 independent experiments show the means and standard deviations. Statistical significance was determined by one-way analysis of variance (*F*-test) followed by individual two-tailed *t*-test or Dunnett's multiple comparison test using Microsoft Excel for Mac 2011 with the add-in software Statcel 4 (OMS publisher Ltd., Japan) unless otherwise specified. Linear regression analyses were performed using Microsoft Excel for Mac.

Immunoblotting analysis

Immunoblotting was performed essentially as described in a previous report[39]. We used the following antibodies as primary antibodies: p53 (clone DO-1, sc-126 HRP, Santa Cruz Biotechnology), p21 (clone EA10, Calbiochem), PUMA (Ab-1, Calbiochem), p53DINP1 (NB100-56627, Novus Biologicals), GAPDH (clone 6C5, GeneTex), β-Actin (clone AC-15, Sigma), caspase-3 (ab90437, abcam), or caspase-7 (clone 4G2, MBL, Japan).

Quantitative PCR (qPCR) analysis

qPCR analysis was performed on a Step one plus Real-Time PCR system (Applied Biosystems) as described previously [13]. An absolute quantification was performed by

comparing the Ct of the unknown samples with the standard curve obtained from purified amplicons using PCR Clean-up kit (Macherey Nagel). Nascent RNA transcripts were captured by labeling intracellular nascent RNA with 5-ethynyl-uridine (EU) using the Click-iT Nascent RNA Capture Kit (Invitrogen).

The primers used in these analyses were as follows:

TP53 (which encodes p53),

(forward) 5'-AGGCCTTGGAACTCAAGGAT-3'

(reverse) 5'-CCCTTTTTGGACTTCAGGTG-3'

ACTB (which encodes β-Actin),

(forward) 5'-TGGCACCCAGCACAATGAA-3'

(reverse) 5'-CTAAGTCATAGTCCGCCTAGAAGCA-3'

GAPDH,

(forward) 5'-CCCCGGTTTCTATAAATTGAGC-3'

(reverse) 5'-CTTCCCCATGGTGTCTGAG-3'

CDKN1A (which encodes p21),

(forward) 5'-GGTGGCAGTAGAGGCTATGGACA-3'

(reverse) 5'-GGCTCAACGTTAGTGCCAGGA-3'

TP53INP1 (which encodes p53DINP1),

(forward) 5’-CTGTCTAGCTGTGCATAACTCCT-3’

(reverse) 5’-CCCCATTTCATTTTGAGCTT-3’

BBC3 (which encodes PUMA),

(forward) 5’-AGCCAAACGTGACCACTAGC-3’

(reverse) 5’-GCAGAGCACAGGATTCACAG-3’

DNA melting-curve analysis

Thermal denaturation experiments of calf thymus DNA (ctDNA; Sigma) in 10 mM HEPES-NaOH buffer (pH 7.4) with I = 0.1 ($NaNO_3$) were performed on a JASCO V-550 UV/vis spectrophotometer (JASCO, Japan) equipped with a thermoelectric temperature controller (±0.5 °C), a stirring unit, and a 10 mm quartz cuvette. Thermal melting curves for 50 μM ctDNA were obtained by following the absorption change at 260 nm as an effect of the raising temperature (1 °C /min). The melting temperature (*T*m) value was graphically determined from the spectral data, and the Δ*T*m value for each condition was calculated from the results in the presence and absence of additives.

Chapter 6.

References

References

1. Chandra, R. A.; Keane, F. K.; Voncken, F. E. M.; Thomas, C. R. Contemporary radiotherapy: present and future. *Lancet* **2021**, *398*, 171–184.

2. (a) Bentzen, S. M.; Tucker, S. L. Quntifying the position and steepness of radiation dose-response curve. *Int. J. Radiat. Biol*. **1996**, *71*, 531–542. (b) He, L.; Yu, X.; Li, W. Recent progress and trends in X-ray-induced photodynamic therapy with low radiation doses. *ACS Nano* **2022** ASAP.

3. (a) Kamran, M. Z.; Ranjan, A.; Kaur, N.; Sur, S.; Tandon, V. Radioprotective agents: strategies and translational advances. *Med. Res. Rev.* **2016**, *36*, 461–493. **(**b) Mum, G.; Kim, S.; Choi, E.; Kim, C. S.; Lee, Y. S. Pharmacology of natural radioprotectors. *Arch*. *Pharm*. *Res*. **2018**, *41*, 1033−1050.

4. Obrador, E.; Salvador R.; Villaescusa, J., I.; Soriano, J. M.; Estrela, J. M.; Montoro, A. Radioprotection and radiomitigation: from the bench to clinical practice. *Biomedicines* **2020**, *8*, 461.

5. Levine, A. J.; Oren, M. The first 30 years of p53: growing ever more complex. *Nat. Rev. Cancer* **2009**, *9*, 749–758.

6. Hafner, A.; Bulyk, M. L.; Jambhekar, A.; Lahav, G. The multiple mechanisms that regulate p53 activity and cell fate. *Nat. Rev. Mol. Cell Biol.* **2019**, *20*, 199–210.

7. Moding, E. J.; Kaston, M. B.; Kirsch, D. G. Strategies for optimizing the response of cancer and normal tissues to radiation. *Nat. Rev. Drug Discov.* **2013**, *12*, 526–542.

8. Komarov, P. G.; Komarova, E. A.; Kondratov, R. V.; Christov-Tselkov, K.; Coon, J. S.; Chernov, M. V.; Gudkov, A. V. A. A chemical inhibitor of p53 that protects mice from the side effects of cancer therapy. *Science* **1999**, *285*, 1733−1737.

9. (a) Arienti, K. L.; Brunmark, A.; Axe, F. U.; McClure, K.; Lee, A.; Blevitt, J.; Neff, D. K.; Huang, L.; Crawford, S.; Pandit, C. R.; Karlsson, L.; Breitenbucher, J. G. Checkpoint kinase inhibitors: SAR and radioprotective properties of a series of 2-arylbenzimidazoles. *J. Med. Chem.* **2005**, *48*, 1873–1885. (b) Christophorou, M. A.; Ringshausen, I.; Finch, A. J.; Swingart, L. B.; Evan, G. I. The pathological response to DNA damage does not contribute to p53-mediated tumour suppression. *Nature* **2006**, *443*, 214−217. (c) Ventura, A.; Kirsch, D. G.; McLaughlin, M. E.; Tuveson, D. A.; Grimm, J.; Lintault, L.; Newman, J.; Reczek, E. E.; Weissler, R.; Jacks, T. Restoration of p53 function leads to tumor regression *in vivo*. *Nature* **2007**, *445*, 661–665. (d) Li, T.; Kon, N.; Jiang, L.; Tan, M.; Ludwig, T.; Zhao, Y.; Baer, R.; Gu, W. Tumor suppression in the absence of p53-mediated cell-cycle arrest, apoptosis, and senescence. *Cell* **2012**, *149*, 1269−1283. (e) Wang, X.; Wei, L.; Cramer, J. M.; Leibowitz, B. J.; Judge, C.; Epperly, M.; Greenberger, J.; Wang, F.; Li, L.; Stelzner,

M. G.; Dunn, J. C. Y.; Martin, M. G.; Lagasse, E.; Zhang, L.; Yu, J. Pharmacologically blocking p53-dependent apoptosis protects intestinal stem cells and mice from radiation. *Sci. Rep*. **2015**, *5*, 8566. (f) Stewart-Ornstein, J.; Iwamoto, Y.; Miller, M. A.; Prytyskach, M. A.; Ferrentti, S.; Holzer, P.; Kallen, J.; Furet, P.; Jambhekar, A.; Forrester, W. C.; Weissleder, R.; Lahav, G. p53 dynamics vary tissues and are linked with radiation sensitivity. *Nat. Commun*. **2021**, *12*, 898.

10. Cho, Y.; Gorina, S.; Jeffrey, P. D.; Pavletich, N. P. Crystal structure of a p53 tumor suppressor-DNA complex: understanding tumorigenic mutations. *Science* **1994**, *265*, 346–355.

11. (a) Morita, A.; Zhu, J.; Suzuki, N.; Enomoto, A.; Matsumoto, Y.; Tomita, M.; Suzuki, T.; Ohtomo, K.; Hosoi, Y. Sodium orthovanadate suppresses DNA damage-induced caspase activation and apoptosis by inactivating p53. *Cell Death Differ.* **2006**, *13*, 499–511. (b) Morita, A.; Ariyasu, S.; Ohya, S.; Takahashi, I.; Wang, B.; Tanaka, K.; Uchida, T.; Okazaki, H.; Hanaya, K.; Enomoto, A.; Nenoi, M.; Ikekita, M.; Aoki, S.; Hosoi, Y. Evaluation of zinc(II) chelators for inhibiting p53-mediated apoptosis. *Oncotarget* **2013**, *4*, 2439–2450. (c) Morita, A.; Wang, B.; Tanaka, K.; Katsube, T.; Murakami, M.; Shimokawa, T.; Nishiyama, Y.; Ochi, S.; Satoh, H.; Nenoi, M.; Aoki, S. Protective effects of p53 regulatory agents against high-LET radiation-induced

injury in mice. *Front. Public Health* **2020**, *8*, 601124. (d) Nishiyama, Y.; Morita, A.; Wang, B.; Sakai, T.; Ramadhani, D.; Satoh, H.; Tanaka, K.; Sasatani, M.; Ochi, S.; Tominaga, M.; Ikushima, H.; Ueno, J.; Nenoi, M.; Aoki, S. Evaluation of sodium orthovanadate as a radioprotective agent under total-body irradiation and partial-body irradiation conditions in mice. *Int. J. Rad. Biol.* **2021**, *97*, 1241–1251.

12. Ariyasu, S.; Sawa, A.; Morita, A.; Hanaya, K.; Hosoi, M.; Takahashi, I.; Wang, B.; Aoki, S. Design and synthesis of 8-hydroxyquinoline-based radioprotective agents. *Bioorg. Med. Chem.* **2014**, *22*, 3891–3905.
13. Morita A.; Takahashi, I.; Sasatani, M.; Aoki, S.; Wang, B.; Ariyasu, S.; Tanaka, K.; Yamaguchi, T.; Sawa, A.; Nishi, Y.; Teraoka, T.; Ujita, S.; Kawate, Y.; Yanagawa, C.; Tanimoto, K.; Enomoto, A.; Nenoi, M.; Kamiya, K.; Nagata, Y.; Hosoi, Y.; Inaba, T. A chemical modulator of p53 transactivation that acts as a radioprotective agonist. *Mol. Cancer Ther.* **2018**, *17*, 432–442.
14. Jean-Jacques, C.; Jianmin, F.; Rajender, K.; Kashinath, S.; Zaihui, Z. Pyrazole and pyrrole compounds useful in treating iron disorders. US2009058730.
15. Matten, B.; Kostermans, M.; Baelen, G. V.; Swet, M.; Dahaen, W. Synthesis of 5-aryl-2-oxopyrrole derivatives as synthons for highly substituted pyrroles. *Tetrahedron*. **2006**, *62*, 6018−6028.
16. (a) Braun, W.; Go, N. Calculation of protein conformations by proton-proton distance

constraints: a new efficient algorithm. *J. Mol. Biol.* **1985**, *186*, 611–626. (b) Marintchev, A.; Frueh, D.; Wagner, G. NMR methods for studying protein-protein interactions involved in translation initiation. *Methods Enzymol.* **2007**, *430*, 283–331.

17. Strohmeier, G. A.; Kappe, C. O. Rapid parallel synthesis of polymer-bound enones utilizing microwave-assisted solid-phase chemistry. *J. Comb. Chem*. **2002**, *4*, 154–161.
18. Ballatore, C.; Huryn, D. M.; Smith, A. B. Carboxylic acid (bio)isosteres in drug design. *ChemMedChem* **2013**, *8*, 385–395.
19. Chernova, O. B.; Chernov, M. V.; Agarwal, M. L.; Taylor, W. R.; Stark, G. R. The role of p53 in regulating genomic stability when DNA and RNA synthesis are inhibited. *Trends Biochem. Sci.* **1995**, *20,* 431–434.
20. Ljungman, M.; Zhang, F.; Chen, F.; Rainbow, A. J.; McKay, B. C. Inhibition of RNA polymerase II as a trigger for the p53 response. *Oncogene* **1999**, *18,* 583–592.
21. Arima, Y.; Nitta, M.; Kuninaka, S.; Zhang, D.; Fujiwara, T.; Taya, Y.; Nakao, M.; Saya, H. Transcriptional blockade induces p53-dependent apoptosis associated with translocation of p53 to mitochondria. *J. Biol. Chem.* **2005**, *280*, 19166–19176.
22. Ross, W. E.; Bradley, M. O. DNA double-stranded breaks in mammalian cells after exposure to intercalating agents. *Biochim. Biophys. Acta* **1981**, *654,* 129–134.
23. Chen, A. Y.; Liu, L. F. DNA topoisomerases: essential enzymes and lethal targets. *Annu. Rev. Pharmacol. Toxicol.* **1994**, *34,* 191–218.

24. Ferguson, L. R.; Baguley, B. C. Topoisomerase II enzymes and mutagenicity. *Environ. Mol. Mutagen.* **1994**, *24,* 245–261.

25. Chodosh, L. A.; Fire, A.; Samuels, M.; Sharp, P. A. 5,6-Dichloro-1-beta-D-ribofuranosylbenzimidazole inhibits transcription elongation by RNA polymerase II in vitro. *J. Biol. Chem.* **1989**, *264,* 2250–2257.

26. Prelich, G. RNA polymerase II carboxy-terminal domain kinases: emerging clues to their function. *Eukaryot. Cell* **2002**, *1,* 153–162.

27. Sims, R. J.; Belotserkovskaya, R.; Reinberg, D. Elongation by RNA polymerase II: the short and long of it. *Genes Dev.* **2004**, *18,* 2437–2468.

28. Sellins, K. S.; Cohen, J. J. Gene induction by gamma-irradiation leads to DNA fragmentation in lymphocytes. *J. Immunol*. **1987**, *139,* 3199–3206.

29. Yamada, T.; Ohyama, H. Radiation-induced interphase death of rat thymocytes is internally programmed (apoptosis). *Int. J. Radiat. Biol. Relat. Stud. Phys. Chem. Med.* **1988**, *53,* 65–75.

30. Lowe, S. W.; Schmitt, E. M.; Smith, S. W.; Osborne, B. A.; Jacks, T. p53 is required for radiation-induced apoptosis in mouse thymocytes. *Nature* **1993**, *362,* 847–849.

31. Clarke, A. R.; Purdie, C. A.; Harrison, D. J.; Morris, R. G.; Bird, C. C.; Hooper M. L.; Wyllie, A. H. Thymocyte apoptosis induced by p53-dependent and independent pathways. *Nature* **1993**, *362*, 849–852.

32. Petrova, G. V.; Donchenko, G. V. Effect of alpha-tocopherol and its derivatives on actinomycin D induced apoptosis of rat thymocytes. *Ukr. Biokhim. Zh. (1999)* **2005**, *77,* 72–77.

33. Kasai, T.; Ohguchi, K.; Nakashima, S.; Ito, Y.; Naganawa, T.; Kondo, N.; Nozawa, Y. Increased activity of oleate-dependent type phospholipase D during actinomycin D-induced apoptosis in Jurkat T cells. *J. Immunol.* **1998**, *61,* 6469–6474.

34. Caelles, C.; Helmberg, A.; Karin, M. p53-dependent apoptosis in the absence of transcriptional activation of p53-target genes. *Nature* **1994**, *370,* 220–223.

35. Marchenko, N. D.; Zaika, A.; Moll, U. M. Death signal-induced localization of p53 protein to mitochondria: a potential role in apoptotic signaling. *J. Biol. Chem.* **2000**, *275,* 6202–6212.

36. Mihara, M.; Erster, S.; Zaika, A.; Petrenko, O.; Chittenden, T.; Pancoska, P.; Moll, U. M. p53 has a direct apoptogenic role at the mitochondria. *Mol. Cell* **2003**, *11,* 577–590.

37. Marchenko, N. D.; Wolff, S.; Erster, S.; Becker, K.; Moll, U. M. Monoubiquitylation promotes mitochondrial p53 translocation. *EMBO J.* **2007**, *26*, 923–934.

38. Taylor, M. H.; Buckwalter, M. R.; Stephenson, A. C.; Hart, J. L.; Taylor, B. J.; O'Neill, K. L. Radiation-induced apoptosis in MOLT-4 cells requires de novo protein synthesis independent of de novo RNA synthesis. *FEBS Lett.* **2002**, *514,* 199–203.

39. Ito, A.; Morita, A.; Ohya, S.; Yamamoto, S.; Enomoto, A.; Ikekita, M. Cycloheximide suppresses radiation-induced apoptosis in MOLT-4 cells with Arg72 variant of p53 through translational inhibition of p53 accumulation. *J. Radiat. Res.* **2011**, *52,* 342–350.

40. Clark, R. L.; Johnston, B. F.; Mackay, S. P.; Breslin, C. J.; Robertson, M. N.; Harvey, A. L. The Drug Discovery Portal: a resource to enhance drug discovery from academia. *Drug Discov. Today* **2010**, *15,* 679–683.

41. (a) Dumont, P.; Leu, J. I.; Della Pietra, A. C. 3rd; George, D. L.; Murphy, M. The codon 72 polymorphic variants of p53 have markedly different apoptotic potential. *Nature Genet.* **2003**, *33,* 357–365. (b)Liu, Y.; Zhang, X.; Han, C.; Wan, G.; Huang, X.; Ivan, C.; Jiang, D.; Rodriguez-Aguayo, C.; Lopez-Berestein, G.; Rao, P. H.; Maru, D. M.; Pahl, A.; He, X.; Sood, A. K.; Ellis, L. M.; Anderl, J.; Lu, X. TP53 loss creates therapeutic vulnerability in colorectal cancer., *Nature* **2015**, *520,* 697-701.

42. Pim, D.; Banks, L. p53 polymorphic variants at codon 72 exert different effects on cell cycle progression. *Int. J. Cancer* **2004**, *108,* 196–199.

43. Ye, H.; Liu, X.; Lv, M.; Wu, Y.; Kuang, S.; Gong, J.; Yuan, P.; Zhong, Z.; Li, Q.; Jia, H.; Sun, J.; Chen, Z.; Guo, A.Y. MicroRNA and transcription factor co-regulatory network analysis reveals miR-19 inhibits CYLD in T-cell acute lymphoblastic leukemia. *Nucleic Acids Res*. **2012**, *40,* 5201–5214.

44. Aguilar, N.; Fernandez, J.; Terricabras, E.; Carceller, G. E.; Salas, S. J. Substituted tricyclic compounds with activity towards EP1 receptors. WO/2013/149997 A1.

45. Rodrigues, D. A.; Ferreira-Silva, G. À.; Ferreira, A. C. S.; Frnandes, R. A.; Kwee, J. K.; Sant'Anna, C. M. R.; Ionta, M. and Fraga, C. A. M. Design, Synthesis, and Pharmacological Evaluation of Novel *N*-Acylhydrazone Derivatives as Potent Histone Deacetylase 6/8 Dual Inhibitors *J. Med. Chem*. **2016**, *59*, 655−670.

46. Tsuboi, S.; Sakamoto, J.; Yamashita, H.; Sakai, T.; Utaka, M. Highly enantioselective synthesis of both enantiomers of γ-substituted butenolides by Bakers' yeast reduction and lipase-catalyzed hydrolysis. Total synthesis of (3AS, 6aS)-Ethisolide, Whisky Lactone, and (-)-Avenaciolide. *J. Org. Chem*. **1998**, *63*, 1102–1108.

47. Tintori, C.; Brai, A.; Lang, M. C. D.; Deodato, D.; Greco, A. M.; Bizzarri, B. M.; Cascone, L.; Casian, A.; Zamperini, C.; Dreassi, E.; Crespan, E.; Maga, G.; Vanham, G.; Ceresola, E.; Canducci, F.; Ariën, K. K.; Botta, M. Development and in vitro evaluation of a microbicide gel formulation for a novel non-nucleoside reverse transcriptase inhibitor belonging to *N*-dihydro-alkyloxy-benzyl-oxopyrimidines (N-DABOs) family. *J. Med. Chem*. **2016**, *59,* 2747–2759.

48. Dolomanov, O. V.; Bourhis, L. J.; Gildea, R. J.; Howard, J. A. K.; Puschmann, H.

OLEX2: a complete structure solution, refinement and analysis program. *J. Appl. Cryst.* **2009**, *42*, 339–341.

49. Sheldrick, G. M. SHELXT-integrated space-group and crystal-structure determination. *Acta. Cryst.* **2015**, *A71*, 3–8.
50. Sheldrick, G. M. Crystal structure refinement with SHELXL. *Acta. Cryst.* **2015**, *C71*, 3–8.
51. Cheng, J.; Haas, M. Frequent mutations in the p53 tumor suppressor gene in human leukemia T-cell lines. *Mol. Cell Biol.* **1990**, *10,* 5502–5509.
52. Oconnor, P. M.; Jackman, J.; Bae, I.; Myers, T. G.; Fan, S.; Mutoh, M.; Scudiero, D. A.; Monks, A.; Sausville, E. A.; Weinstein, J. N.; Friend, S.; Fornace Jr, A. J.; Kohn, K. W. Characterization of the p53 tumor suppressor pathway in cell lines of the National Cancer Institute anticancer drug screen and correlations with the growth-inhibitory potency of 123 anticancer agents. *Cancer Res.* **1997**, *57,* 4285–4300.
53. Gong, B. D.; Chen, Q.; Endlich, B.; Mazumder, S.; Almasan, A. Ionizing radiation-induced, Bax-mediated cell death is dependent on activation of cysteine and serine proteases. *Cell Growth Differ.* **1999**, *10,* 491–502.
54. Jia, L. Q.; Osada, M.; Ishioka, C.; Gamo, M.; Ikawa, S.; Suzuki, T.; Shimodaira, H.; Niitani, T.; Kudo, T.; Akiyama, M.; Kimura, N.; Matsuo, M.; Mizusawa, H.; Tanaka, N.; Koyama, H.; Namba, M.; Kanamaru, R.; Kuroki, T. Screening the p53 status of human cell lines using a yeast functional assay. *Mol Carcinog.* **1997**, *19,* 243–253.

55. Nakano, H.; Kohara, M.; Shinohara, K. Evaluation of the relative contribution of p53-mediated pathway in X-ray-induced apoptosis in human leukemic MOLT-4 cells by transfection with a mutant p53 gene at different expression levels. *Cell Tissue Res.* **2001**, *306,* 101–106.

56. Jia, L. Q.; Osada, M.; Ishioka, C.; Gamo, M.; Ikawa, S.; Suzuki, T.; Shimodaira, H.; Niitani, T.; Kudo, T.; Akiyama, M.; Kimura, N.; Matsuo, M.; Mizusawa, H.; Tanaka, N.; Koyama, H.; Namba, M.; Kanamaru, R.; Kuroki, T. Screening the p53 status of human cell lines using a yeast functional assay. *Mol. Carcinog.* **1997**, *19,* 243–253.

57. Sugimoto, K.; Toyoshima, H.; Sakai, R.; Miyagawa, K.; Hagiwara, K.; Ishikawa, F.; Takaku, F.; Yazaki, Y.; Hirai, H. Frequent mutations in the p53 gene in human myeloid leukemia cell lines. *Blood* **1992**, *79,* 2378–2383.

58. Murai, Y.; Hayashi, S.; Takahashi, H.; Tsuneyama, K.; Takano, Y. Correlation between DNA alterations and p53 and p16 protein expression in cancer cell lines. *Pathol. Res. Pract.* **2005**, *201,* 109–115.

59. (a) Morita, A.; Yamamoto, S.; Wang, B.; Tanaka, K.; Suzuki, N.; Aoki, S.; Ito, A.; Nanao, T.; Ohya, S.; Yoshino, M.; Zhu, J.; Enomoto, A.; Matsumoto, Y.; Funatsu, O.; Hosoi, Y.; Ikekita, M. Sodium orthovanadate inhibits p53-mediated apoptosis. *Cancer Res.* **2010**, *70,* 257–265. (b) Morita, A.; Ariyasu, S.; Wang, B.; Asanuma, T.;

Onoda, T.; Sawa, A.; Tanaka, K.; Takahashi, I.; Togami, S.; Nenoi, M.; Inaba, T.; Aoki, S. AS-2, a novel inhibitor of p53-dependent apoptosis, prevents apoptotic mitochondrial dysfunction in a transcription-independent manner and protects mice from a lethal dose of ionizing radiation. *Biochem. Biophys. Res. Commun.* **2014**, *450,* 1498–1504.

Acknowledgement

本研究の遂行、本論文の執筆、そして日々の研究生活に際して、日頃から温かく熱心に御指導、御鞭撻を賜りました東京理科大学薬学部 青木 伸 教授に心より感謝申し上げます。

本論文の副査を引き受けて頂き、適切な御助言を賜りました東京理科大学薬学部 内海 文彰 教授、内呂 拓実 教授、月本 光俊 教授、早田 匡芳 准教授に厚く御礼申し上げます。

本研究の遂行ならびに本論文の執筆に際して、徳島大学大学院医歯薬学研究部 森田 明典 教授には数多くのご指導、ご助言を賜りました。心より感謝申し上げます。

本研究を進めるにあたり、化合物の生物学的評価に関して徳島大学 越智 進太郎氏、氏田 将平氏、豊田 美裕氏、多田 佳寿美氏には、多大なご助力を頂きました。心より感謝申し上げます。

本研究の遂行ならびに本論文の執筆に際して、徳島大学 西山 祐一 助教、松下 洋輔 助教、長崎大学 田中 義正 教授、植田 弘師 教授、出口 雄一 准教授、鈴木 啓司 准教授、広島大学 稲葉 俊哉 教授、東北大学 細井 義夫 教授 には数々のご指導、ご助言を賜りました。心より感謝申し上げます。

前 東京理科大学薬学部助教 嵯峨 裕 先生（現 大阪大学大学院工学研究科 助教）には研究活動でのご助言、また有機化学の楽しさを教えて頂きました。心より感謝申し上げます。

前 東京理科大学薬学部助教 田中 智博 先生（現 岡山大学大学院医歯薬学総合研究科 准教授）には公私を問わずご相談に乗っていただき、研究活動に際して数多くのご指導をいただきました。心より感謝申し上げます。

前 東京理科大学薬学部ポストドクトラルフェロー Babita Shashni 先生（現 筑波大学数理物質系 特任助教）、Chandrasekar Balachandran 先生（現 東京理科大学生命医科学研究所 助教）、前 日本学術振興会 外国人特別研究員 Jebiti Haribabu 博士（現 University of Atacama ポストドクトラルフェロー）、東京理科大学薬学部ポストドクトラルフェロー Surajit Haldar 博士には実験に関するご指導ならびに英語でのディスカッションを行っていただきました。心より感謝申し上げます。

質量分析を引き受けてくださいました前 東京理科大学薬学部質量分析室 長谷川 富貴子 技術専門職員、東京理科大学薬学部質量分析室 吉村 弥生 博士に深く感謝申し上げます。

NMR 測定法をご教示いただきました前 東京理科大学薬学部核磁気共鳴分析室 澤邉 紀子 技術専門職員、松田 諭 技術専門職員、東京理科大学薬学部核磁気共鳴分析室 飯田 基雄 技術専門職員に深く感謝申し上げます。

元素分析を引き受けてくださいました前 東京理科大学研究推進機構研究機器センター 中村 里子 技術専門職員、東京理科大学研究推進機構研究機器センター 倉持 裕生 技術専門職員に深く感謝申し上げます。

私の研究生活を支えて頂きました同級生（安藤 涼輔氏、風間 彩水氏、小林 由佳氏、口石 博斗氏、直井 竜大氏、廣瀬 真澄氏、水野 皓介氏）に心より御礼申し上げます。

多くの有益な御助言を下さり、研究生活を支えて頂いた先輩方（伊藤 太基 博士、染谷 英寿 博士、宮澤 有哉 博士、Akib Bin Rahman 博士、田村 裕一 博士、上田 大貴 博士、横井 健汰 博士、加藤 萌氏、菊池 千陽氏、田村 佳氏、寺岡 達朗氏、今福 浩輝氏、萱野 蒔人氏、関根 禎亮氏、内藤 佳奈氏）に深く感謝申し上げます。

いつも温かく接してくださった後輩の皆さん（2018 年度配属: 川端 凌矢氏、清水 舜氏、関 健仁氏、中川 聖也氏、2019 年度配属: 石上 剛大氏、内山 遥氏、小山田 有沙氏、芝内 涼太氏、山口 晃平氏、2020 年度配属: 岡本 紘知氏、笠井 貴文氏、神戸 梓氏、藤田 絢子氏、森田 都望恵氏、2021 年度配属: 磯部 理沙氏、垣花 真輝氏、川本 健太氏、新居 真由香氏、宮内 奈津子氏、2022 年度配属: 大瀧 正太郎氏、河野 航周氏、成島 希海氏、野本 彩音氏、山田 竜也氏）に心より感謝申し上げます。

筆末ながら、ここまで惜しみない支援をくださいました家族、友人に厚く御礼申し上げます。

2023 年(令和 5 年) 2 月

東京理科大学大学院　薬学研究科薬科学専攻

生物有機化学研究室

佐藤 秀哉

List of Publications

主論文を構成する論文

1. Design, synthesis and biological evaluation of 2-pyrrolone derivatives as radioprotectors

   Hidetoshi Satoh, Shintaro Ochi, Kosuke Mizuno, Yutaka Saga, Shohei Ujita, Miyu Toyoda, Yuichi Nishiyama, Kasumi Tada, Yosuke Matsushita, Yuichi Deguchi, Keiji Suzuki, Yoshimasa Tanaka, Hiroshi Ueda, Toshiya Inaba, Yoshio Hosoi, Akinori Morita, Shin Aoki

   Bioorganic & Medicinal Chemistry, Vol. 67, 116764 (2022 年 5 月)
   DOI: 10.1016/j.bmc.2022.116764

2. A Novel RNA Synthesis Inhibitor, STK160830, Has Negligible DNA-Intercalating Activity for Triggering A p53 Response, and Can Inhibit p53-Dependent Apoptosis

   Akinori Morita, Shintaro Ochi, Hidetoshi Satoh, Shohei Ujita, Yosuke Matsushita, Kasumi Tada, Mihiro Toyoda, Yuichi Nishiyama, Kosuke Mizuno, Yuichi Deguchi, Keiji Suzuki, Yoshimasa Tanaka, Hiroshi Ueda, Toshiya Inaba, Yoshio Hosoi, Shin Aoki

   Life, Vol. 11, Issue 10, 1087 (2021 年 10 月)
   DOI: 10.3390/life11101087

参考論文

1. Protective Effects of p53 Regulatory Agents Against High-LET Radiation-Induced Injury in Mice

   Akinori Morita, Bing Wang, Kaoru Tanaka, Takanori Katsube, Masahiro Murakami, Takashi Shimokawa, Yuichi Nishiyama, Shintaro Ochi, Hidetoshi Satoh, Mitsuru Nenoi, Shin Aoki

   Frontiers in Public Health, Vol. 8, 601124 (2020 年 12 月)
   DOI: 10.3389/fpubh.2020.601124

2. Evaluation of sodium orthovanadate as a radioprotective agent under total-body irradiation and partial-body irradiation conditions in mice

   Yuichi Nishiyama, Akinori Morita, Bing Wang, Takuma Sakai, Dwi Ramadhani, Hidetoshi Satoh, Kaoru Tanaka, Megumi Sasatani, Shintaro Ochi, Masahide Tominaga, Hitoshi Ikushima, Junji Ueno, Mitsuru Nenoi, Shin Aoki

   International Journal of Radiation Biology, Vol. 97, Issue 9, 1241–1251 (2021 年 7 月)
   DOI: 10.1080/09553002.2021.1941377